Institute of Physics of Latvian University

Mn-Zn FERRITE NANOPARTICLES FOR WATER- AND HYDROCARBONE-BASED FERROFLUIDS: PREPARATION AND PROPERTIES

Dr. Chem. THESIS

by Eduards Auzāns

Supervisors: Prof. E.Blūms
Prof. R.Massart

Rīga 1999

Promocijas darbs izstrādāts LU Fizikas institūtā un P. un M. Kirī Universitātē Ķīmijas fakultātē (Francijā) laika posmā no 1993. gada līdz 1998. gadam.

Darba raksturs: disertācija ķīmijas nozarē fizikālās ķīmijas apakšnozarē.

Darba recenzenti:

Dr. habil. phys. J. Tīliks (Latvijas Universitāte)
Dr. habil. chem. I. Vītiņa (RTU Neorganiskās Ķīmijas institūts)
Dr. chem. V. Cabuil (P. un M. Kirī Universitāte)

Darba aizstāvēšana notiks Latvijas Universitātes ķīmijas nozares habilitācijas un promocijas padomes atklātā sēdē 1999. g. 28. jūnijā plkst. 14^{00} Latvijas Universitātes Ķīmijas fakultātē Kr. Valdemāra ielā 48.

Ar disertāciju un tās kopsavilkumu var iepazīties Latvijas Universitātes bibliotēkā, Kalpaka bulvārī 4, un Latvijas Akadēmiskajā bibliotēkā, Rūpniecības ielā 10.

Habilitācijas un promocijas padomes priekšsēdis:

Dr. habil. chem. prof. A. Zicmanis

Table of content

This work is carried out mainly at the University P. et M. Curie in Paris, France and at the Institute of Physics of Latvian University in Latvia.

Preparation of Mn-Zn ferrite nanoparticles, cationic and hydrocarbon-based ferrofluids, as well as chemical analysis, X-rays powder diffraction, electronic microscopy, thermogravimetry, IR spectroscopy and magnetic measurements (at ambient temperature) of samples are carried out at the University P. et M. Curie under guidance of Prof. René Massart and Dr. D. Zins.

Magnetisation measurements at the temperature range of 280-473 K as well as processing of magnetisation curves and obtaining the spectra of magnetic moments are carried out at the Institute of Physics under direction of Prof. Elmārs Blūms and Dr. M. Maiorov.

Magnetisation measurements at low temperatures (100-293 K) of several samples are made in Department of Solid State Physics at Chalmers University of Technology and Göteborg University in Sweden.

I am very grateful to Prof. Elmārs Blūms for encouraging me to prepare and study Mn-Zn ferrite ferrofluids, for his persistant interest in my work, for his support and valuable advises.

I express special thanks to Prof. René Massart for offered opportunity to work at the Laboratoire de Colloides Magnétiques in Paris, his benevolence and permanent support in my work.

I address particular gratitude to Dr. Daniel Zins for taking care of me during my work in Paris, for his enthusiasm, help in experimental work as well as in discussing results.

I am very thankful to Prof. Jean-Claude Bacri and Prof. Regine Perzynsky for their great efforts in providing possibility for Latvian Ph. D. students to work in Paris. I am grateful for their support, interest to my work and helpful discussions.

I am grateful to Madame Fanton for teaching me many useful experimental things, especially in preparation of samples and their chemical analysis.

I would like to thank Dr. M.Robineau for his help in making X-rays diffraction measurements and his useful advises.

I would like to thank Madame Carpentier, Dr. V. Cabuil, Dr. A. Bee, Dr. S. Neveu, Dr. C. Menager, M-lle S. Lefebure and all people from Laboratoire de Colloides Magnétiques for their help and creative atmosphere.

I am thankful to my teachers and colleges in the Heat Physics Laboratory of Institute of Physics - Dr. M. Maiorov and Dr. G. Kronkalns for their enthusiasm, technical support and advises in preparing ferrofluids, making magnetic measurements and discussing of results.

Without support of Prof. M. Hanson from Chalmers University of Technology magnetisation measurements at low temperatures would be impossible.

Introduction

Ferrofluids present a new class of magnetic materials. They consist of a magnetic nanoparticles colloidally dispersed in a carrier liquid and combine both fluid and magnetic properties. This gives rise to the numerous unusual fundamental phenomena as well as to the interesting applications. Eight international conferences have been devoted to this field in recent twenty five years.

A promising application is using ferrofluids as liquid heat carriers in different heat-exchange devices as well as in devices for magnetocaloric energy conversion. Such systems may require ferrofluids with high thermomagnetic coefficients, however the most widely used ferrofluids with the magnetite nanoparticles do not satisfy these requirements. Therefore the development and synthesis of the special temperature sensitive magnetic nanoparticles for ferrofluids is of great interest. Among different temperature sensitive magnetic materials Zn-containing spinel type ferrites $Me_{1-x}Zn_xFe_2O_4$ are attractive as substances in which variation of content of initial components (Zn substitution degree **x**) allows to change their magnetic parameters in a wide range of values. This allows to obtain materials exhibiting different thermomagnetic coefficients. Moreover, Zn-containing ferrites can be obtained in a form of ultrafine particles by using a comparatively simple chemical coprecipitation method. Among different Zn-substituted ferrites Mn-Zn ferrites are preferred due to their lower Curie temperatures and high magnetisation, which lead to rather high thermomagnetic coefficients.

Crystalline and magnetic properties of bulk Mn-Zn ferrites are well known. However, properties of ferrite nanoparticles significantly differ from those of a bulk material. Therefore a detailed study of conditions of synthesis and their influence on the properties of Mn-Zn ferrite nanoparticles is necessary. Magnetisation measurements of these nanoparticles in a wide temperature range may clarify the regularities of behaviour of their magnetic parameters upon temperature.

The size of particles plays a significant role in their solubilisation in a liquid medium. Therefore, it seems important to study the dependence of properties of nanoparticles upon their size.

According to the type of carrier liquid two different types of ferrofluids are known: an aqueous ionic ferrofluid and a surfacted organic-based one. Ionic ferrofluids demonstrate several specific phenomena as well as may be used as precursors for a wide class of surfacted ferrofluids. Surfacted ferrofluids based on low-evaporating non-polar liquids keep their fluid properties in a rather wide temperature range that is important for practical applications. Synthesis of these two types of ferrofluids requires an elaboration of appropriate solubilisation procedures for Mn-Zn ferrite particles.

Chapter 1.

STATE OF PROBLEM: REVIEW OF LITERATURE

1.1. Intrinsic properties of Mn-Zn ferrite particles

Crystalline and magnetic properties of bulk Mn-Zn ferrites ($Mn_{1-x}Zn_xFe_{2.0}O_4$)) are described in 1.1.1. However, properties of ultrafine Mn-Zn ferrite nanoparticles obtained by coprecipitation method differ from those of bulk Mn-Zn ferrites (see 1.1.2.).

Magnetic properties of ferrofluids and powders of nanoparticles are discussed in 1.2.

Formation of Mn-Zn ferrite fine particles by coprecipitation method, influence of synthesis conditions and parameters on the properties of particles are discussed in 1.3.

Questions connected with solubilisation of ferrite nanoparticles in aqueous solution and in non-aqueous medium are described in 1.4.1. and 1.4.2., respectively.

1.1.1. Crystalline and magnetic properties of bulk Mn-Zn ferrite

Mn-Zn ferrites as magnetic materials are widely used for cores of intermediate frequency transformers, inductors, loudspeakers and other electromagnetic devices. Usual ceramic preparation of bulk ferrites is carried out by means of a high-temperature reaction between finely milled oxide (or carbonate) powders followed by shaping and successive pressing and sintering [1]. Crystalline and magnetic properties of bulk Mn-Zn ferrites have been intensively studied since 50-ies.

1.1.1.-A. Crystalline structure of bulk Mn-Zn ferrites

Ferrites $Zn_xMn_{1-x}Fe_2O_4$ ($0 \le x \le 1$) have crystalline structure of spinel type. In spinels the elementary cell is of faces-centred cubic symmetry. The elementary cell (with rib length **d** of ~0.84 nm) is formed by 32 oxygen atoms and 24 cations. There are 64 tetraedric and 32 octaedric possible positions for cations in the elementary cell. Only 8 tetraedric and 16 octaedric positions are occupied by cations. They are named A- and B- positions, respectively. B- positions are usually shown by square brackets.

According to distribution of cations there are following types of ferrospinels:

1) normal spinel structure, where all Me^{2+} ions occupy A-sites; structural formula of such ferrites is $Me^{2+}[Fe_2^{3+}]O_4^{2-}$. This type of distribution takes place in the zinc ferrite: $Zn^{2+}[Fe^{3+}Fe^{3+}]O_4^{2-}$.

2) inversed spinel structure, where all Me^{2+} are in B- positions and Fe^{3+} ions are equally distributed between A- and B-sites: structural formula of these ferrites is $Fe^{3+}[Me^{2+}Fe^{3+}]O_4^{2-}$. Magnetite Fe_3O_4, ferrites $NiFe_2O_4$ and $CoFe_2O_4$ have inversed spinel structure.

3) mixed spinel structure, when cations Me^{2-} and Fe^{3+} occupy both A- and B-positions; structural formula of such ferrites is $Me^{2+}_{(1-\delta)}Fe^{3+}_{\delta}[Me^{2+}_{\delta}Fe^{3+}_{2-\delta}]O_4^{2-}$, where parameter δ indicates the degree of inversion. $MnFe_2O_4$ represent this type of structure and has an inversion degree of $\delta=0.2$ and its structural formula reads: $Mn^{2+}_{0.8}Fe^{3+}_{0.2}[Mn^{2+}_{0.2}Fe^{3+}_{1.8}]O_4^{2-}$. Mn-Zn ferrites have also a same type of spinel structure (Zn^{2+} prefers to occupy A-sites): $Zn^{2+}_xMn^{2+}_yFe^{3+}_{1-x-y}[Mn^{2+}_{1-x-y}Fe^{3+}_{1+x+y}]O_4^{2-}$, $\delta=1-x-y$ [1-3].

Increase in Zn substitution degree **x** leads to a linear decrease in the lattice constant from 0.851-0.852 nm for $MnFe_2O_4$ down to 0.844 nm for $ZnFe_2O_4$. This occurs due to a smaller ion size of Zn^{2+} (0.83 Å) than that of Mn^{2+} (0.91 Å) [4].

1.1.1.-B Magnetic properties of bulk Mn-Zn ferrite ferrites

Mn-Zn ferrites are distinguished for their low Curie temperatures, low remaining magnetisation and low values of the magnetic crystalline anisotropy constant. In the magnetism this is called "magnetic softness".

Magnetic properties of ferrites were explained by Neel, who postulated that magnetic moments of ferrites are the sum of magnetic moments of individual sublattices. In ferrospinels these are: sublattice A consisting of cations in tetraedric positions and sublattice B with cations in octaedric positions. Exchange interaction between electrons of ions in these sublattices has different value. Usually interaction between magnetic ions of sublattices A and B (AB-interaction) is the strongest. AA-interaction is almost ten times weaker and BB-interaction is the weakest. This interaction leads to complete or partial (noncompensated) antiferromagnetism (ferrimagnetism) [1, 2].

In the inversed ferrites one half of Fe^{3+} is placed in A-sites and another half in B-sites. Their magnetic moments are mutually compensated and resulting moment of the ferrite is due to the magnetic moments of bivalent cations Me^{2+} in B-positions.

A	[B	]
Fe^{3+}	$[Me^{2+}\ Fe^{3+}]$	O^{2-}_4
↓	↑ ↑	0

Magnetisation of $MnFe_2O_4$ which has inversion degree δ=0.2 is described by the following scheme:

A		[B		]	
$Mn^{2+}_{0.8}$	$Fe^{3+}_{0.2}$	$[Mn^{2+}_{0.2}$	$Fe^{3+}_{0.8}$	$Fe^{3+}]$	O^{2-}_4
↓	↓	↑	↑	↑	0

Substitution of Mn^{2+} with Zn^{2+} leads to introduction of nonmagnetic Zn^{2+} ions into A-sites and thus increasing of σ_s occurs as originally shown by Guillaud and co-workers [5]. Increasing **x** up to 0.4 (at 0 K) leads to linear increase in magnetisation and may be described by the following formula [3]:

A		[B		]	
Zn^{2+}_x	Mn^{2+}_y Fe^{3+}_{1-x-y}	$[Mn^{2+}_{1-x-y}$	Fe^{3+}_{1+x+y}	$Fe^{3+}]$	O^{2-}_4
0	↓ ↓	↑	↑	↑	0

For higher Zn concentrations (**x**>0.4-0.5) ferrite becomes normal spinel. It means that there are no more Mn^{2+} in B-sites and no more Fe^{3+} in A-sites. For **x**>0.4 weakening of the A-B exchange interaction and increasing of role of B-B interaction takes place. Due to that magnetic moments of a part of Fe^{3+} ions (which are now only in B position) become oriented reversibly and as a result the decrease of the total magnetic moment in ferrite follows. The higher is the temperature **T**, the greater is the relative effect of the A-B exchange weakening due to the thermal fluctuations. As a result the decrease in magnetisation occurs. In Tab. 1.1.-1. the saturation magnetisation σ_s and the Curie temperatures T_c of bulk ceramic Mn-Zn ferrites with a different Zn substitution degree **x** at three different temperatures are shown [1,5-6]. At 0 K maximum of magnetisation lies at **x**=0.4-0.6, but the increase in temperature to 293 K leads to lower σ_s values. In the other words, increasing of **T** up to the

ambient temperature leads to shift of σ_s maximum to lower **x** values (0.2-0.3). At the same time increase in **x** leads also to the decrease of Curie temperature and for **x**=0.6 T_c becomes close to the room temperature (see Tab. 1.1.-1).

Values of the thermomagnetic coefficient k_{T_s} are calculated as $-\Delta\sigma_s/\Delta T$ in the range of 293-373 K and also shown in Tab. 1.1.-1.

Increase in **x** of Mn-Zn ferrite leads to lower values of the constant of the crystalline magnetic anisotropy K_1. $|K_1|$ decreases from $3.3\cdot10^4$ erg/cm^3 for Mn ferrite to a small values down to less than $1\cdot10^4$ erg/cm^3 for **x**=0.3-0.55 [4,7,8] (see Tab. 1.1.-1.). For Mn-Zn ferrites with higher Zn substitution degrees (**x**>0.5) the determination of K_1 at room temperature becomes difficult due to a small magnetisation and for these ferrites there are no data in the literature.

Values of σ_s, k_{T_s}, T_c and K_1 are given also for magnetite Fe_3O_4, particles of which are commonly used for ferrofluids (see Tab. 1.1.-1.). The Curie temperature T_c of magnetite is almost for 300 K higher than that of Mn ferrite. Therefore magnetite exibits a very small values of k_{T_s}=0.06 emu/g*K.

Table 1.1.-1. Magnetic properties for bulk Mn-Zn ferrites with a different Zn substitution degree **x** and for magnetite Fe_3O_4: saturation magnetisation σ_s at different temperatures, Curie temperature T_c (from refs. [1] [5], and [6] if not specially mentioned) and constant of crystalline magnetic anisotropy K_1. Data for Fe_3O_4 are taken from ref. [2].

Zn substitution degree **x**	σ_s extra-polated to 0 K	σ_s at 293 K, emu/g	σ_s at 373 K, emu/g	Thermomagn. coefficient k_{T_s} (293-373 K), emu/g*K	Curie tempe-rature T_c, K	Constant of magnetic crystalline anisotropy K_1 at 293 K, erg/cm^3	Critical superpara-magnetic size D_s, nm
0	112	80	62	0.23	573	$-3.3\cdot10^4$ **[7]	53 [9]
0.2	139	91	66	0.31	513	$-1.8\cdot10^4$ **[7]	
0.4	169	79	44	0.44	438	~0 **[7]	
0.45						$+0.7\cdot10^4$ ** [7]	
0.5	164	65	-	-	398		
0.55						$-0.38\cdot10^4$ [8]	103 [8]
0.6	160	55*	-	-	343	-	
0.8	115	12*	-	-	-	-	
Magnetite Fe_3O_4 [2]	98	92	87	0.06	868	$-11\cdot10^4$	25 [9]

* - σ in H=18 500 Oe at 285 K

** in [7] K_1 values are for Mn-Zn ferrites with 52 mol % Fe_2O_3

For Zn substitution degrees **x** close to 1.0 B-B interaction becomes dominant and in $ZnFe_2O_4$ magnetic moments of Fe^{3+} have antiparallel orientations. As Zn^{2+} cations, which occupy A-positions, have no magnetic moments the resulting magnetic moment of $ZnFe_2O_4$ is zero. $ZnFe_2O_4$ is the compensated antiferromagnetic and is described by the following scheme [1, 2]:

$$\begin{array}{c} Zn^{2+}[Fe^{3+}\ Fe^{3+}]O_4^{2-} \\ 0 \quad \uparrow\downarrow \quad 0 \end{array}$$

However, there are some cases when a small magnetism is observed in $ZnFe_2O_4$, for example, after fast cooling from high temperatures a small part of Zn^{2+} may remain in the B-positions and a part of Fe^{3+} - in the A-positions, respectively. Inversion degree δ reaches values ~0.1 and such Zn ferrite manifests a non-compensated antiferromagnetism. [10].

1.1.2. Crystalline and magnetic properties of ultrafine Mn-Zn ferrite particles

Bulk ferrites are synthesised by sintering at high temperatures (at 1200-1300 °C). At these temperatures the diffusion rate of cations is sufficiently high and a perfect crystalline lattice with the high chemical homogeneity can be formed [10].

Ultrafine Mn-Zn ferrite particles are prepared by the chemical coprecipitation method at temperatures near 100 °C and their properties differ from the corresponding bulk ferrite [11-13].

Mn-Zn ferrite particles of 12-20 nm contain up to 10 w% of associated water, which cannot be eliminated by heating in aqueous solution at 373 K (100°C) [13]. Lattice parameter of these particles is slightly increased in respect to the samples subjected to high temperature heating.

Ultrafine Mn-Zn ferrite particles demonstrate a lower magnetisation than that of corresponding bulk ferrite [12,13]. In Tab. 1.1-2 the saturation magnetisation σ_s at 293 K is shown for particles of two different sizes: 12-20 nm [13] and 120 nm [13] with a different Zn substitution degree **x**.

Table 1.1.-2. Saturation magnetisation at 293 K for particles with a different Zn substitution degree **x** of two different sizes: 120-130 nm [12] and 12-20 nm [13].

Zn substitution degree **x**	σ_s, D=120-130 nm	σ_s at 293 K D=12-20 nm
0	70.5	45.6
0.19	75.4	-
0.20	-	48.9
0.27	-	49.2
0.29	76.8	-
0.40	69.1	46.7
0.50	51.4	35.4
0.60	45.6	18.3
0.80	-	9.1

It can be seen that a smaller size of particles leads to a lower magnetisation. Particles of 120 nm demonstrate 80-90 % of $\sigma_{s\,bulk}$, whereas particles of 12-20 nm show only 54-60 % of $\sigma_{s\,bulk}$.

Small Mn-Zn ferrite nanoparticles (6 - 10 nm) with $x \geq 0.5$ are found to be far from magnetic saturation even in a very strong magnetic field of 120 kOe due to significant paramagnetic contribution [14]. This may hinder correctly determinate their saturation magnetisation. Authors of ref. [14] made an attempt to divide superparamagnetic and paramagnetic contributions of the whole magnetisation on the base of calculated spectrum of magnetic moments. Then a "spontaneous intrinsic magnetisation" is calculated as saturation of superparamagnetic part of magnetisation. However, for samples with $x \geq 0.8$ as well as for samples with lower Zn content at elevated temperatures it becomes not possible to divide these two parts of magnetisation.

Influence of the size of particles of different ferrites (ferrites of Co, Mn, Ni and $Ni_{0.3}Zn_{0.7}$) on their magnetisation was studied by T.Sato et al [9]. Authors have found a gradual decrease of $\sigma_s/\sigma_{s\,bulk}$ with decreasing of particles size in the range from 50 to 15 nm and rather sharp decrease below 15 nm. Comparing of $\sigma_s/\sigma_{s\,bulk}$ for different ferrites with equal particle sizes have shown a relatively larger loss in magnetisation for materials with low K_1 (constant of magnetic crystalline anisotropy): for Mn ferrite and $Ni_{0.3}Zn_{0.7}$ ferrite ($|K_1|$ are $3.3 \cdot 10^4$ and $3 \cdot 10^3$ erg/cm^3 respectively) 10 nm particles had $\sigma_s/\sigma_{s\,bulk}$ 0.47 and 0.40 respectively, whereas for magnetite particles of the same size it was 0.65. Decrease of σ_s for Mn ferrite particles of smaller sizes was also reported by Z.X.Tang et al [15]: for particles of

7.5 nm size the normalised magnetisation $\sigma_s/\sigma_{s\,bulk}$ was found to be ~0.4. These particles demonstrated also an increase of T_c for ~100 K in comparison with the bulk material.

Value of $|K_1|$ determines so called critical superparamagnetic size D_s (see Tab.1.1.-1). For particles with size less than D_s a magnetic moment is not rigidly fixed within particle, but can turn inside it (Neel mechanism of magnetic relaxation occurs) [16]. In the macroscopic level (for powder or ferrofluid) it means that there is no the remaining magnetisation or the magnetic hysteresis. Nanoparticles of Mn and Mn-Zn ferrites with sizes suitable for ferrofluids (D<11 nm) are completely super-paramagnetic because their D_s exceeds 50 nm.

Due to decrease of σ_s and increase of T_c in nanoparticles one may expect also a lower values of the thermomagnetic coefficients k_T. However, there are no systematic studies of magnetisation dependence on temperature for Mn-Zn ferrite nanoparticles. T.Fujita reported thermomagnetic coefficient k_T~0.2 emu/g•K for Mn-Zn ferrite nanoparticles of 9 nm with Ca^{2+} additions ($Mn_{0.3}Ca_{0.1}Zn_{0.6}Fe_2O_4$) [17].

Bigger and smaller particles fractionated from a polydispersed sample of $Mn_{0.5}Zn_{0.5}$ ferrite ferrofluid demonstrate different thermomagnetic coefficients k_T [14, 18].

In an ultrasmall particles of Zn ferrite, obtained by the chemical coprecipitation method, noncompensated antiferromagnetism was observed. Moreover, the inversion degree and magnetisation depend on the size of particles and are higher in a smaller ones (of 6-10 nm) [19-21].

1.2. Magnetic properties of ferrofluids and powders

Ferrofluid usually demonstrates superparamagnetic behaviour. Each particle (monodomen) in solution bears magnetic moment μ which can freely orientate in the direction of external magnetic field H. Thermic motion tends to disorientate parallel alignment of magnetic moments to H. The concurrence of these two forces determine the resulting value of magnetisation I (magnetic moment per volume $I=\mu/V$). Classic Langevin theory for the ensemble of independent paramagnetic gas molecules is usually applied to description of magnetic behaviour of ferrofluid, where the individual magnetic moments of particles are considered instead of the moments of gas molecules. Magnetisation of ferrofluid is described by the following formula: $I = I_\infty \cdot L(\xi)$, where Langevin function $L(\xi)=cth(\xi)-1/\xi$. Langevin argument ξ represents the ratio of magnetic interaction energy of the particle μH to the thermal energy kT: $\xi = \frac{\mu_0 \cdot \mu H}{kT}$, the magnetic interaction of particle moment tends to orientate it in the direction of the external magnetic field, while the thermic energy disorientates it [22]. For spherical particles $\xi = \frac{\pi}{6} \cdot \frac{\mu_0 I_S H \cdot D^3}{kT}$

$I_\infty = \varphi_M I_S$ – saturation magnetisation of ferrofluid;

φ_M – volume concentration of the magnetic phase;

I_S – saturation magnetisation of magnetic particles material;

μ – magnetic moment of particle;

kT – thermic energy;

μ_0 – absolute magnetic permeability.

In a small magnetic fields ($\xi<<1$) Langevin function has a linear asymptotic $L(\xi)= \xi/3$, and the initial magnetic susceptibility for spherical particles $\chi_0=I/H$ is $\chi_0 = \frac{\pi}{18}\cdot\frac{\mu_0 I_\infty I_S}{kT}\cdot D^3$, In a strong magnetic fields ($H>> kT/(\mu_0 \mu)$ or $\xi >>1$) the magnetisation is inversely proportional to the **H**:

$$I=I_\infty - \frac{6\cdot I_\infty kT}{\pi\cdot\mu_0\cdot I_S\cdot H\cdot D^3}$$

From the experimental dependence for ferrofluid **I(H)** versus 1/**H** in strong magnetic fields it is possible to determine the value of saturation magnetisation I_∞ by extrapolation **I(H)** values up to $H \rightarrow \infty$ ($1/H \rightarrow 0$).

In practice the above mentioned regularities mean that the smaller particles have less steep magnetisation curve than the bigger ones.

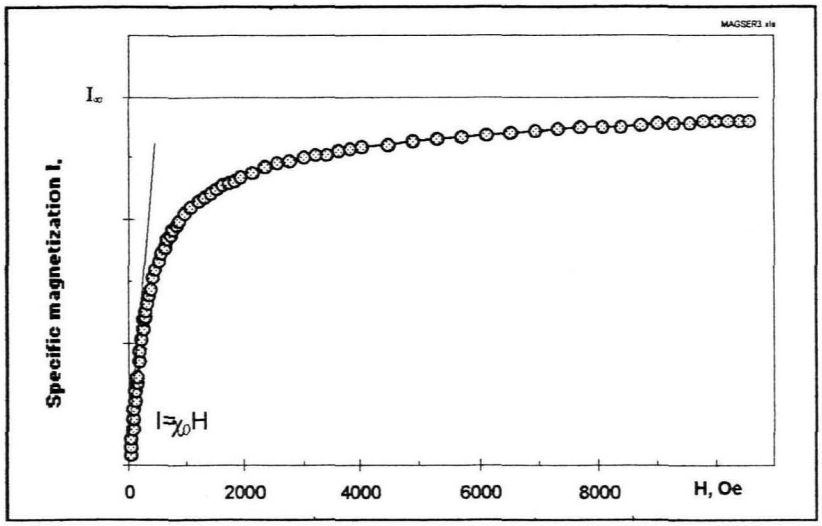

Figure 1.2.-1. Typical magnetisation curve for Mn-Zn ferrofluid (Zn substitution degree **x**=0.24).

For dried powders the initial section of magnetisation curve may differ from the Langevin shape, because of interaction between particles. Therefore the correct determination of χ_0 is impossible for powders.

Interaction between particles depends on their magnetic moments, distance and mutual orientation of their magnetic moments. The maximal interaction is when two particles are placed one under another and their magnetic moments are oriented parallel to this direction:

In this case the local field of one particle in the centre of another is $H_0=2\mu/D^3$, where μ is the magnetic moment and **D** - particles diameter. For **D**=10 nm, σ_s =50 emu/g and μ =$2.5\cdot10^{-16}$ emu evaluation of maximal interaction field gives H_0=500 Oe. If the external magnetic field **H** exceeds H_0 than the magnetic interaction may be neglected. For characterisation of dried powders of nanoparticles the specific mass magnetisation σ is usually used $\sigma=\mu/m=I/\rho$, where ρ is a ferrite density.

1.3. Synthesis of Mn-Zn ferrite fine particles: coprecipitation and heating in alkaline solution

Ferrites (including Mn-Zn ones) with the most perfect crystalline and magnetic structure are produced by sintering of Me(II) and Fe(III) oxides or carbonates at high temperatures (up to 1200 °C) [1-2]. This method, however, can not be used for producing the ultrafine particles for ferrofluids.

Ultrafine particles can be synthesised by so called "coprecipitation method" or "low temperature method". It can provide nanoparticles (size less than 12 nm) with surface allowing to adsorb ions or surfactants, which is necessary for the further formation of the stable colloidal solution (ferrofluid) [22] .

Synthesis of such nanoparticles was described for magnetite [23], ferrites of Co and Mn [25] as well as for Zn ferrite [20].

There are also a few publications concerning the properties of ferrofluids based on Mn-Zn ferrite nanoparticles of 5-12 nm [17, 18, 26-28], but unfortunately no much details are given about the particles synthesis process. However, for bigger Mn-Zn ferrite particles (**D**>15 nm) obtained by the coprecipitation method, several synthesis parameters and their influence on particles properties have been studied and described [13, 29].

1.3.1. Principle of reaction

Mn-Zn ferrite fine particles are obtained by the coprecipitation (polycondensation) from aqueous solutions of Fe^{3+} and bivalent metal Me^{2+}, where as Me^{2+} may serve Fe^{2+}, Mn^{2+}, Co^{2+}, Ni^{2+} and (or) Zn^{2+} cations [30].

At first solid hydroxides of metals in the form of colloidal particles are obtained by the coprecipitation of metal cations in alkaline medium (coprecipitation step). For the case of Mn with a partly substituted by Zn this reaction is following:

$$(1-x)Mn^{2+} + xZn^{2+} + 2Fe^{3+} + OH^- \rightarrow (1-x)Mn(OH)_2 \cdot xZn(OH)_2 \cdot 2Fe(OH)_3 \downarrow$$

Then this product is subjected to heating in the precipitation alkaline solution to provide the transformation of solid solution of metal hydroxides to the Mn-Zn ferrite (ferritisation step):

$$(1-x)Mn(OH)_2 \cdot xZn(OH)_2 \cdot 2Fe(OH)_3 \xrightarrow{aq.,\ t^\circ} Mn_{(1-x)}Zn_x Fe_2O_4 \cdot nH_2O$$

The peculiarity of "the coprecipitation method" of synthesis (in comparison with the high temperature synthesis of ceramic ferrites) is that the product contains a certain amount of associated water (up to 10 w%) even after several hours of heating in alkaline solution [13].

1.3.2. Parameters of synthesis and their influence on the properties of Mn-Zn ferrite particles

1.3.2.-A. Role of anions

The type of anions in the coprecipitation solution effect properties of obtained primary colloid differently for three metals. Precipitation of individual hydroxides of Fe(III) and Zn gives more pure hydroxides (with a less presence of the basic salts, which facilitate a further ferritisation) in the following sequence of anions: $SO_4^{2-} \rightarrow Cl^- \rightarrow NO_3^-$ [30]. In the case of Mn the sequence of anions for obtaining more pure hydroxide is opposite: $NO_3^- \rightarrow Cl^- \rightarrow SO_4^{2-}$ [30].Therefore for formation of the Zn ferrite particles it is better to take nitrates $Zn(NO_3)_2$ and $Fe(NO_3)_3$, whereas for the Mn ferrite chlorides $MnCl_2$ and $FeCl_3$ are preferable as a compromise. To have a more equal conditions for all three metals in the whole range of Zn substitution degree $0 \leq x \leq 1$, metals may be taken in the form of their chloride salts.

1.3.2.-B. The rate of mixing of reagents

Coprecipitation consists of two processes: nucleation (formation of centres of crystallisation) and a subsequent growth of particles. The relative rates of these two processes determine the size and polydispersity of obtained particles. Polydispersed colloids are obtained as a result of simultaneous formation of a new nuclei and growth of the earlier formed particles [31, 32]. Less dispersed in size colloid is formed when the rate of nucleation is high and the rate of particles growth is low [32]. This situation corresponds to a rapid addition and a vigorous mixing of reagents in the reaction.

Slow addition of reagents in the coprecipitation reaction leads to the formation of bigger nuclei than rapid one. It was observed for formation of $MnFe_2O_4$ particles [33].

It must be also taken into account that in the case of slow addition of the base to solution of metal salts a separate precipitation takes place due to the different pH of precipitation pH_p for different metals [13]. It is just actual in a three metal system where Fe(III) has pH_p~1.6, Zn – pH~5.8 and Mn(II) – pH~8.6 [30]. Separate precipitation may increase the chemical inhomogenity in the particles.

To obtain ferrite particles of a smaller size, less dispersed in size and more chemically homogeneous one must use as rapid rate of mixing of reagents as possible.

1.3.2.-C. Influence of temperature

Increasing of temperature (in the range 20-100 °C) significantly accelerates formation of ferrite particles. It is shown for ferrite particles coprecipitated with NaOH: Mn ferrite [34], Zn ferrite [35] and Mn-Zn ferrite [29]. For Mn-Zn ferrite particles with x=0.33 formed at 80 °C the yield of ferrite estimated from magnetisation of the product is only 2/3 of that at 100 °C [29].

Activation energy for formation of ferrites of different metals is not equal. Activation energy calculated from kinetics of the formation reactions for three different ferrites in the temperature range of 20-100 °C decreases in the following sequence: $E_{A(Mn\ ferrite)} > E_{A(Ni\ ferrite)} > E_{A(Zn\ ferrite)}$ [34]. This sequence is also in agreement with the decreasing of dehydration temperature of the individual hydroxides of the corresponding metals. Authors of ref. [34] conclude that the formation of $ZnFe_2O_4$ proceeds more readily and starts at lower temperatures than that of $MnFe_2O_4$.

As a conclusion of above mentioned, heating at temperatures close to 100 °C are preferable for easier and more rapid formation of the Mn-Zn ferrite particles.

1.3.2.-D. Influence of the pH of the reaction

For the formation of Zn ferrite the yield of ferrite grows when the pH of the reaction is increased from 6.8 to 8.6. Increase of pH value from 8.6 up to 10 leads only to a slight growing of the yield. The most interesting fact is that a further increasing pH up to 13.5–14 leads to a significant growth of the yield. At high pH values the time of formation of Zn ferrite becomes very short [35]. Authors conclude that at high values of pH the reaction of ferrite formation takes place not between solid hydroxides as at pH<10, but between soluble hydroxocomplexes $Zn(OH)_3^-$ and $Fe(OH)_4^-$ in the liquid phase.

For formation of Mn ferrite (NaOH coprecipitating agent) the increasing of pH value up to 12.5 accelerates the formation of the ferrite in a similar manner as for Zn ferrite. But the further increase of pH up to 14 leads to a reduction of the ferrite yield due to formation of nonmagnetic $Na_2[Mn(OH)_4]$ and paramagnetic hydro-hausmanite $Mn_3O_4 \cdot nH_2O$ at high pH [36].

Varying of the value of pH of the reacting solution (NaOH coprecipitating agent) leads to different size of particles. For Zn ferrite pH=8 gives the smallest size of 2 nm and pH=13 - the largest size of 6 nm [20].

On the contrary to the Zn ferrite, increasing of pH in the case of Mn ferrite (NaOH - coprecipitation agent) leads to formation of particles of smaller size [37].

For formation of the Mn-Zn mixed ferrite particles optimal pH range is found to be near 12.5 [13]. Increasing pH up to 14 leads to decrease in magnetisation of the product due to the same reasons as for pure Mn ferrite.

1.3.2.-E. Influence of the concentration of reagents

No significant difference was found in the yield of Mn-Zn ferrite when the concentration of metal salts in the coprecipitated reaction is varied from 0.05 to 4 mol/l [13].

Concentrations of 0.1–0.2 mol/l are usually taken for the synthesis of ferrite particles for ferrofluids [33], because this allows to obtain non-viscosius primary suspension of particles that is important for better mixing of the reacting volume. At higher concentrations ([Me]>0.5 mol/l) suspension becomes viscous, and it is difficult to provide intensive stirring.

1.3.2.-F. The type of the coprecipitating base

The type of the coprecipitating base has a significant influence on the size of obtained ferrite particles. For Mn ferrite it was shown that three different bases give particles with size diminishing in the following sequence, which coincides with the sequence of reducing strength of the base: $D_{NaOH} > D_{CH_3NH_2} > D_{NH_3}$ [25]: NaOH gives the particles of 16.8 nm, CH_3NH_2 - 11 nm and NH_3 - 7.3 nm.

Attempts to obtain Zn ferrite with NH_3 did not succeed. Coprecipitation of Fe^{3+} and Zn^{2+} with NH_3 does not lead to the formation of Zn ferrite even after heating for 8 hours at 60 °C [38].

1.3.2.-G. Duration of heating after coprecipitation

F.Tourinho investigated influence of the duration of heating (at 100°C) after coprecipitation on the size of Mn ferrite particles. Slight growth of particles is found: from 11 nm after 10 min to 12.4 nm after 30 min of heating [33].

V.P.Chalyi and co-workers reported a significant increasing of magnetisation of Mn-Zn ferrite particles (with **x**=0.33) during the process of boiling in alkaline solution from 1 hour to 24 hours [13]. Coprecipitation took place in a concentrated system, but no information is given on growing of particles size, which may take place in a such system during long heating process.

1.3.2.-H. Varying of the Zn substitution degree

Size of Mn-Zn ferrite particles was found to decrease with the increasing of Zn content in the particles [29]. Mn ferrite and $Mn_{0.67}$ $Zn_{0.33}$ ferrite particles had sizes of 15.5 nm and - 14.2 nm respectively.

Increasing of Zn content leads to a higher amount of associated water in the particles [13, 29]. Associated water content (determined by thermogravimetry technique) decreased to a certain level after 24-36 hours of boiling and did not changed for further boiling. Products at this stage are characterised by the following formula: $MnFe_2O_4 \cdot 0.4H_2O$, $Mn_{0.66}Zn_{0.33}Fe_{2.0}O_4 \cdot 0.6H_2O$ and $ZnFe_2O_4 \cdot 1.2H_2O$ [29,35,36].

1.3.2.-I. Varying of the ratio Me(II)/Fe(III)

Varying of the initial proportion of the molar ratio X=Mn(II)/ (Mn(II) +Fe(III)) was investigated for Mn ferrite formation by [23]. High magnetisation is found for X=0.3-0.45 with a maximum in the magnetisation near stoichiometric ratio X=0.33. Deviation from stoichiometric proportion leads also to the increase in particles size.

1.3.2.-J. Influence of the gas atmosphere

Boiling of coprecipitated Mn, Zn and Fe(III) hydroxides in alkaline solution under argon atmosphere did not lead to a significant changes in the yield and magnetisation of ferrite in comparison with the samples prepared in air atmosphere [13]. Authors conclude that the role of Mn(II) oxidation products (α-MnOOH, α-, β-Mn_3O_4 and β-Mn_2O_3) in the process of ferrite formation is negligible.

1.4. Solubilisation of ferrite nanoparticles into liquid carrier: formation of ferrofluid

Ferrofluids consist of fine particles suspended in the carrier liquid. One of the essential points for elaboration of such systems is their chemical and physical stability. The density of the ferrite particles is more higher than that of solvents. Reaction of the coprecipitation under certain conditions leads to a fine grains of the ferrite, to whom the brownian movement may compensate action of gravitational force. But even if particles are sufficiently small, the brownian movement can not compensate the attraction raised by the magnetic and Van-der-Waals forces. It is necessary to introduce supplementary repulsive interaction between the grains for stabilisation of magnetic colloid in the given solvent. This interaction may be created by the electrostatic repulsion in the aqueous solution (ionic ferrofluids) or by the absorbed surfactant layer in a non-aqueous media (surfacted ferrofluid).

1.4.1. Solubilisation of ferrite nanoparticles into aqueous solution: formation of ionic ferrofluid

The method of producing of the ionic water-based ferrofluids is based on the principle described by R.Massart for ferrofluids on the base of magnetite [40]. Particles synthesised by this reaction are macroanions. Electric charges appear due to the specific adsorption of the amphoteric hydroxyl group, which leads to superficial negative charges in the alkaline medium and a positive charges in the acidic one [41]. Because of these charges particles are peptizable in water. But this is only possible with a low polarising counterions. Ferrite particles formed after coprecipitation and heating in alkaline solution can not be directly solubilised in water-based medium. The presence of 'the primary' too polarising counterions such as Na^+, $(CH_3)NH_3^+$ or NH_4^+ remained from the coprecipitation reaction has a strong screening effect on charged particles, and as a result the repulsion between particles is less effective and particles aggregate [40].

It is found by R.Massart [40] that a non-aggregating colloidal sols (ionic ferrofluids) can be obtained by the substitution of above mentioned primary counterions with a low polarising cations $N(CH_3)^+$ and NO_3^- anions in appropriate concentration [40]. Surface charge density can be

progressively and reversibly modified through the acid-base equilibrium. Because of the OH^- ligand, the Zero Charge Point is located at pH~7.5-8.0. Around this point the surface charge density is too small and particles flocculate. In practice it does not allow to get such ionic ferrofluids at pH in the range between 5.5 and 10 [41]. Effective desorbtion of the primary counterions may be obtained by the exposition of particles to HNO_3 solution (so called 'surface acid treatment') to replace them with NO_3^- counterions.

During HNO_3 treatment the degradation of part of ferrite particles material takes place. For example, for Co ferrite particles treatment of 2 mol/l HNO_3 for 1 hour leads to a degradation of 30 % of particles material and degradation is complete in 48 h [25].

Cationic (acidic) sols for Mn and Co ferrites prepared directly after HNO_3 treatment appear to be not chemically stable in time. Specific surface electric charge density on the particles after HNO_3 treatment is too high (40-60 mC/cm^{-2}) and particles slowly degradate in acid medium (at pH=2 - conditions of cationic sol). Therefore an additional treatment of particles was proposed and applied to the synthesis of Mn and Co ferrite ionic ferrofluids [33]. The scheme of preparation used by F.Tourinho is shown on Fig. 1.4.-1. After surface treatment with HNO_3 an additional $Fe(NO_3)_3$ treatment of particles was carried out [33]. It leads to modification of particle surface, namely to decrease of acid fixation on the surface (surface becomes more passive). The surface electric charge density decreases to ~20-30 mC/cm^{-2}. Stable ferrofluids correspond to less reactive surfaces [25], therefore F.Tourinho is called $Fe(NO_3)_3$ treatment as 'surface stabilisation' procedure.

A change of chemical composition during $Fe(NO_3)_3$ treatment procedure is observed: the content of Fe^{3+} significantly increases, in another words molar ratio $X=[Me^{2+}]/[Me^{2+}+Fe^{3+}]$ falls from the stoichiometric value 0.33 down to 0.25. F.Tourinho reports also the decrease of magnetisation after $Fe(NO_3)_3$ treatment procedure. Formation of superficial nonmagnetic, relatively chemically inactive shell on the ferrite particles after $Fe(NO_3)_3$ treatment is considered [25].

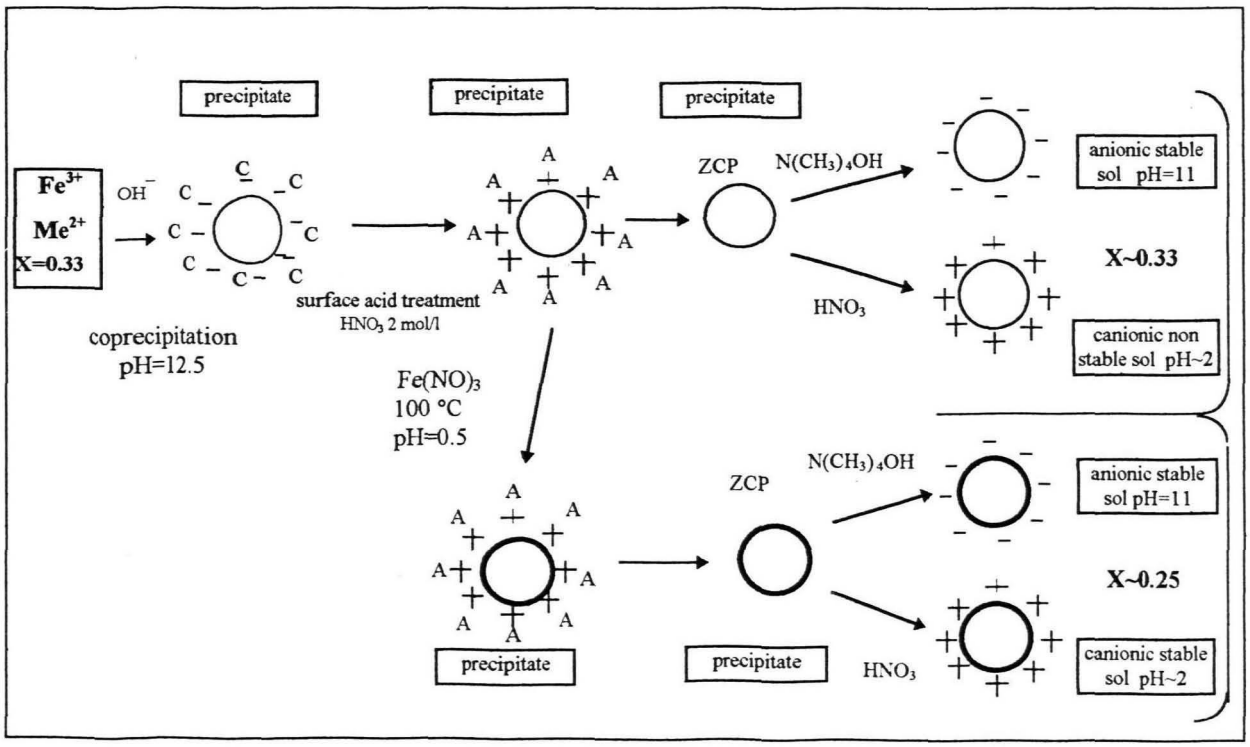

Figure. 1.4.-1. Scheme of preparation of cationic and anionic sols.
ZCP - zero charge point; $A = NO_3^-$; $C = Na^+$, NH_4^+ or $CH_3NH_3^+$ from [24].

After 'the surface treatment' (HNO_3 and subsequent $Fe(NO_3)_3$ treatments) particles are transformed into anionic or cationic sols through ZCP (zero charge point). For anionic sol this stage is not obligate [25]. For anionic ferrofluids their chemical composition is close to that of coprecipitated particles [24]. Anionic sols must be kept under inert (free of CO_2) atmosphere to avoid the neutralisation of TMAOH ($N(CH_3)_4OH$) [25].

1.4.2. Solubilisation of ferrite nanoparticles in nonaqueous medium

In the chapter 1.4.1. synthesis of aqueous ferrofluids is described. It is shown how Mn-Zn ferrite particles of definite size can transferred into a water solution.

These particles can be as well dispersed in a non-polar solution. To do this it is necessary "to surfact" them, in other words surround them with amphiphil molecules [42]. Repulsion between particles is caused by these surfactants and is of steric type. The surface adsorbed layer must have a definite thickness (not less than 1-2 nm), which limits the action of attractive forces between particles.

In ref. [43] the competition between the attractive energies (Van der Waals and magnetic energies) and the energy of steric repulsion between particles versus distance between their surfaces is considered. The diameter of magnetite particles is 10 nm and the surface cover of surfactant is 10^{18} molecules per m^2, and the length of surfactant chain is 2 nm. The resulting summary interaction energy has a potential barrier with height of about 20 kT and a only few particles can overcome it (see Fig. 1.4.-1.). As a result an agglomeration is negligible and particles remain in colloidally stable condition [44].

Surfactants used for steric stabilisation of particles usually consist of polar part (hydrophilic head) and more extended hydrocarbon tail. Oleic acid is one of the most widely used surfactants of this class. It is fat acid with 18 carbon atoms and has the following chemical formula:

$$CH_3\text{-}(CH_2)_7\text{-}CH{=}CH\text{-}(CH_2)_7\text{-}\overset{\overset{O}{\|}}{C}\text{-}OH$$

nonpolar tail polar head

Double bond (=) provides a bend of the hydrocarbon chain at 9th atom of C. This bend is important for creating not densely surfacted layer. The kinetic heat motion of hydrocarbon tail prevents merging of surfactant molecules with each other and formation of the liquid crystal type structure. Stearine acid which has also 18 atoms, but has no double bond does not provide effective surfactation [43, 44].

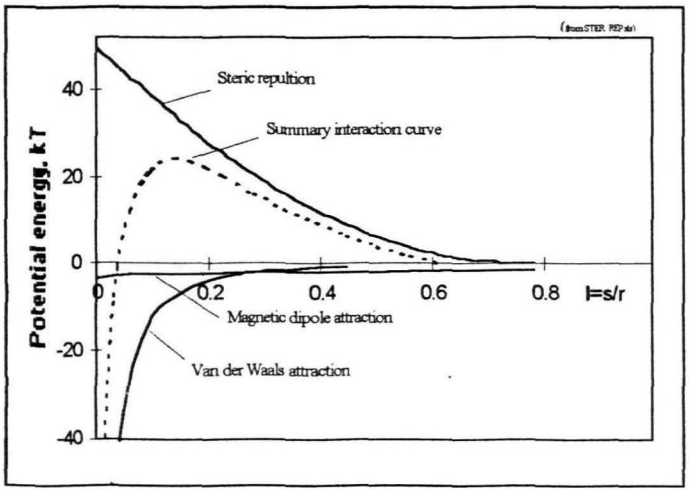

Figure 1.4.-2. Potential interaction energies expressed in number of **kT** for two magnetite particles (diameter 10 nm) surfacted by oleic acid (number of molecules of surfactant on the surface unit - 10^{18} per m^2, l=2 nm) as function of the distance between surfaces of particles (from [43]).

Adsorption isotherm for oleic acid on maghemite particles of 6-7 nm shows linear section to 0.5 g of the adsorbed oleic acid per 1 g of maghemite. Further increase of added oleic acid leads only to slight adsorption of it [45].

Surfactation with oleic acid allows to obtain stable ferrofluid in different non-polar solvents: cyclic hydrocarbons, straight chain hydrocarbons, paraffin oils, etc. [44].

1.5. Purpose and the tasks of the thesis

The survey of the literature on Mn-Zn ferrite particles reveals that synthesis conditions and properties are mostly studied for particles of size higher than 12 nm. However, these particles are too large to form colloidally stable ferrofluids. Therefore detailed studies of smaller nanoparticles are necessary. There are no systematic studies of magnetisation dependence on temperature for Mn-Zn ferrite nanoparticles. Publications on ferrofluids with Mn-Zn ferrite nanoparticles are mostly concerning the applications, but almost do not touch the problem of preparation of these ferrofluids.

On the base of that **the purpose of the present work** is formulated as **investigation of synthesis conditions for Mn-Zn ferrite nanoparticles of size less than 12 nm, study of their physical and chemical properties and preparation of ferrofluids with these particles**. In this context the following tasks are to be solved:

1. To prepare and investigate the properties of Mn-Zn ferrite nanoparticles:
   a) to synthesise Mn-Zn ferrite nanoparticles in the whole range of Zn substitution degree: $0 \le x \le 1$;
   b) to investigate the effect of several synthesis parameters (the type of coprecipitation base, time of heating after coprecipitation) on properties of obtained particles;
   c) to clarify the effect of increasing of Zn substitution degree **x** on properties of obtained particles (especially magnetic parameters);
   d) to study magnetic properties of ferrite nanoparticles in the temperature range of 293-473 K and for samples with higher **x** also at lower temperatures of 100-293 K.
2. To prepare chemically and colloidally stable ferrofluids with Mn-Zn ferrite nanoparticles in aqueous and non-aqueous media:
   a) to prepare cationic water-based ferrofluid and to study changes in properties of nanoparticles arised by preparation procedures;
   b) to prepare surfacted hydrocarbon-based ferrofluid directly from precipitated particles as well as cationic ones. To compare properties of particles in these two ferrofluids.
3. To compare physical and chemical properties of different size particles fractionated from the polydispersed samples.

Chapter 2.

EXPERIMENTAL METHODS FOR CHARACTERISATION OF Mn-Zn FERRITE FINE PARTICLES AND FERRO-FLUIDS

2.1. Chemical analysis

2.1.1. Determination of Fe^{3+} ions concentration

2.1.1.-A. Principle of the method

Fe^{3+} ions are determined by chemical titration, namely by complexion of Fe^{3+} with bi-Na salt of ethylendiamin tetraacetic acid (EDTA) which has following formula:

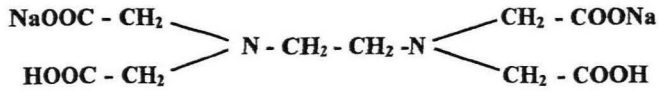

The Fe^{3+} ion forms with EDTA noted as Y^- stable chelate in proportion 1:1 :

$$Fe^{3+} + Y^{4-} = FeY^- \qquad pK=25.1$$

The titration is controlled by indicator, which forms coloured complex with metallic cation. This complex is less stable than that of EDTA. The change of colour with restoration of characteristic colour of free indicator shows that all Fe^{3+} is fixed with EDTA. In general, these indicators are also indicators of pH, therefore it is important that the pH remains constant during titration, it must be fixed with buffer. The EDTA is an agent, which forms complexes with all transition metals. In the titration solution three metallic cations are present: Fe^{3+}, Mn^{2+} and Zn^{2+}. By choosing convenient pH range ($2<pH<3$), it is possible to dose only one of them, namely Fe^{3+}. On the contrary, complexion of Mn^{2+} and Zn^{2+} takes place in the same zone of pH (basic). Therefore, it is not possible to determine these cations selectively by the present method. In acid range of pH complexes EDTA-Mn^{2+} and EDTA-Zn^{2+} are not forming.

Coloured indicator used here is sulfosalicylic acid:

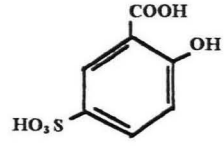

2.1.1.-B. Detailed procedure

0.3 ml (in formula designated as V_{sol}) of titrated solution is taken. 10 ml of concentrated HCl is added (easy destruction of ferrite particles). Solution is brought to boiling under stirring. Having at first orange colour it becomes then bright yellow. Then sodium acetate is added for fixing pH about 2-3 (conditions for optimal observation of the transition). After addition sodium of acetate solution becomes dark-yellow. The volume of the solution is brought to 100 ml with addition of distilled water. An indicator is added: 1 ml of sulfosalicylic acid. The solution becomes wine-coloured. At the end of the titration with 0.05 mol L^{-1} EDTA a colour change to bright yellow takes place. Fe^{3+} ion concentration is determined by following formula:

$$[Fe^{3+}] = \frac{V_{EDTA} \times 0.01}{V_{sol}}$$ Value of $[Fe^{3+}]$ is calculated as mean value of two titrations.

2.1.2. Determination of Mn^{2+} and Zn^{2+} concentration ofby flame spectroscopy

For titration of cations of Mn^{2+} and Zn^{2+} a method of flame spectroscopy by the atomic absorption is applied. Spectrophotometer Perkin-Elmer (series X100) is used.

2.1.2.-A Principle of the method

Emission and adsorption of light are caused by the processes of transition of atoms from one energetic state to another. The most intensive adsorption takes place at a resonance frequencies, which are specific for each chemical element. Conditions of the flame allow to obtain metal elements in the form of dissociated atoms.

Solution of analysed substance is atomised and advanced to the flame of gas in the form of fine droplets, where it is transformed to a vapour state; atoms of the analysed element are absorbing light from a special lamp. Absorption at resonance wavelength is registered by photoelement and then transformed to electrical signal. Absorption is linearly proportional to the concentration of analysed element within a certain concentration range. The extent of absorption is also dependent on the conditions of atomisation, temperature of the flame, etc. Therefore it is necessary to calibrate apparatus with solutions of known concentration for each series of measurements.

2.1.2.-B. Experimental conditions

- the choice of the gas couple oxidant-reductant, which maintains the temperature of flame in a convenient range: here mixture of air and acetylene;
- the choice of the lamp, specific for determined cation: the titrations of Mn^{2+} and Zn^{2+} are carried out with two different lamps.

The measured value is the absorption. Within a certain limits it is connected with concentration by the Beer-Lamber law: $D=\varepsilon\, l\, c$, where c – concentration in [mg l^{-1}];
ε – coefficient of extinction in [l mg^{-1} cm^{-1}];
l – optical length, in [cm].

The resonance wavelengths used are:
for Mn^{2+} λ=279.5 nm;
for Zn^{2+} λ=213.9 nm.

The lower and the upper limits of concentration (sensibility and the limit of linearity), which can be determined by a given technique are following:
for Mn^{2+} : 0.05 – 3 mg l^{-1}; for Zn^{2+} : 0.02 – 1 mg l^{-1}.

Therefore, it is necessary to make a careful dilution of the initial solutions (for concentrated samples up to 10 000 times) to fall within the above mentioned concentration ranges.

The chemical composition of ferrite particles is expressed in a mol % of convential MnO, ZnO and Fe_2O_3. Two molar ratios are also used: the Zn substitution degree x=[Zn]/([Mn]+[Zn]) and the molar ratio X= ([Mn]+[Zn])/([Mn]+[Zn]+[Fe]).

2.2. X-rays powder diffraction

X-rays powder diffraction allows to identify the crystalline structure of obtained particles.

X-rays powder diffraction diagrams are measured on the automatised diffractometer Philips 1130, which uses Co-Kα radiation source with the wavelength λ=1.7902 Å.

Diagrams are measured for powders dried and pounded with a pestle.

Measuring of the X-rays powder diffraction diagrams at the different steps of synthesis allows to control if obtained particles correspond to the ferrite spinel structure, which is identified by the ASTM tables data. The typical X-rays powder diffraction diagram for Mn-Zn ferrite fine particles powder (initial proportion Mn0.5/Zn0.5/Fe2.0) is shown on Fig.2-1. Widening of peaks is related to a size of crystallites . A particles mean diameter is determined from the measurements of the widening at half height through the Scherrer formula:

$$D_{XR} = \frac{0.9 \times \lambda}{\Delta\Theta \times \cos\Theta}$$

where $\Delta\Theta$ is the half-height width of the line in radian in a 2Θ scale, Θ – the Bragg angle; λ - radiation wavelength.

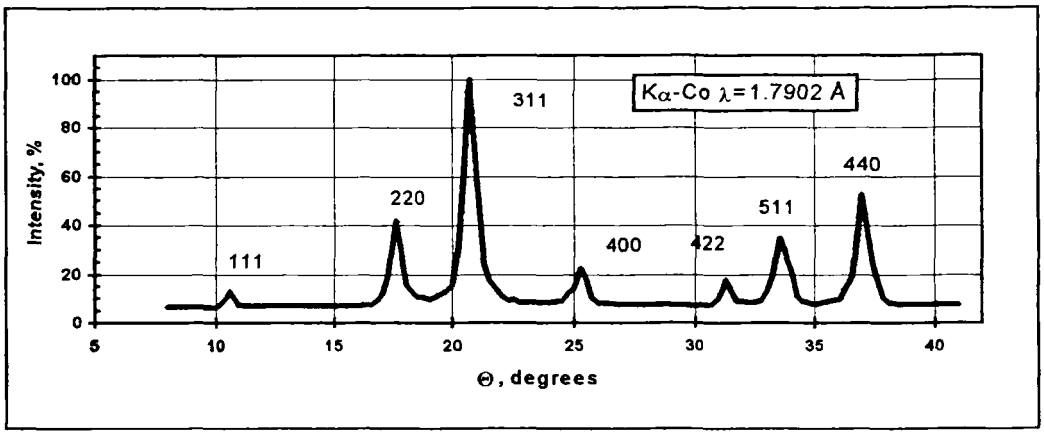

Figure 2.-1. Roethgen diffraction powder diagram for Mn-Zn ferrite spinel type fine particles.

From the experimental values of Θ it is possible to calculate values of **d** – distances between atomic planes using the relation of Bragg: $2\mathbf{d} \times \sin\Theta = \mathbf{n}\lambda$

Experimentally determined values of **d** for above mentioned sample, as well as values taken from the ASTM tables for the bulk Mn and Zn ferrites are shown in Tab. 2.-1.

Table 2.-1. Values of interatomic plane distances **d** and corresponding intensities for Mn-Zn ferrite fine particle powder and for the bulk Mn and Zn ferrites as well as for synthesised Mn-Zn ferrite particles.

Experimental		ASTM 10-319 $MnFe_2O_4$			ASTM 22-1012 $ZnFe_2O_4$		
d (Å)	I/I_{max}, %	d (Å)	I/I_{max}, %	hkl	d (Å)	I/I_{max}, %	hkl
4.843	7	4.906	20	111	4.873	7	111
2.968	38	3.005	35	220	2.984	35	220
2.534	100	2.563	100	311	2.543	100	311
2.101	16.5	2.124	25	400	2.109	17	400
1.718	11	1.734	20	422	1.723	12	422
1.624	30.5	1.636	35	511	1.624	30	511
1.491	48	1.503	40	440	1.491	35	440
–	–	1.296	20	533	1.287	9	533
–	–	1.106	30	731	1.099	11	553
–	–	0.982	20	555	–	–	–

2.3. Infra-red (IR) absorption spectroscopy

IR absorption spectroscopy allows to identify the spinel structure as well as a presence of certain types of chemical substances adsorbed on the surface of particles.

IR spectra of dried samples are recorded on the Bio-Rad IR computerised spectrophotometer in waverange of 4000 - 200 cm^{-1}. Preparation of samples included a dilution with KBr powder (highly transparent substance in IR range) and a subsequent formation of pellet. For the majority of samples the following proportion is taken: 10 mg powder /300 mg KBr. Both substanses are mixed and pounded with a pestle. Then a thin pellet is formed under a special press.

In the IR spectra of hydrated oxids the following vibrations, with a corresponding (approximate) wavenumber are possible [46]:

(1) $O \Longleftrightarrow H$ stretching vibration 3400 cm^{-1}

(2) 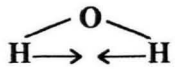 bending vibration 1600 cm^{-1}

(3) 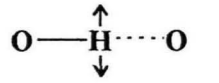 bending vibration 900-1000 cm^{-1}

(4) $Me_T — \overset{\longleftrightarrow}{O} — Me_O$ stretching vibration 600-550 cm^{-1}

(5) $Me_O \Longleftrightarrow O$ stretching vibration 450 -385 cm^{-1}

(6) $Me_T \Longleftrightarrow Me_O$ stretching vibration 350-330 cm^{-1}

where **O** is oxygen, **H** - hydrogen, Me_O is metal in the octaedric site and Me_T -in the tetraedric site.

The OH stretching vibration (1) causes a strong absorption band at about 3400 cm^{-1}. The bending vibration (2) at about 1600 cm^{-1}, typical of the H_2O molecule, is less intensive. The third absorption band (3) is due to the OH deformation vibration. For strong hydrogen bridges its maximum lies at about 900-1000 cm^{-1}. These first three bands indicate the presence of free and crystalline associated water. The metal-oxygen absorption bands (4) and (5) are characteristically pronounced for all spinel structures and for ferrites in particular. The band (6) is less intensive than bands (4) and (5), sometimes it merges with the band (5) and gives one wide band at 420-330 cm^{-1} [47].

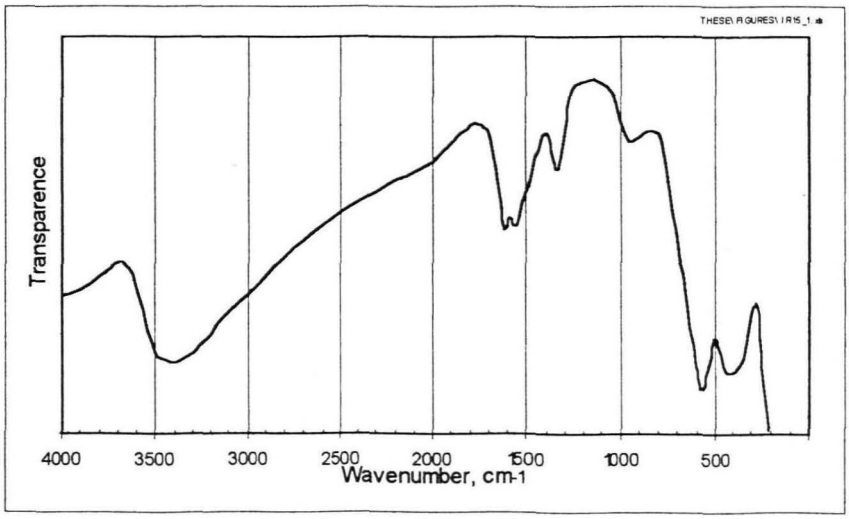

Figure 2.-2. Typical IR-absorption spectra for Mn-Zn ferrite nanoparticles.

Comparing the IR-spectra of samples at a different steps of synthesis as well as with high temperature treated Mn-Zn ferrite allows to see the product structure transformations.

2.4. Determination of associated water content in particles by the thermogravimetry and by the calculation from metal content

The associated water content is estimated independently by the thermogravimetry and by the calculation from metal content.

Samples are previously washed with acetone and ether and then dried at room temperature. Thermogravimetrical (TG) measurements are performed using a Perkin-Elmer TG-Analyser up to 750 °C in an inert gas (nitrogen) atmosphere. The TG heating rate is 5-10 °C/mn. Weight loss of the sample in the process of the heating is registered. The difference in weight measured at 750 °C and 20 °C is considered as an estimate of the content of water retained in the particles.

Estimation of water content by calculation is made in the assumption that the chemical composition of particles may be described by the following formula $\{(Mn_aZn_bO_{a+b})(Fe_cO_{3c/2})\}(nH_2O)$, where a+b+c=3, and thus the mass attributed to oxygen may be calculated knowing the content of metals from the chemical analysis. Comparing the mass of ferrite corresponding to the part of formula in { } with directly measured weight of powder gives the difference which may be attributed to the quantity of associated water.

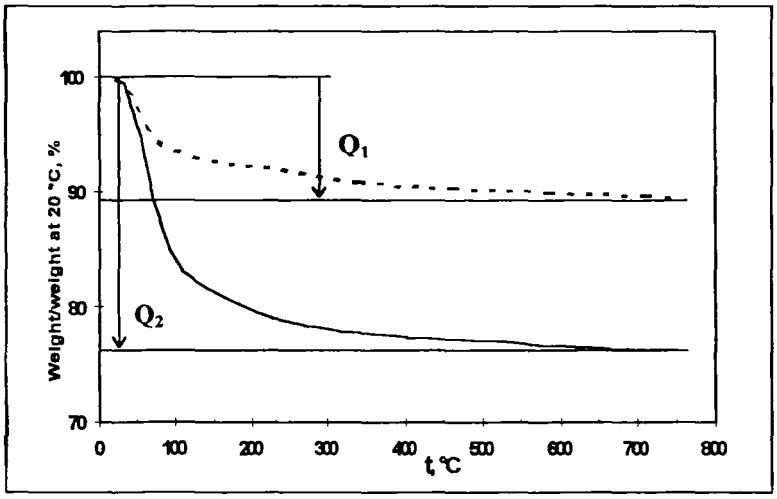

Figure 2.-3. Thermogravimetrical curves (weight related to the initial weight at 20 °C versus temperature) for Mn-Zn ferrite nanoparticles. Arrows correspond to weight difference attributed to assoociated water content Q.

2.5. Electronic microscopy

The mean size of particles for some samples is determined electronic microscopy.

Glass plates photographs of nanoparticles are obtained by the Electronic Microscope JEOL 100 CX2. The microscope allowed to obtain the magnification up to 120 000 - 230 000 times. Samples are prepared from dried powders obtained by drying of precipitates or directly from the cationic ferrofluids.

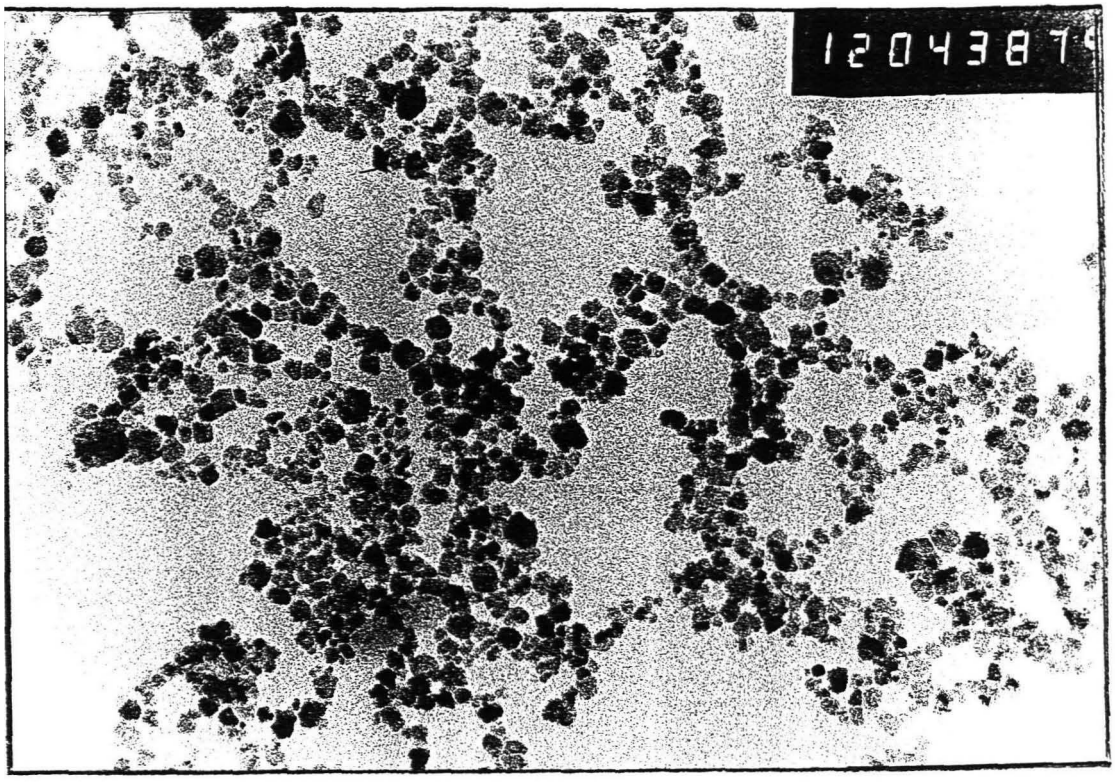

Figure 2.-4. Picture of electronic microscopy of Mn-Zn ferrite nanoparticles.

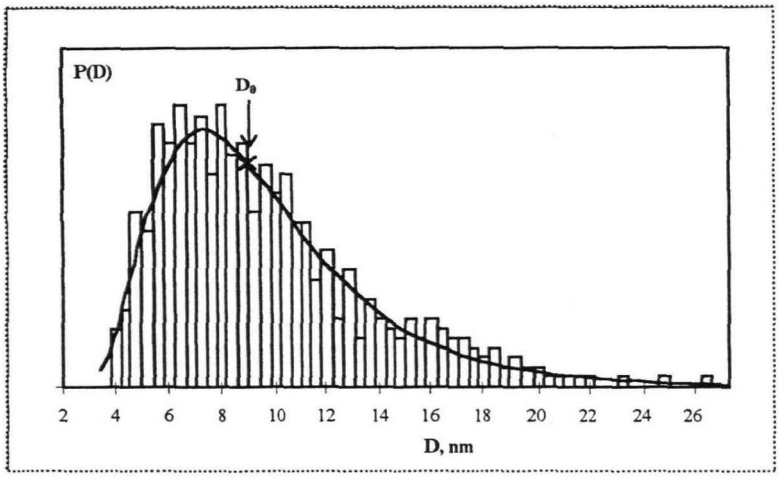

Figure 2.-5. Particles size histogram and a corresponding log-normal distribution curve for Mn-Zn ferrite nanoparticles from cationic ferrofluid obtained from electronic microscopy photograph.

Powders are dispesed by the ultrasound in distilled water or in the organic solvents as acetone or cyclohexane. Then the dispersion is deposed on carbon membrane and dried. Usually 5 pictures from different parties of samples are taken.

Cationic ferrofluid is diluted with distilled water and deposed directly on the carbon membrane. Photographs on paper are made from glass plates with the magnification of 3 times. The particles mean sizes are determined from measuring of 500 particles by the light microscope with eyepiece build-in scale. All samples are strongly polydispersed. Their size histograms are approximated with the log-normal distributions with probability function: $p(D) = \frac{1}{\sqrt{2\pi}\cdot\sigma_D\cdot D_0}\cdot e^{-\ln^2(D/D_0)/2\sigma_D^2}$, where

p(D)ΔD represent the part of all particles with size in the interval from **D** to **D+ΔD**; **lnD₀** is the mean value for **lnD** distribution; σ_D - the standard deviation. **D₀** does not coincides with the maximum of **p(D)**, which corresponds to $D_0 e^{-\sigma^2}$.

Further in the text the size D_0 is called "mean" and signified as D_{EM}.
For some samples the lower and the upper size limits are also estimated.

2.6. Magnetic measurements and processing of magnetisation curves

2.6.1. Measuring of magnetisation curves

The magnetisation curves are measured on the automatised vibrating sample magnetometers (AVSM).

The principal block-scheme of AVSM at Institute of Physics of LU in Salaspils is shown in Fig. 2-6. Measurements in magnetic fields up to 20 kOe in temperature range from ambient temperature up to 473 K (200 °C) are made on this AVSM.

The action of AVSM is based on a measuring of the magnetic field of sample (1) oscillating in a uniform magnetic field. Oscillations of magnitude ~0.2 mm at frequency 71 Hz are produced by a special vibrator (2). The uniform field is produced by a powerful electromagnet (3), which supply block (4) is controlled by the computer (5) via CAMAC interface (6). Uniform magnetic field is measured by the Hall gauge (7).

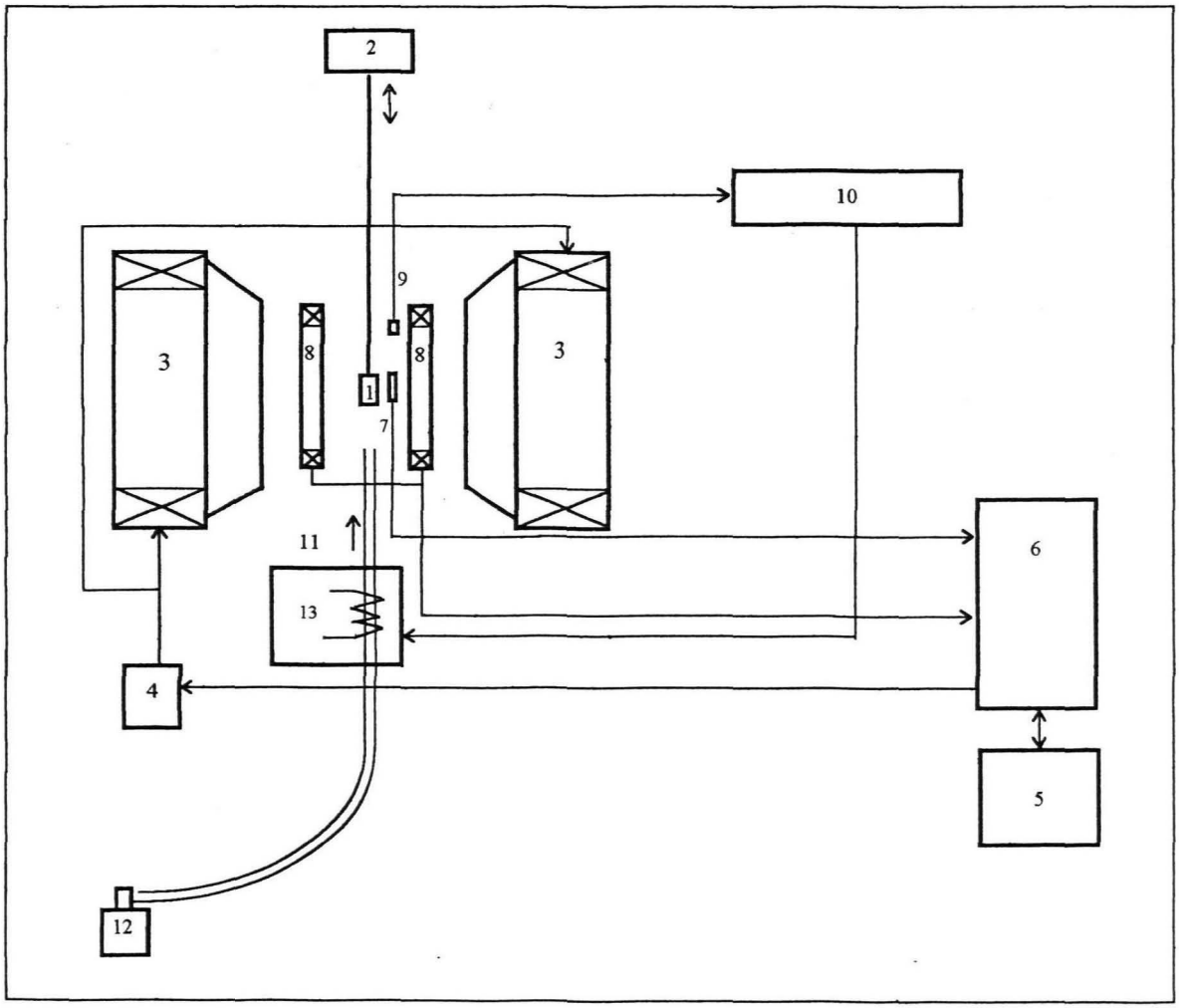

Figure 2.- 6. The principal block scheme of automatised vibrating magnetometer (AVSM) in Institute of physics in Salaspils.

Signal from a measuring coils (8) is amplified and through CAMAC interface transferred to the computer. Temperature is measured by a temperature gauge (9) and regulated by a temperature controller (10). Heating of the measuring chamber is realised by blowing through an inert gas (argon, nitrogen, CO_2) (11, 12) heated by a special thermostat (13). Liquid samples are capsuled in the spherical 4 mm small glass vessel, but powder ones in a 3 mm cylindrical tubes from aluminium folio.

2.6.2. The distributions (spectra) of magnetic moments

It is assumed that the particles are non-interacting single-domain polydispersed ones. Magnetization curve is approximated by a sum of Langevin functions to obtain the spectrum of magnetic moments, which characterise the orientation processes of the magnetization of mono-domain particles:

$$\mathbf{M(H) = \sum_{i}^{N} n_i m_i L(m_i H/ kT)}$$

Here μ_i are the fixed parameters - the values of magnetic moments, n_i are the calculated parameters- the weights of μ_i. The parameters n_i are calculated by the variation method of regularisation described in [48]. N value is taken 40. Magnetic moments μ_i are taken in a logarithmic order and cover a wide range from a very weak values (10^{-18} emu) to the strong ones (10^{-14} emu).

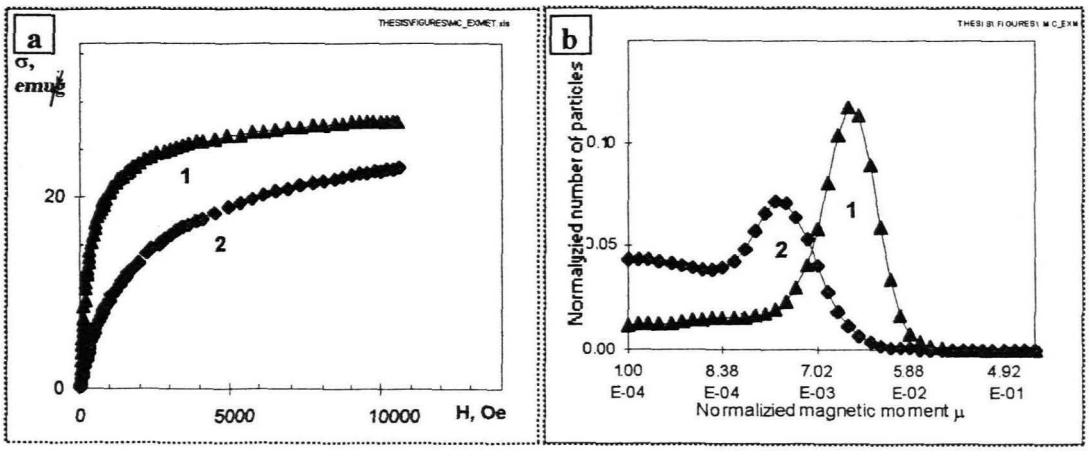

Figure 2.-7. Magnetisation curves (a) for Mn-Zn ferrite cationic ferrofluids with a different Zn substitution degree **x** (1 - **x**=0.24; 2 - **x**=0.62) and a corresponding spectra of magnetic moments (b).

Chapter 3.

FORMATION AND PROPERTIES OF Mn-Zn FERRITE FINE PARTICLES

Introduction

Ultrafine manganese-zinc ferrite particles (6-11 nm) are obtained by *the chemical coprecipitation and the ferritisation*. These are two sequential processes: the proper coprecipitation of metal salts into hydroxides in alkaline medium, which occurs immediately, and the transformation of hydroxides into ferrite which starts at the coprecipitation moment but requires a certain time and usually occurs when the precipitate phase is heated. To prevent the particle growth and to keep the surface of particles able for later adsorption of ions or surfactants, coprecipitated particles are heated in an aqueous alkaline medium (in a mature precipitation solution).

Samples after coprecipitation and ferritization are further named *'coprecipitated and heated'* or *'non treated'* in comparison with the surface treated ones (see chapter 4).

In this chapter the influence of the type of coprecipitation base, the Zn substitution degree **x** and some other synthesis parameters on the properties of particles, such as mean size, content of associated water, chemical composition and magnetisation is studied.

3.1. Synthesis of Mn-Zn ferrite fine particles

3.1.1. Initial parameters of synthesis. Fixed parameters

Coprecipitation is performed in the aqueous solutions of $MnCl_2$, $ZnCl_2$ and $FeCl_3$ mixtures in alkaline medium. The initial molar proportion ([Mn]+[Zn])/[Fe] is always taken as the stoichiometric 1/2. The initial concentration of salts is taken of 0.1-0.2 $mol \cdot L^{-1}$ of the total metal content Me ([Me]=[Fe]+[Mn]+[Zn]).

Three different bases are taken as the coprecipitating agents: sodium hydroxide (NaOH), methylamine (CH_3NH_3OH) and ammonia (NH_4OH). Formation of Mn-Zn ferrite occurs at the elevated temperatures. For coprecipitation with NaOH temperatures of 95-100°C are taken. For CH_3NH_3OH and NH_4OH the reaction temperatures do not exceed 90°C and 60°C respectively due to high evaporation of these bases.

In the case of NaOH, the concentration of the base is ~0.4 $mol \cdot L^{-1}$. It provides pH=12.5-13 after coprecipitation, whereas for two other bases (CH_3NH_3OH and NH_4OH) the concentration is 0.8 - 1 mol/l and a pH after coprecipitation is 10.5-11 and 9.5 respectively.

For majority of samples the reaction time (time of heating in an alkaline medium after coprecipitation) is fixed: for NaOH as 40 min, for CH_3NH_3OH and NH_4OH as 30 min and 10 min respectively. For samples coprecipitated by NaOH a special study of the heating time upon their properties is carried out (see 3.1.2.-B).

The reaction volume is ussually 2 liters.

3.1.2. Influence of some synthesis parameters on the properties of Mn-Zn ferrite particles

3.1.2.-A Influence of the type of coprecipitation base on the properties of Mn-Zn ferrite particles

The nature of the coprecipitating base has a significant influence on a size of obtained ferrite particles. For Mn ferrite it was shown earlier that three bases give particles with size diminishing in the following sequence: $D_{(NaOH)}>D_{(CH_3NH_3OH)}>D_{(NH_4OH)}$. Results presented here confirm this observation for Mn ferrite and allow to spread it on Mn-Zn ferrite. The relationship of acting of the above mentioned bases to the size of Mn-Zn ferrite particles is the same: reductant (see Table 3.2.-1. and scheme on Fig. 3.2.-1.). Mn ferrite particles coprecipitated by NaOH, CH_3NH_3OH and NH_4OH have the mean sizes of 19, 10 and 6 nm respectively. $Mn_{0.5}Zn_{0.5}$ ferrite particles obtained by NaOH and CH_3NH_3OH have the mean sizes 8.6 and 7 nm respectively.

Coprecipitation by NaOH leads to formation of ferrite in all range of the initial Zn substitution degree x_0 from ferrite of Mn (x_0=0) up to ferrite of Zn (x_0=1) (see Table 3.2.-1. and Fig. 3.2.-1.). For CH_3NH_3OH and NH_4OH formation of ferrite takes place only within a limited range of x_0. When the initial Zn substitution degree x_0 exceeds a certain threshold value (x_0~0.6 for CH_3NH_3OH and x_0~0.2 for NH_4OH), a nonmagnetic roentgenamorphous product is obtained (see Fig. 3.2.-1). This may be due to a complexation of Zn^{2+} and partly Mn^{2+} with NH_4OH and CH_3NH_3OH. Samples obtained in conditions of the edge of ferrite formation zone (for example sample D2: x_0=0.5 coprecipitated with CH_3NH_3OH) demonstrate lower resistance to acid attack at HNO_3 treatment step in preparation of cationic ferrofluid (see 4.1.1. Surface treatment procedures.).

Table 3.1.-1. Mean sizes D_{XR} (obtained by the Scherrer formula from X-ray powder diffraction) for particles obtained at different Zn substitution degree x_0.

Initial Zn substitution degree x_0	Coprecipitating base					
	NaOH		CH_3NH_3OH		NH_4OH	
	Name of sample	D_{XR}, nm	Name of sample	D_{RX}, nm	Name of sample	D_{XR}, nm
0.0	A1	18.8	A2	9.9	A3	6.0
0.2	B1	11.4	B2	7.6		
0.4	C1	9.4			r.a	
0.5	D1	8.6	D2	7.0	r.a	
0.6	E1	7.3			r.a	
0.8	G1	6.6	r.a		**r.a**	
1.0	J1	6.2	r.a		r.a	

r.a. - renthgenoamorphous

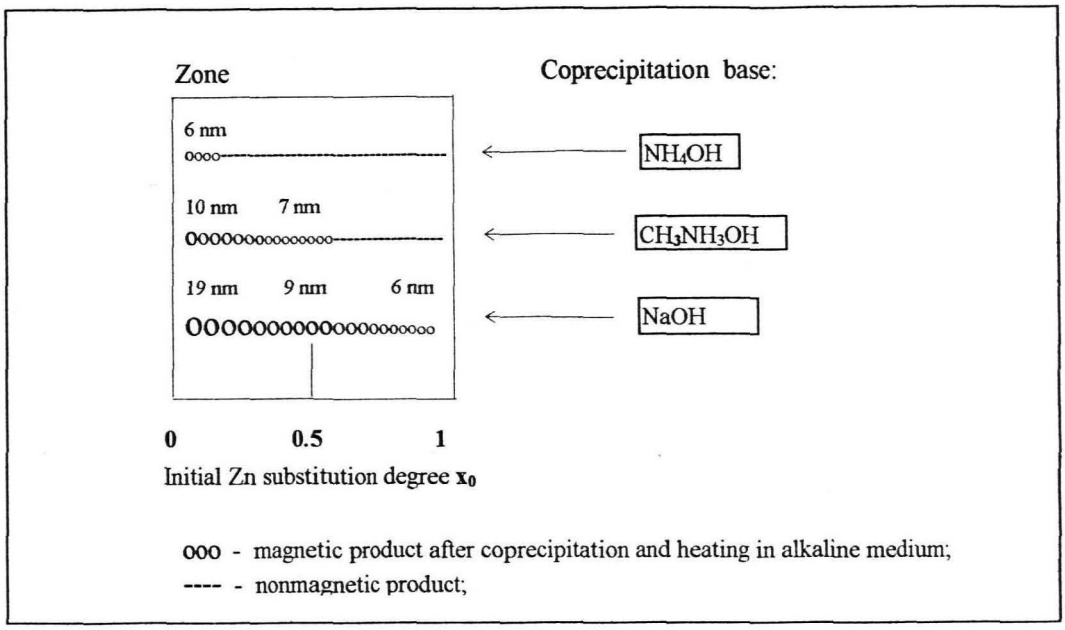

Figure 3.1.-1. Zones of initial Zn substitution degree x_0 for obtaining ferrite particles with three different coprecipitation bases: NaOH, CH_3NH_3OH and NH_4OH. Size of circles corresponds to mean size of particles, determined by Scherrer formula from X-rays diffraction.

The chemical composition of samples obtained by NaOH and CH_3NH_3OH is summarised in Tab. 3.1.-2. It can be seen that the chemical composition of particles is rather close to the initial one in the initial reagent mixture. Some minor deviations are observed: for almost all samples a slight excess of Fe and a slight deficit of Zn content in respect to the initial stoichiometric proportion is found. A little more pronounced deficit in Zn is found in samples precipitated by CH_3NH_3OH (samples B2 and D2).

Table 3.1.-2. Chemical composition of samples obtained by the precipitation with NaOH and CH_3NH_3OH

Initial Zn substitution degree x_0	Name of sample	Chemical composition of particles after coprecipitation and heating				
		MnO mol%	ZnO mol%	Fe_2O_3 mol%	Molar ratio **X**	Zn substitution degree **x**
0.2	B1	39.0	10.0	51.0	0.32	0.20
0.4	C1	29.5	19.5	51.0	0.32	0.40
0.5	D1	24.5	22.0	53.5	0.30	0.47
0.6	E1	20.0	27.5	52.5	0.31	0.58
0.8	G1	10.5	37.5	52.0	0.32	0.78
1.0	J1	0.0	48.9	51.1	0.32	1.00
0.0	A2	50.9	0.0	49.1	0.34	0.00
0.2	B2	41.2	7.7	51.1	0.32	0.16
0.5	D2	26.1	22.3	51.6	0.32	0.46

3.1.2.-B Time of heating of particles in alkaline solution

For particles coprecipitated with NaOH the process of ferrite formation takes place at temperatures close to 100 °C and requires a certain time. Influence of the heating time of coprecipitated particles (at initial proportion of $Mn_{0.5}/Zn_{0.5}/Fe_{2.0}$) on their properties is studied. Namely, the chemical composition, the particles mean size and the associated water content are determined. The chemical composition of the sample remains approximately the same for all times of heating and is close to the initial proportion (see Tab. 3.1.-3.). In the particles heated for 1 min content of Fe is slightly increased in comparison with those heated for 20-90 min.

X-rays powder diffraction diagrams for 1 min., 20 min. and 90 min. boiled samples are shown on Fig. 3.1-2. Particles after 1 min. of boiling show only hardly pronounsed wide peaks of spinel structure, whereas after 20 min. of boiling these peaks become well pronounced. Further boiling up to 90 min. leads to more narrow width of peaks at their foot, but does not change their width at half-height, which is related to the mean size of particles. The mean sizes $\mathbf{D_{XR}}$, obtained from X-rays powder diffraction and the size limits estimations $\mathbf{D_{EM}}$ made from electronic microscopy pictures show that a significant growth of particle size occurs in the first 20 min.

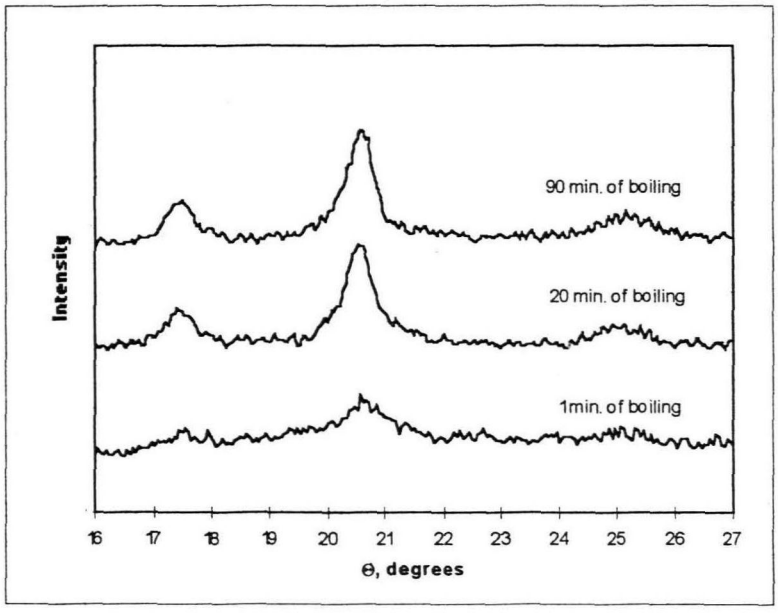

Figure 3.1.-2. X-rays spectra of the coprecipitated particles boiled for different times.

Table 3.1.-3. Properties of coprecipitated particles, heated in alkaline coprecipitation solution for different time: mean size from X-rays powder diffraction $\mathbf{D_{XR}}$, size limits from electronic microscopy $\mathbf{D_{EM}}$, chemical composition and associated water content **Q**.

Time of heating, min	Chemical composition, mol%			Content of associated water **Q**, w%		Particles mean size	
	MnO	ZnO	Fe_2O_3	Calculated	TG** 750 °C	$\mathbf{D_{XR}}$, nm	$\mathbf{D_{EM}}$, nm
1	23.3	22.2	54.5	22.0	23.7	4.9	2.0-2.5
20	24	23.3	52.7	9.8	10.3	9.0	-
40	23.1	23.3	53.6	11.8	11.5	8.2	3.0-10.0
90	24	23.3	52.6	12.5	10.4	8.6	5.0-10.0

* Additional peaks corresponding to hydroxide of Fe are present.

** Thermogravimetry with the upper temperature 750 °C.

For coprecipitated particles heated for 1 min the associated water content determined by the thermogravimetry is about 24 w % and calculation gives 22 w%, while heating already for 20 min decreases the water content to 10 w % (see Tab. 3.1.-3. and Fig. 3.1.-3.). Further heating up to 90 min does not lead to decrease of the associated water content.

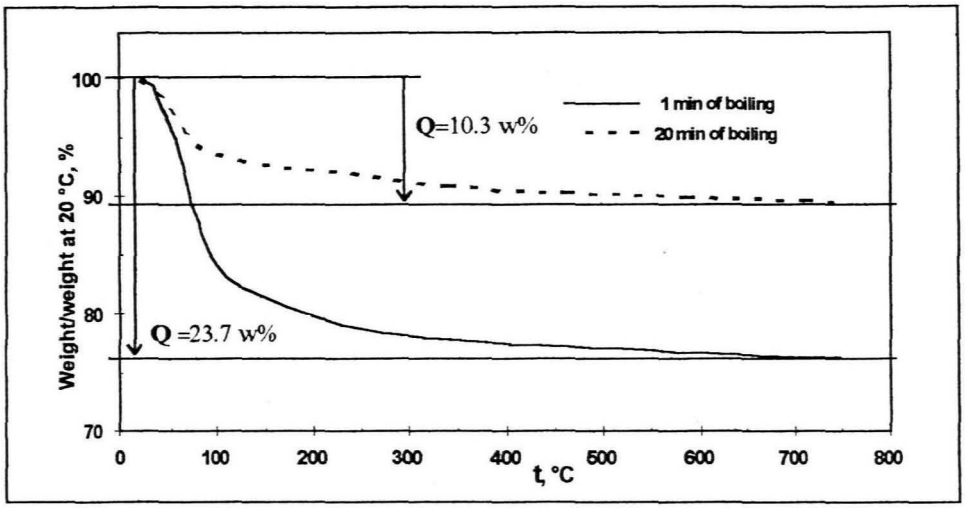

Figure 3.1.-3. Thermogravimetrical curves (relative weight related to initial weight at 20 °C versus temperature) for coprecipitated samples heated at 100°C in mature precipitation solution for different time. Content of associated water **Q** in particles is attributed to the lost weight at 750°C and is shown by arrows.

The IR spectroscopy allows to follow qualitatively the process of the ferrite formation and leaving of associated water from particles. The IR-spectra of coprecipitated samples boiled for 1 min and 20 min are shown on Figure 3.1.-4. Sample after 1 min boiling fails to demonstrate very intensive absorption wavebands at 580 and 460 cm^{-1}, which correspond to metal-oxygen bonds and are considered as confirmation of the existence of ferrite. After 20 min of heating these wavebands become much more intense, while adsorption at 3400-3440 cm^{-1}, which corresponds to the associated water decreases. Adsorption at 1490 cm^{-1} shifts to higher wavenumbers reaching a maximum at 1560 cm^{-1}.

It is remarkable that if coprecipitated sample is heated at high temperature (at ~900°C) in an inert gas atmosphere, absorption wavebands of 3430 cm^{-1} and 1640-1380 cm^{-1} disappear and only ones at 580 and 460 cm^{-1} remain. This means that associated water completely quits from ferrite particles.

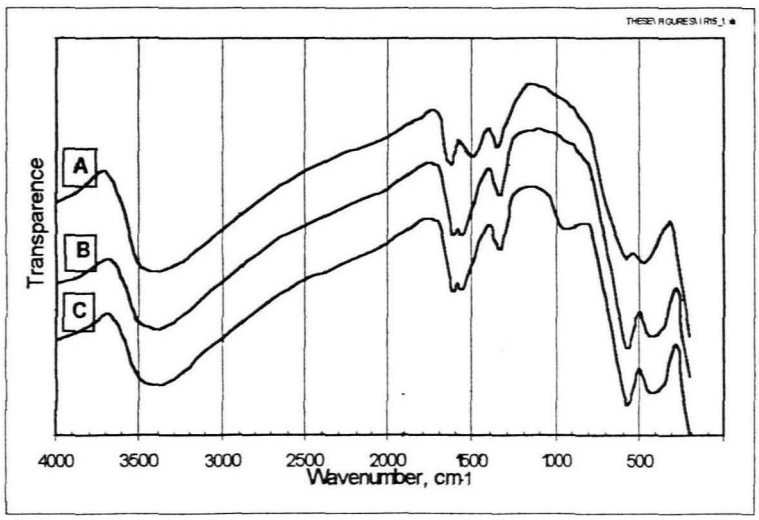

Figure 3.1.-4. IR-spectra of coprecipitated samples heated in an alkaline solution for different time: (A) - for 1 min., (B) - 20 min., (C) - 90 min.

Thus, the peculiarity of Mn-Zn ferrite particles, obtained by the chemical coprecipitation method is that they contain ~10-12 w % of the associated water even after 90 min of heating in alkaline medium.

3.1.3. Experimental operation protocol for preparation of Mn-Zn ferrite particles

On the basis of studied synthesis parameters the optimal operation protocol for preparation of Mn-Zn ferrite particles is developed. All data are given for total reaction volume of 2 liters.

Initial solutions:

Solution A-1 is prepared by mixing of :

160 ml $FeCl_3$ of 1 $mol \cdot L^{-1}$, $(80-q_0)$ ml $MnCl_2$ of 1 $mol \cdot L^{-1}$ and q_0 ml $ZnCl_2$ 1 $mol \cdot L^{-1}$, where $0 \le q_0 \le 80$; $q_0 = 80 \cdot x_0$.

Solution A-2 is prepared by dilution of *solution A-1* in 1770 ml of distilled water, addition of 10 ml concentrated HCl and heating to boiling.

Solution B-1: 70 ml of 10 $mol \cdot L^{-1}$ NaOH is diluted in 1750 ml of distilled water to a concentration of 0.37 mol/l and heated to boiling.

Solution B-2: 128 ml of 13 $mol \cdot L^{-1}$ (40%) CH_3NH_3OH water solution.

Procedure:

1. Step of coprecipitation:
   a) for NaOH:
   Solution A-1 is poured as quickly as possible into a boiling *solution B-1* under vigorous stirring produced by the glass mechanical stirrer (~500 r/min). After coprecipitation pH is 12.5-13.
   b) for CH_3NH_3OH (the order of reagents mixing is opposite):
   Solution B-2 is poured into *solution A-2*. pH after coprecipitation is 10.5-11.
2. Step of heating:
   The reaction vessel is covered with a plastic cover to to diminish evaporation of solution. The reaction is continued for 30-40 min at temperature 90-100 °C under vigorous stirring.
3. Step of washing:
   The reacting vessel is cooled to the ambient temperature and particles precipitate.
   The total volume is reduced to ~500 ml by aspiration of supernatant.
   The suspension is centrifuged in 4 beakers at 7000 rpm for 10 min.
   The precipitate is washed with distilled water of ~900 ml and centrifuged once more at the same parameters.

3.2 Influence of Zn substitution degree on physical and chemical properties of Mn-Zn ferrite particles

Different compositions $(1-x_0)$Mn / x_0Zn / 2.0 Fe within the stoichiometric ferrite proportion, where x_0 is 0; 0.2; 0.4; 0.5; 0.6; 0.8; 1.0 are taken for the initial mixtures of metal salts.

3.2.1. Influence of Zn substitution degree on the size of particles

It is found that for the same other conditions increasing of the Zn substitution degree x_0 leads to the formation of particles of smaller sizes. Mean sizes of particles obtained from the X-ray powder diffraction peak enlargement are summarized in Table 3.1.-1 and in Figure 3.2.-1. This tendency occurs both for samples coprecipitated with NaOH and CH_3NH_3OH .

The most strong decrease in size is observed for small values of x_0: 0-0.2. For particles obtained with NaOH the mean size in this range decreases from 18.7 to 11.4 nm and for CH_3NH_3OH from 9.9 nm to 6.8 nm. The mean size of particles for x_0 growing from 0 to 1 in the case of NaOH decreases approximately 3 times.

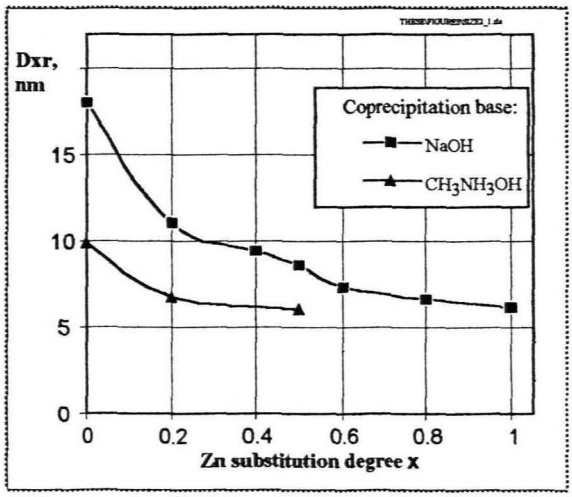

Figure 3.2.-1. Mean sizes of coprecipitated particles D_{XR} (determined by the Sherrer formula from X-ray powder diffraction) for samples with different Zn substitution degree **x**.

3.2.2. Influence of Zn substitution degree on the content of associated water

Changing of Zn substitution degree **x** acts significantly on the associated water content **Q**. Data for samples coprecipitated by NaOH and CH_3NH_3OH and heated for 40 and 30 min respectively, are summarized in Table 3.2.-1. Results from thermogravimetry and calculation are in agreement with each other and show a significant enhancing of **Q** in particles with the increasing of the Zn substitution degree **x**. In the case of NaOH **Q** grows from 3.4-6.0 w% for ferrite of Mn up to 14 w% for Zn ferrite. This effect may be connected with the higher affinity of the remaining hydroxide of Zn to water. Particle size diminishing (and correspondent surface role increase) with the increasing of Zn initial substitution degree **x** must also be taken into account.

Table 3.2.-1. The associated water content **Q** in particles coprecipitated and heated in alkaline solution. Data for samples with a different Zn substitution degree **x** coprecipitated with a two different bases NaOH or CH_3NH_3OH are presented. Water content is determined by the thermogravimetry (TG) and by the calculation from metals content

Name of sample	Coprecipitation base	Zn substitution degree **x**	Mean size of particles D_{XR}, nm	Content of associated water **Q**, w %	
				TG	Calculation
A11	NaOH	0	23.5	3.4	6.0
C1	NaOH	0.40	9.4	4.5	5.6
D1	NaOH	0.47	8.6	9.5	10.0
E1	NaOH	0.58	7.3	10.1	10.6
G1	NaOH	0.78	6.6	12.0	12.7
J1	NaOH	1.0	6.2	13.6	n.d.
A2	CH_3NH_3OH	0.0	9.9	6.0	6.5
D2	CH_3NH_3OH	0.47	6.0	10.0	13.9

n.d. - not determined

3.2.3. Influence of Zn substitution degree on magnetic properties

Introduction

The magnetic properties of Mn-Zn ferrite particles (magnetisation σ, parameter i_m, thermomagnetic coefficient k_T) are strongly dependent on the Zn substitution degree **x**. The initial Zn substitution degrees x_0 are varied in the range of 0.2-1.0. As coprecipitation with NaOH gives particles in the whole range of $0 \leq x \leq 1$, the magnetic properties of samples obtained with this base are studied.

Samples coprecipitated with NaOH and heated in alkaline solution for 40 min are then dried at the room temperature and grinded. Magnetisation curves are measured at different temperatures in the range of 293-473 K and for samples with **x**=0.58 and 0.78 also at lower temperatures down to 100 K.

3.2.3.-A. Magnetic properties at the room temperature

Magnetisation curves for samples with different **x** measured at the room temperature are shown in Fig. 3.2.-2.(a). The same magnetisation curves with the H-axis in log scale plotted on 3.2.2 -2(b) allow better observe initial (low field) parts. It can be seen that increasing of **x** from 0.2 to 0.5 leads to a more sloping shape of magnetisation curve. In a low and medium magnetic fields (H<7.5 kOe) magnetisation of sample with **x**=0.2 is higher than that of sample with **x**=0.5, whereas in high fields (H>7.5 kOe) situation is opposite (see also Figure 3.2.-2. (a)).

The magnetisation curve for Zn ferrite practically concise with that for **x**=0.8 and is not shown on the figures.

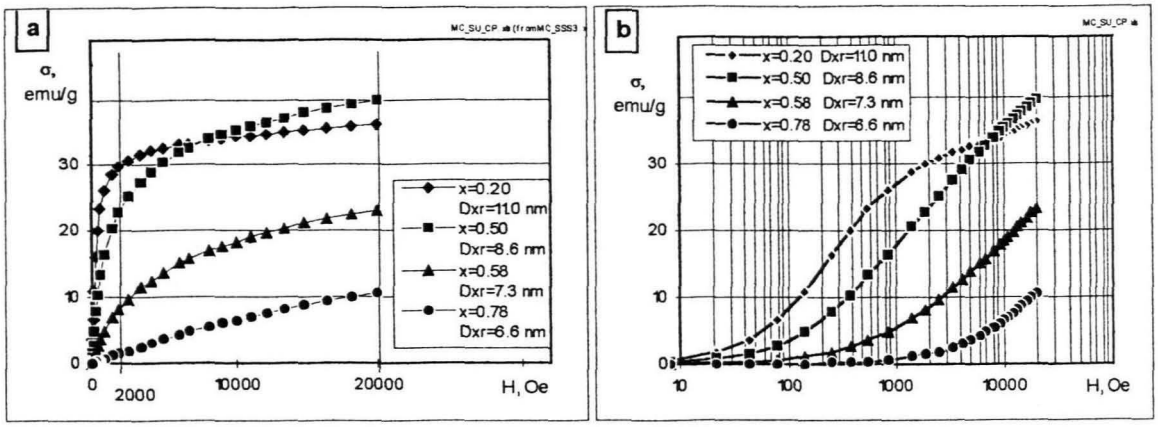

Figure 3.2.-2. Magnetisation curves for samples with different Zn substitution degree **x**: (a)- abscise axe normal; (b)- abscise axe logarithmic.

Magnetisation of samples versus Zn substitution degree **x** is shown on Figure 3.2.-3. (a). The magnetisation in magnetic field of two different intensities is taken: σ_{2000} in **H**=2 kOe and σ_m in $\mathbf{H_m}$=20 kOe. When **x** increases from 0.5 to 0.58 a dramatic fall of magnetisation is observed. For σ_m this fall is 1.7 times and for σ_{2000} it reaches 3 times. Further growing of **x** from 0.58 to 0.78 leads to a continued decrease of magnetisation (not so strong). For samples with **x**=0.78-1.0 σ_m is only 10-11 emu/g and σ_{2000} is very small ~1.8 emu/g. Growing of **x** from 0.78 up to 1.0 (Zn ferrite) does not lead to the further decrease of magnetisation to zero as occurs for the bulk ferrites, but keeps it at the same constant level. The chemical composition of obtained Zn ferrite sample is close to the stoichiometric. For the bulk stoichiometric $ZnFeO_4$ antiferromagnetic (non magnetic) behaviour at the room temperatures is known [1, 2].

The shape of magnetisation curve undergoes changes with **x** growing as well. To characterise evolution of the shape with **x** growing, the parameter $\mathbf{i_m}=\sigma_{2000}/\sigma_m$ is calculated and dependence $\mathbf{i_m(x)}$ is plotted on Figure 3.2.-3.(b). For **x** growing from 0.2 to 0.5 $\mathbf{i_m}$ decreases only from 0.84 to 0.66, whereas the most dramatic decrease takes place (as in the case of σ) for 0.5<**x**<0.58. Further growth of **x** leads to a continuos fall of $\mathbf{i_m}$ to very small value (~0.17) for **x**=0.8-1.0. This means that the sample with such **x** are in a great extent paramagnetic ($\mathbf{i_m}$=0.1).

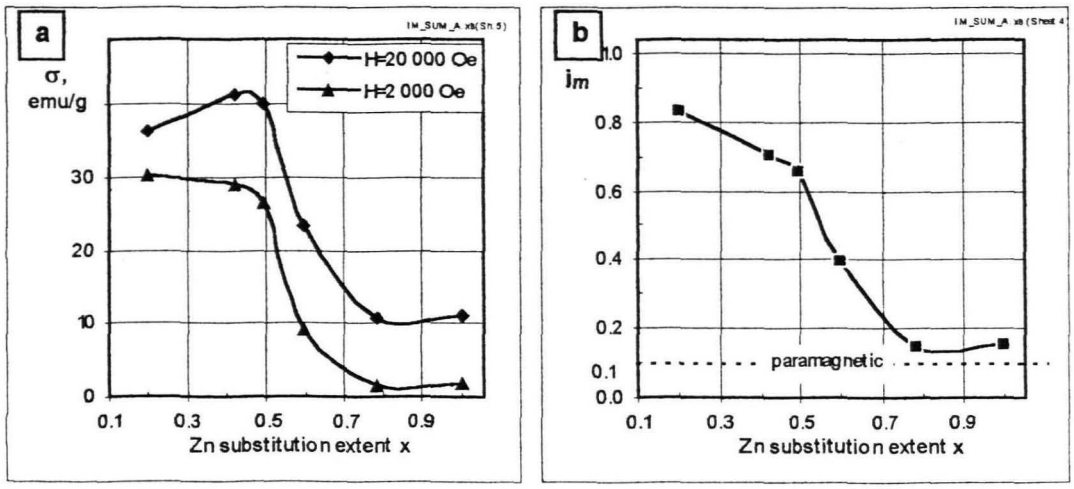

Figure 3.2.-3. (a) - Magnetisation in $\mathbf{H_m}$= 20 kOe and **H**= 2 kOe at **T**=293 K for samples with different Zn substitution degree **x**; (b)- parameter $\mathbf{i_m}$ characterising the shape of magnetisation curve: $\mathbf{i_m} = \sigma_{2000}/\sigma_m$ versus Zn substitution degree **x** at **T**=293 K. Paramagnetic state corresponds to $\mathbf{i_m}$=0.1.

3.2.3.-B. Magnetic properties at different temperatures

Magnetisation of Mn-Zn ferrite particles is decreasing with the temperature growing.

The magnetisation σ_m (in H_m=20 kOe) and σ_{2000} (in H=2 kOe) for samples with a different Zn substitution degree **x** at a different temperatures in the range of 293 - 473 K is shown in Figure 3.2.-4.(a) and (b) respectively.

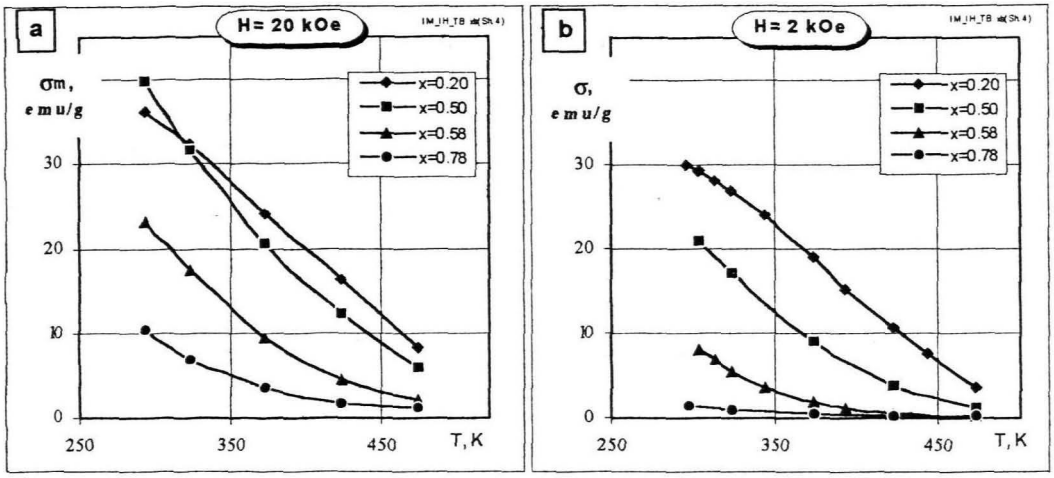

Figure 3.2.-4. Magnetisation of samples with a different Zn substitution degree **x** versus temperature in the temperature range of 293-473 K : (a)- in H_m =20 kOe; (b)- in **H** =2 kOe.

A great difference in magnetisation for samples with **x**=0.5 and 0.58 occurs for all the range of taken temperatures. In a smaller fields (**H**=2 kOe) this difference is even more pronounced than in H_m. For samples with **x**=0.58 and 0.78 the measurements of magnetisation curves at lower temperatures down to 100 K are also carried out. The magnetisation in H_m for these samples in temperature range of 100-473 can be seen on Figure 3.2. -5. This wide temperature range allows to conclude that the whole $\sigma(T)$ dependence has \-like shape with less steep sections at a low temperatures and at a higher temperatures with the linear intermediate section with a higher slope.

The Curie temperatures T_C are estimated by the linear extrapolation of a linear sections of $\sigma(T)$ up to the intersection with T-axis. T_C values for four samples with a different **x** as well T_C values for the corresponding ceramic ferrites are summarised in Table 3.2.-2. (from ref. [5]). T_C value for nanoparticles with **x**=0.2 is only of 10 K higher than the value for bulk ceramic ferrite with the same **x**. For samples with higher **x** this difference is already of 50-60 K. For samples with a different **x** the most used temperature range of 293-423 K falls on a different parts of \-like $\sigma(T)$ curve: for **x**=0.2 - in a linear part of curve, whereas for x=0.5-0.6 partly in the linear and partly in the non-linear 'tail'. For **x**=0.78 the non-linear 'tail' lies in 293-423 K range (T_C is only 350 K).

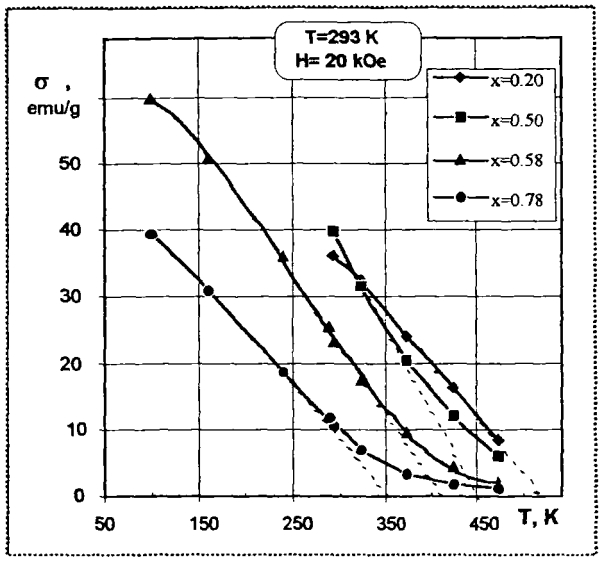

Figure 3.2.-5. Magnetisation of samples with a different Zn substitution degree **x** versus temperature in the range 100-473 K (in H_m=20 kOe). Extrapolation of the linear sections for determination of T_C is shown by the dashed lines.

Table 3.2-2. Estimated Curie temperatures T_C for samples with a different **x** values and the corresponding ceramic Mn-Zn ferrites.

	The Curie temperatures T_C, K			
Zn substitution degree **x**	**0.20**	**0.50**	**0.58**	**0.78**
Prepared nanoparticles	523	450	405	350
Ceramic ferrite [5]	513	402	345	-

The slope of dependence σ(T) is characterised by the thermomagnetic coefficient $k_T = -\Delta\sigma/\Delta T$, where ΔT is taken 20-50 K. The thermomagnetic coefficients for samples with a different **x** values at two temperatures: 313 K and 383 K (in H=5 kOe) are shown on Fig. 3.2.-6. (a). For T=313 K there is a pronounced maximum at **x**~0.4-0.5 and the maximal values of k_T reach 0.21 emu/g*K. Increasing the temperature to 383 K lowers the absolute values of k_T at **x**~0.5 to 0.17 emu/g*K and transforms maximum into the constant section for range $0.2 \le x \le 0.5$. For **x** exceeding 0.5 a dramatic decrease of k_T occurs both at 313 K and 383 K.

For samples with **x**=0.58 and 0.78 measurements of the magnetisation curves at lower temperatures down to 100 K are also carried out. On the basis of that k_T for these samples in the temperature range of 100-300 K are calculated and shown together with k_T for all samples in 303-448 K on Fig 3.2.-6. (b). It is seen that the maximum of k_T for samples with a different **x** lies at a different temperatures. The temperature ranges of maximal k_T and maximal k_T values themselves for samples with a four different **x** values are summarised in Tab. 3.2.-3. The constant behaviour of k_T(T) corresponds to the linear dependence for σ(T) (see Fig. 3.2.-4.). It can be seen from the Tab. 3.2.-3. that the growing of **x** shifts the maximum of k_T to a lower temperatures. These results may allow to choose samples with an appropriate **x** values for using in definite temperature range. High coefficients k_T (0.13-0.21 emu/g*K) in the most important for practice temperature range 313-413 K are reached only by samples with **x**=0.2-0.5. For sample with **x**=0.78 k_T reaches its maximum at very low temperatures (T<160 K) and at the room temperature it falls to a very small value of 0.05 emu/g*K.

Other interesting feature is that the maximal values of all samples for $0.2 \le x \le 0.8$ lie in the approximately same range of 0.16-0.21 emu/g*K.

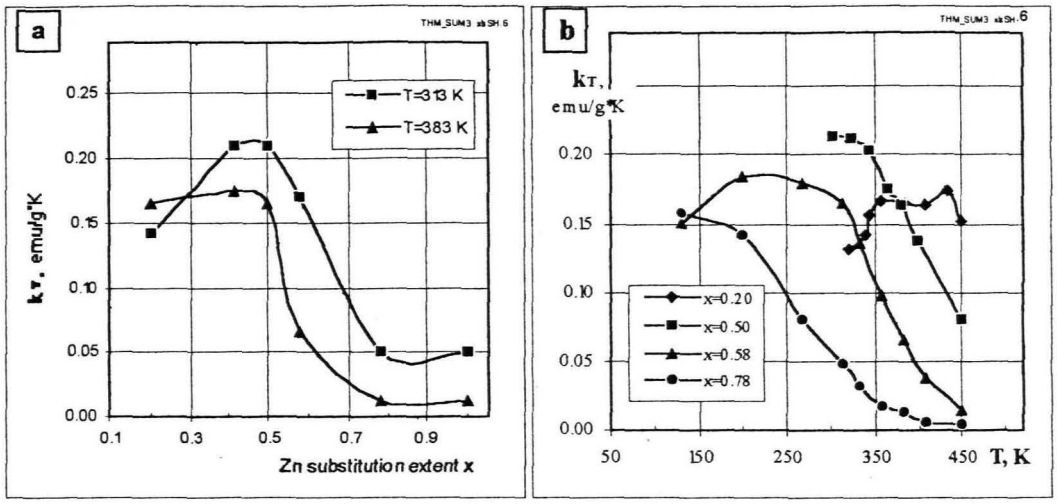

Figure 3.2.-6. (a)- Thermomagnetic coefficients k_T versus Zn substitution degree **x** at 313 K and 383 K; (b)- k_T versus temperature for four samples with different Zn substitution degree **x** in the range of 100-473 K.

Behaviour of $k_T(T)$ for Zn ferrite (**x**=1.0), which is not shown on Fig.3.2.-6. (b) is very close to that for sample with **x**=0.8.

Table 3.2.-3. Temperature range of maximal k_T and maximal k_T values in studied temperature range.

Zn substitution degree **x**	**0.2**	**0.5**	**0.58**	**0.78**
Studied temperature range	315-448 K	303-413 K	120-448 K	120-448 K
Temperature range of maximal k_T	350-430 K	260-310 K	200-260 K	≤160 K
Maximal k_T in studied temperature range, emu/g*K	0.175	0.23	0.18	0.16
Curie temperature T_C, K	523	450	405	350

Conclusions

Syntesis of Mn-Zn ferrite nanoparticles

1. The particles size can be partly controlled by choosing the type of the coprecipitating base. Three bases yield particles with the respective sizes decreasing in the following order: $D_{NaOH}>D_{CH_3NH_3OH}>D_{NH_4OH}$.

Coprecipitation with NaOH leads to the formation of ferrite within the entire range of Zn substitution degree x_0, whereas CH_3NH_3OH and NH_4OH. yield ferrite only under the condition that the x_0 does not exceed a certain value.

2. Chemical composition of the particles is rather close to the stoichiometric proportion in the initial reagents mixture. Small deficit in Zn in respect to the initial stoichiometric proportion is more pronounced in samples precipitated by CH_3NH_3OH.

3. The most relevant increase of particles size and decrease of associated water content takes place in the first 20 min of heating. Even after 90 min of heating particles contain 10-12 w % of associated water.

4. On the basis of studied synthesis parameters the optimal protocol for reproducible preparation of Mn-Zn ferrite particles is developed.

Influence of Zn substitution degree x on particles properties

5. Increasing of Zn substitution degree **x** leads to the decrease of mean size of particles **D**: for **x** growing from 0 to 1 (coprecipitation by NaOH), D_{XR} decreases from 19 down to 6 nm.

6. Increasing of **x** caused a significant enhancing of the associated water content **Q** in particles. For particles coprecipitated by NaOH, the associated water content for **x** growing in the range 0-1 increases from 3-4 to 14 w. %.

7. Near the room temperature magnetic parameters - magnetisation σ and thermomagnetic coefficient k_T reach their maximum values at **x**=0.4-0.5: σ_m=41 emu/g and k_T=0,215 emu/g*K respectively in magnetic field of 20 and 5 kOe. For **x** above 0.5 a dramatic decrease in σ and k_T as well as in i_m occurs. However, Zn ferrite particles (**x**=1) show relatively high magnetisation: σ_m value of about 11 emu/g, which is not found for bulk material.

8. Parameter $i_m=\sigma_{2000}/\sigma_m$ progressively decreases with **x** growing. For **x**>0.5 stronger falling occurs down to values close to 0.1 for **x** 0.8-1.0. The shape of magnetisation curve becomes more sloping tending to the linear for high **x**.

9. Particles with different **x** show their maximal values of thermomagnetic coefficients k_T at a different temperatures. Growth of **x** from 0.2 to 0.8 shifts the maximum of k_T to a lower temperatures: from 350-430 to 160 K respectively. These results allow to choose appropriate **x** values for preparing particles with maximal values of thermomagnetic coefficients for a different temperature ranges.

10. Estimated Curie temperatures T_c are higher (for 10-60 K) than T_c values for the corresponding bulk Mn-Zn ferrites. For samples with higher **x** values this difference in T_c more pronounced. Non-linear 'tails' of $\sigma(T)$ above Curie temperatures for **x**=0.58-0.78 reach 80-100 K.

Chapter 4.

FORMATION OF THE IONIC WATER-BASED AND THE SURFACTED HYDROCARBONE-BASED FERROFLUIDS WITH Mn-Zn FERRITE NANOPARTICLES

4.1. Formation of aqueous ionic ferrofluids: surface treatment procedures

4.1.1. Surface acid (HNO_3) treatment. Partial dissolution of particles in an acid medium

To obtain cationic ferrofluid, ferrite particles after coprecipitation and ferrite formation step are subjected to a surface acid treatment with HNO_3. During this procedure OH^- hydroxil anions primary adsorbed on the particles surface are replaced by H_3O^+ ions and floculating counterions remaining from precipitation base (Na^+, $CH_3NH_3^+$ or NH_4^+) replaced by less floculating NO_3^- anions.

The procedure is realised by keeping a precipitate in 2 mol/l HNO_3 under intensive stirring for 10 minutes. Then particles are separated from supernatent solution by the magnetic decantation or by the centrifugation at 7000 r/min for 10 min. In the whole, precipitate is exposed to the acid attack for about 25 min. HNO_3 treatment leads also to degradation of part of particles material. 25 min long acid attack leads to dissolution of 10-30 w % of particles material.

The value of part dissolved at acid treatment depends on duration of heating (boiling) of precipitate in the alkaline medium. This effect is studied for Zn ferrite particles coprecipitated and heated (boiled) in NaOH solution for a different time. Acid solution after HNO_3 treatment is analyzed and the concentrations of Fe^{3+} and Zn^{2+} are determined (see Table 4.1.-1.). It is remarkable that Fe(III) and Zn dissolve from particles differently: Zn always in a greater extent than Fe(III). However, the longer is the heating time, the closer is the molar ratio $X=[Zn^{2+}]/([Zn^{2+}]+[Fe^{3+}])$ in acid supernatant solution to the initial stoihiometric value of 0.5. The longer is the duration of heating, the less is also the part of particles material degradated in the process of acid treatment (see Table 4.1.-1.).

Table 4.1.-1. Dissolution in HNO_3 (2 mol/l) of Zn ferrite particles heated (boiled) in alkaline medium for different time: chemical composition of the particles before the acid treatment and of acid solution after the treatment expressed in the molar ratio $X=[Zn^{2+}]/([Zn^{2+}]+[Fe^{3+}])$.

Time of boiling after coprecipitation, minutes	Molar ratio X in the particles before HNO_3 treatment	Dissolved part during HNO_3 treatment, mol %	Molar ratio X in acid solution after HNO_3 treatment	Molar ratio X in particles after HNO_3 and $Fe(NO_3)_3$ treatments
15	0.29	35.3	0.39	0.19
40	0.32	26.6	0.37	0.26
180	0.29	21.7	0.35	0.25

For Mn-Zn ferrite particles HNO_3 treatment leads to changes in the chemical composition of particles. Chemical analysis of acid solutions after the acid treatment reveal that Mn, Zn and Fe dissolve from particles differently. For all used Zn substitution degrees Mn and Zn dissolve in a greater extent than Fe, and dissolution of Mn is relatively more pronounced than that of Zn (see Table 4.1.-2.). The probable explanation of this may be that the formation of Zn ferrite occurs more readily than that of Mn ferrite. Therefore not all Mn may be included in Mn-Zn ferrite, some part of it may remain in the form of hydroxide and may be more readily dissolved in HNO_3.

Table 4.1.-2. Chemical composition of Mn-Zn ferrite particles (coprecipitated by NaOH) before HNO_3 treatment and of acid solutions after treatment: Zn substitution degree **x**=[Zn]/([Zn]+[Mn]) and molar ratio **X**=([Zn]+[Mn])/ ([Zn]+[Mn]+[Fe]).

Chemical composition of non treated particles		Mean size of non treated particles D_{XR}, nm	Chemical composition of acid solutions after HNO_3 treatment		Particles dissolved part during HNO_3 treatment, mol %
Molar ratio **X**	Zn substitution degree **x**		Molar ratio **X**	Zn substitution degree **x**	
0.32	0.20	11.0	0.37	0.10	11
0.30	0.47	8.6	0.40	0.37	n.d.
0.31	0.58	7.3	0.38	0.51	15
0.32	0.78	6.6	0.38	0.76	22

n.d. - not determined.

The increase of Zn substitution degree **x** in the particles leads to a bigger value of the degradated part during acid treatment. Diminution of particles mean size with increase of **x** may be partly responsible for this.

It is remarkable, that particles mean size D_{XR} and associated water content **Q** do not change much after HNO_3 treatment (see Table 4.1.-3.). Noticeble diminution in size are found only for particles with initially smaller size (see data for sample D2).

Table 4.1.-3. Chemical composition, mean size D_{XR} and associated water content **Q** of Mn-Zn ferrite particles before and after surface acid treatment with HNO_3. (coprecipitation with CH_3NH_3OH).

Coprecipitated and heated particles (before surface treatment)						Particles after HNO_3 treatment					
Name of sample	Molar ratio **X**	Zn substitution degree **x**	Associated water content **Q**, w%		D_{XR}, nm	Name of sample	Molar ratio **X**	Zn substitution degree **x**	D_{XR}, nm	Associated water content **Q**, w%	
			TG	Calc.						TG	Calc.
A2	0.34	0.0	6.0	6.6	9.9	A2a	0.25	0.0	9.9	5.9	n.d.
D2	0.32	0.46	11.0	12.8	7.0	D2a	0.24	0.56	6.2	n.d.	13.0

The acid surface treatment carried out on not completely ferritized Mn-Zn ferrite particles reveal some interesting features of the degradation process. Coprecipitated sample at the Zn substitution extent **x**=0.5 is separated by the natural sedimentation in an alcaline solution into three fractions according to the time of sedimentation. In ligter fraction X-rays powder diffraction reveals not only peaks of spinel, but the additional peaks of FeOOH as well. For the light fraction of separated sample two additional diffraction lines are found in the range of $1.8<\mathbf{d}<3.5$, namely, **d**=2.82 Å and **d**=1.99 Å. They are fair with the lines for FeOOH, obtained by the precipitation of Fe^{3+} by NaOH. After the acid treatment (2 mol/l HNO_3) these additional peaks dissapear and only the peaks of spinel remain. This may indicate that a less crystalized part is readily dissolved during HNO_3 treatment.

The method of sedimentation of ferrite particles after the surface treatment procedures turns out to be important for obtaining stable in time cationic ferrofluid. For Mn, Co ferrite and magnetite particles, separation of particles from supernatant after HNO_3 and $Fe(NO_3)_3$ treatments can be carried out by a simple decantation on the magnetic plate [23, 33]. For Mn-Zn ferrite particles, which are less magnetic, such decantation is not sufficient for good separation of particles. Residues of the treatment

solutions negatively influence stability of ferrofluid. Therefore for majority of samples the cetrifugation for 10 min at 7000 r/min is used.

4.1.2. Surface stabilisation by $Fe(NO_3)_3$ treatment

The Mn-Zn ferrite particles obtained directly after the surface acid treatment procedures are not chemically stable in acid medium (pH~2 - conditions of cationic ferrofluid). Therefore an additional treatment procedure is necessary to stabilise the surface of particles.

The treatment of ferrite particles by the aqueous ferric nitrate $Fe(NO_3)_3$ was ealier developed for Mn and Co ferrites [25] and here it is applied for the surface stabilization of Mn-Zn ferrite particles.

The procedure includes addition of precipitate obtained after acid surface treatment to a ferric nitrate solution of 0.3 mol/l concentration and keeping boiling for half an hour.

A sample with the initial Zn substitution degree x_0=0.5, coprecipitated with CH_3NH_3OH, is chemically analysed at a different stages of synthesis. Namely, the chemical composition is determined for particles after coprecipitation and heating, then after acid surface treatment and at last for particles after the ferric nitrate treatment (see Table 4.1.-4.).

Table 4.1.-4. Chemical composition of sample at different steps of preparation of cationic ferrofluid: for coprecipitated (non treated), for acid treated and for subsequently ferric nitrate treated particles (CH_3NH_3OH coprecipitating agent, initial Zn substitution degree x_0=0.5).

Sample	Chemical composition, mol %			Molar ratio **X**	Zn substitution degree **x**
	MnO	ZnO	Fe_2O_3		
Non treated (D2)	26.1	22.3	51.6	0.32	0.46
After acid treatment (D2a)	16.9	21.6	61.5	0.24	0.56
After acid and subsequent ferric nitrate treatments (D2f)	14.5	18.5	67.0	0.20	0.56

It can be seen that the molar ratio **X** progressively falls (content of Fe increases) after the acid treatment and then after the ferric nitrate treatment, whereas the Zn substitution extent **x** increases only for the first procedure and remains at the same level for the second.

For the majority of samples the chemical composition is determined after both acid and subsequent ferric nitrate treatments, called together as 'the surface treatment'. After a surface treatment, the molar ratio **X** falls from 0.30-0.33 to 0.22-0.25, in other words the molar part of Fe significantly increases (see Table 4.1.-5. and Fig. 4.1.-1.). The Zn substitution degree **x** grows a little due to a higher dissolution of Mn during acid treatment (see also Table 4.1.-2.).

For sample D2 obtained by CH_3NH_3OH in the edge of ferrite formation zone the changes in chemical composition after a surface treatment are more pronounced than for other samples: the molar ratio **X** falls from 0.32 down to 0.20 and the Zn substitution degree **x** increases from 0.46 to 0.56 (see Tables 4.1.-4 and 4.1.-5).

Table 4.1.-5. Chemical composition of particles before and after "surface treatment" (including HNO_3 and subsequent $Fe(NO_3)_3$ treatments).

Coprecipitated and heated particles (before surface treatment)			Surface treated particles		
Name of sample	Molar ratio **X**	Zn substitution degree **x**	Name of sample	Molar ratio **X**	Zn substitution degree **x**
B1	0.32	0.20	B1f	0.24	0.24
C1	0.32	0.40	C1f	0.25	0.47
D1	0.30	0.47	D1f	0.24	0.53
E1	0.31	0.58	E1f	0.24	0.62
G1	0.32	0.78	G1f	0.24	0.79
B2	0.32	0.16	B2f	0.23	0.21
D2	0.32	0.46	D2f	0.20	0.56

Chemical composition of the coprecipitated particles and cationic ferrofluids prepared at a different initial Zn molar part are shown on 3-component diagram (see Fig. 4.1.-1.).

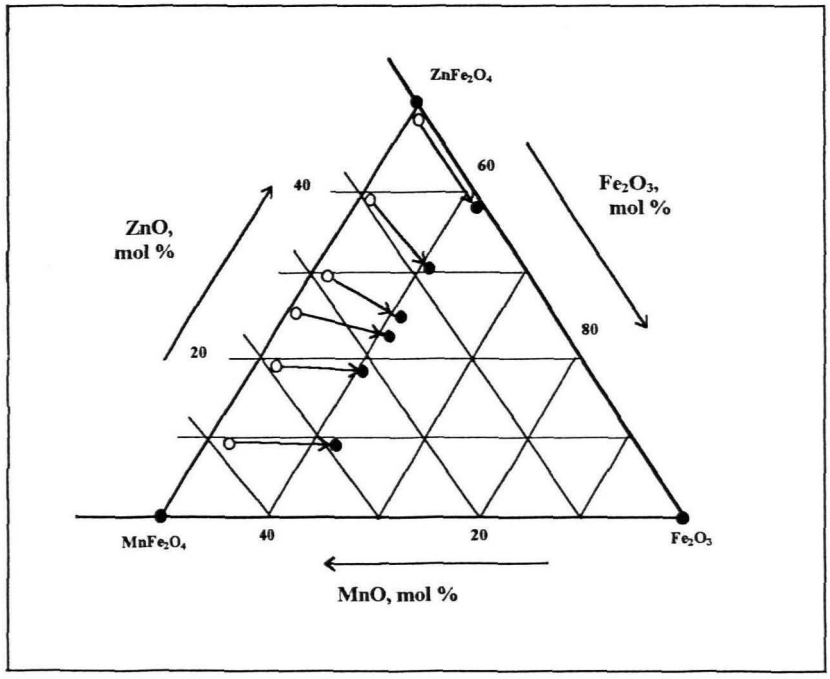

Figure 4.1.-1. The ternary diagram showing chemical composition of coprecipitated (with NaOH) and boiled particles (before surface treatment) - light circles (○) and of particles from cationic ferrofluids obtained after surface treatment - dark circles (●). Samples are synthesised at six different initial x_0 values. Chemical composition is expressed as a combination of three conventional components: MnO, ZnO and Fe_2O_3.

The particles mean size (determined by the Scherrer formula from X-rays powder diffraction) slightly increases after a surface treatment procedures (see Tab. 4.1.-6.). Only for high Zn substitution degree ($0.8 \leq x \leq 1.0$) a slight decrease of the mean size after treatment takes place. After a surface treatment no noticeble changes in X-rays diffraction lines positions or in their relative intensity are observed.

Table 4.1.-6. Mean size for non-treated particles and for a surface treated ones (after HNO_3 and $Fe(NO_3)_3$ treatments) determined by the Scherrer formula from X-rays powder diffraction- D_{XR} and from electronic microscopy photographs - D_{EM}. The size standard deviation σ_{EM} for several surface treated samples is also determined.

Initial Zn substitution extent x_0	Coprecipitating base									
	NaOH						CH_3NH_3OH			
	Sample after coprecipitation and heating		Sample after surface treatment				Sample after coprecipitation and heating		Sample after surface treatment	
		D_{XR}, nm		D_{EM}, nm	σ_{EM}	D_{XR}, nm		D_{XR}, nm		D_{XR}, nm
0.0	A1	18.8	A1f	n.d.	n.d.	19.0	A2s	9.9	A2f	10.0
0.2	B1	11.0	B1f	9.8	0.45	11.4	B2s	7.6	B2f	6.8
0.4	C1	10.4	C1f	n.d.	n.d.	10.4	-	-	-	-
0.5	D1	8.6	D1f	7.1	0.35	8.8	D2s	7.0	D2f	6.0
0.6	E1	7.3	E1f	5.9	0.31	7.6				
0.8	G1	6.6	G1f	5.0	0.33	6.0				
1.0	J1	6.2	J1f	n.d.	n.d.	5.9				

n.d. - not determined

4.1.3. The experimental protocol for surface treatment to produce Mn-Zn ferrite cationic ferrofluid

All data are given for reaction volume of 2 liters.

HNO_3 treatment

- precipitate subjected to HNO_3 2 mol/l (100 ml) at an intensive stirring for 10 min.
- particles are separated by a centrifugation at 7000 r/min for 10 min.

(The supernatent solution is collected and chemically analyzed for Mn, Zn and Fe(III).)

$Fe(NO_3)_3$ treatment

- precipitate is added to a boiling $Fe(NO_3)_3$ solution (270 ml of 0.3 mol/l concentration). The suspension is kept boiling for 30 min.
- the suspension is cooled and precipitate is separated by a centrifugation at 7000 r/min for 10 min.

Washing of precipitate

- precipitate is washed by HNO_3 2 mol/l (120 ml) for 10 min by an intensive stirring and separated by centrifugation.
- precipitate is washed by acetone by an intensive stirring for 10 min and separated by centrifugation.
- distilled water (~50 ml) is added to the precipitate and residues of acetone are eliminated by stirring under a slight vacuum at 30–40 °C.

4.1.4. Magnetic properties of samples after the surface treatment

4.1.4.-A. Magnetic properties of samples after the surface treatment at the room temperature

In the chapter 3 (see 3.2.3.) it is shown that a magnetic parameters of untreated samples are strongly dependent on the Zn substitution degree **x**. A surface treatment leads to some changes in a magnetic parameters, and the magnitude of these changes differs for samples with various **x**.

The magnetization curves at 293 K for particles before and after a surface treatment at four different Zn substitution degrees **x** in the range of 0.2-0.8 are shown on Figure 4.1.-2.

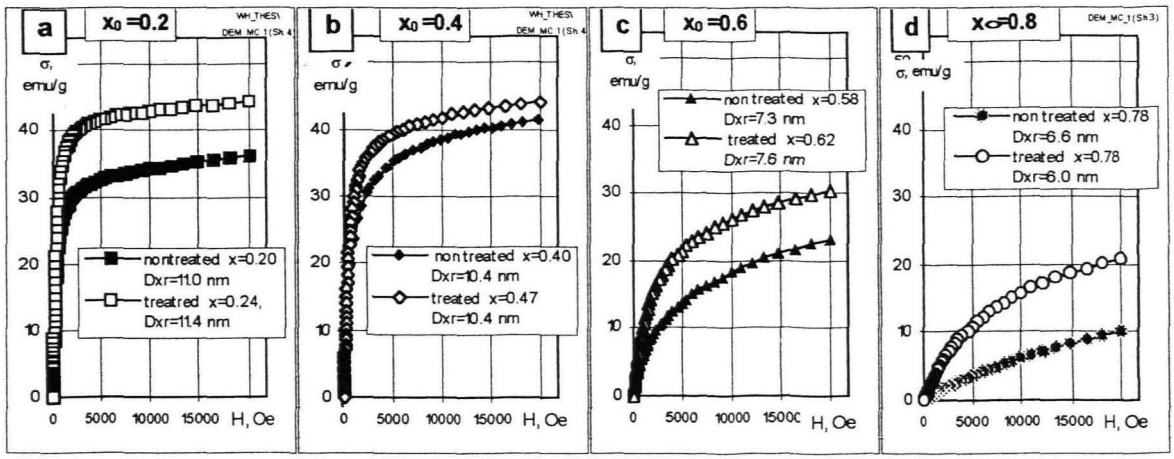

Figure 4.1-2. Magnetization curves at 293 K for samples before and after surface treatment at four different initial Zn substitution degrees x_0: (a) - x_0=0.2; (b) - x_0=0.4; (c) - x_0=0.6; (d) - x_0=0.8.

At x_0=0.2 the magnetisation of particles a after surface treatment increases to ~20 %. A relatively small increase of magnetisation is observed at x_0=0.4 - only 5-10 % (evaluations are made in **H**=5000-20000 Oe). At x_0=0.6 the magnetization of surface treated particles is higher than that of non treated particles for 20-30 %. The maximal relative increase of magnetisation is found for a weakly magnetic sample with x_0=0.8: surface treatment leads to an increase of σ_m in 2 -2.5 times.

The spectrum of magnetic moments of sample with **x**=0.24 has the shape close to the log-normal distribution (see Figure 1.4.-3.). With **x** growing the corresponding spectrum becomes more and more assimetric with a pronounced 'wing' of a low magnetic moments. For **x**=0.62 the spectrum consists of two parts with two maximums. For **x**=0.79 the spectrum has only a weakly magnetic part with one maximum.

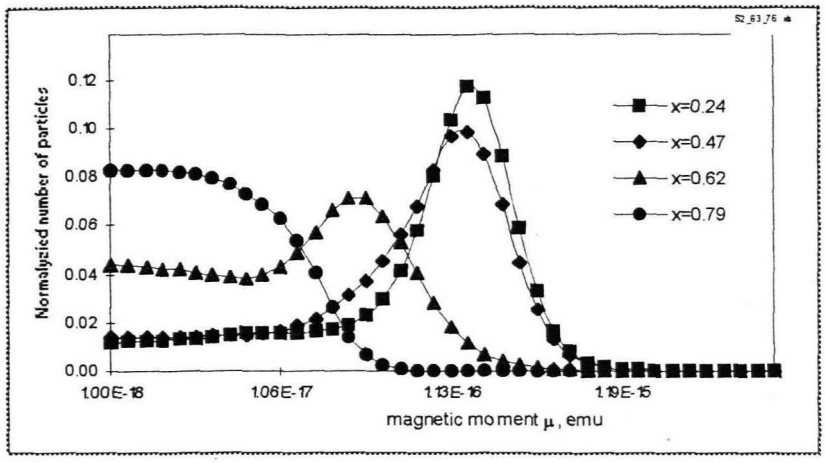

Figure. 4.1.-3. Spectra of magnetic moments obtained by the processing of magnetisation curves of cationic ferrofluids (surface treated particles dispersed in aqueous medium) with different **x**.

The dependences of magnetisation σ (in $\mathbf{H_m}$=20 kOe in $\mathbf{H_{2000}}$=2 kOe) versus Zn substitution degree **x** for particles before and after the surface treatment are shown on Fig. 4.1.-4. (a) and (b) respectively. Pronounced maximum in dependence $\sigma_m(x)$ (in $\mathbf{H_m}$ =20 kOe) for untreated particles transforms after the treatment into a constant section in the **x** range of 0.2-0.5. In $\mathbf{H_{2000}}$ the maximal values of σ are found for **x**~0.2 for both untreated and treated particles. A small decrease of σ in $\mathbf{H_{2000}}$ in the range 0.2-0.5 takes place. The most dramatic decrease of σ for untreated particles occurs when **x** is growing from 0.5 to 0.6: in $\mathbf{H_m}$ for 45 % and in $\mathbf{H_{2000}}$ for 70 %. The surface treatment diminishes these abrupt falls to ~20 % and ~50 % respectively. After the surface treatment this magnetisation decrease shifts to a higher values of **x**: approximetely for 0.5 **x** value. This may be partly connected with a slight increasing of **x** in the samples after a surface treatment.

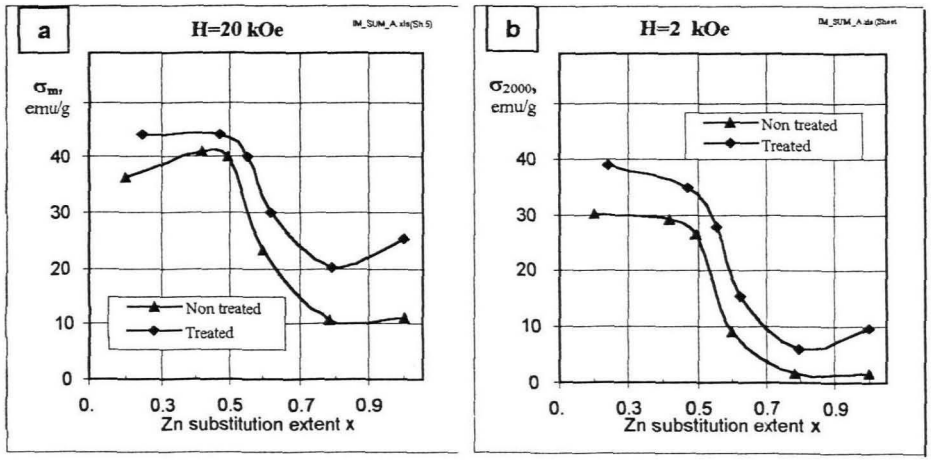

Figure 4.1.-4. Specific magnetization σ at 293 K for particles before (non treated) and after surface treatment versus Zn substitution degree **x**: (a) - in $\mathbf{H_m}$= 20 kOe , (b) - in $\mathbf{H_{2000}}$=2 kOe.

The magnetisation σ of treated particles reaches its minimum at **x**~0.8, and for further growing of **x** up to 1.0 (ferrite of Zn) a slight increase of σ occurs.

The shape of the magnetization curve changes after a surface treatment as well: it becomes more steep. Therefore the increase of magnetisation after a surface treatment is relatively higher in lower fiields. These changes arised by a surface treatment may be better seen by considering the parameter $\mathbf{i_m}$ $\mathbf{i_m}=\sigma_{2000}/\sigma_m$,. The behaviour of $\mathbf{i_m}$ versus Zn substitution degree **x** is shown in Figure 4.1.-5. The higher is the **x** value, the greater is the relative difference in $\mathbf{i_m}$ for non treated and surface treated particles. For untreated sample with **x**~0.8-1.0 the $\mathbf{i_m}$ is close to 0.1 and the corresponding magnetisation curve is almost linear (see also Figure 4.1.-2.(d)), which is feature of paramagnetics.

After a surface treatment the i_m for sample with **x**~0.8 grows to 0.3 and for **x**=1.0 even to 0.4. This means that the paramagnetic component in these samples significantly decreases.

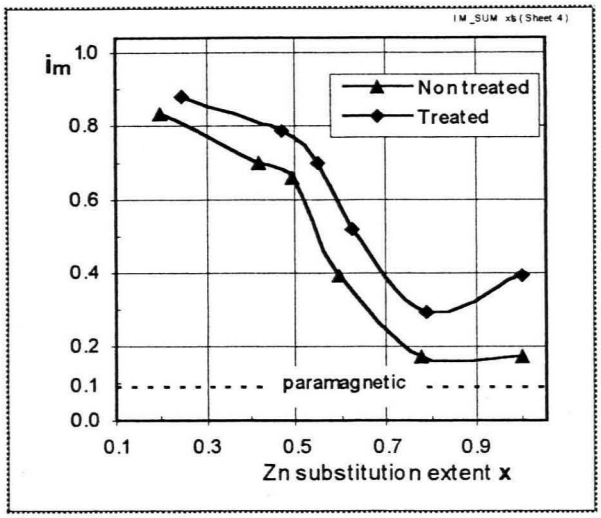

Figure 4.1.-5. Parameter $i_m = \sigma_{2000}/\sigma_m$ at 293 K for particles before (non-treated) and after a surface treatment versus the Zn substitution degree **x**.

4.1.4.-B. Magnetic properties of samples after a surface treatment at different temperatures

After a surface treatment the magnetization σ increases not only at the room temperature, but as well at elevated temperatures in the range of 293-473 K. The magnetisation curves are measured at different temperatures in the range of 293-473 K and for samples with x_0=0.6 and 0.8 also at low temperatures down to 100 K. The dependences of σ_m on temperature for samples before and after surface treatment at four different initial Zn substitution degrees x_0 are shown on Figure 4.1.-6. (a), (b), (c) and (d). For x_0=0.2 the relative increase in magnetisation after a surface treatment is growing from ~20% at the room temperature up to ~50% at 473 K, where the absolute value of σ_m becomes much smaller. Similar peculiarities are observed for samples at x_0=0.6 and 0.8, where the relative increase of σ_m after a surface treatment is higher at elevated temperatures: at 423-473 K σ_m values, which are very small, grow after a surface treatment in 2-3 times.

The Curie temperatures T_c are estimated from dependences σ(T) in the same way as for non-treated samples (see 3.2.3. (b)) and are summarised in the Table 4.1-6. It can be seen that for all studied x_0 the T_c after a surface treatment increase: for x_0=0.2 - for 25 K and for x_0=0.6-0.8 for 50-60 K. The higher is the initial Zn substitution degree x_0, the bigger is the increase of the Curie temperature after a surface treatment.

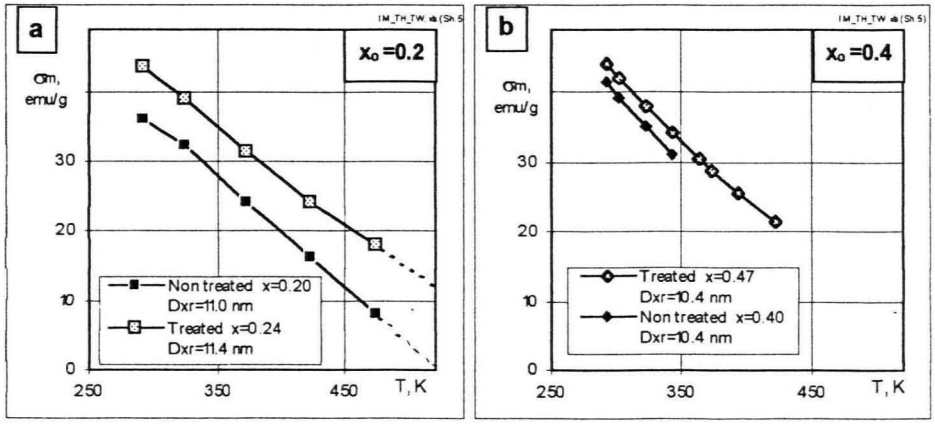

Figure 4.1.-6. (a), (b). The caption see in the next page.

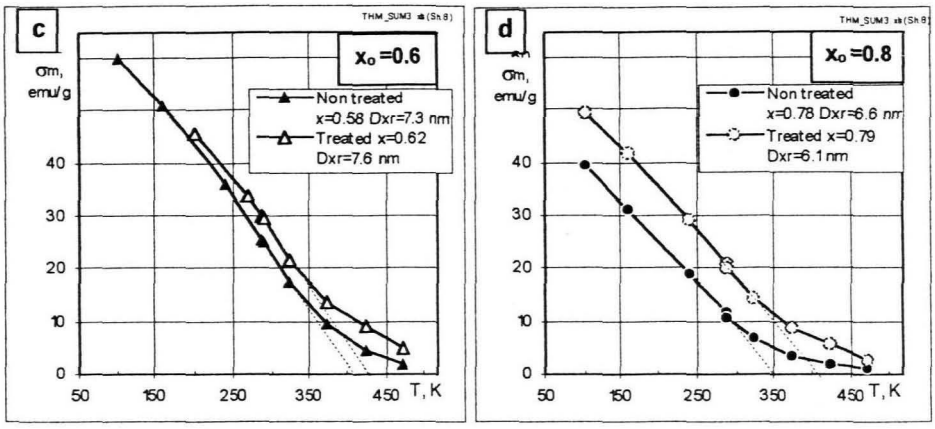

Figure 4.1.-6. Magnetization σ_m versus temperature for non treated and treated samples at a different initial Zn substitution degree x_0: (a)-x_0=0.2; (b)- x_0=0.4; (c)- x_0=0.6; (d)- x_0=0.8.

Table 4.1.-7. The estimated Curie temperatures T_C for samples with a different x values and the corresponding ceramic bulk Mn-Zn ferrites from ref. [1].

	Curie temperatures **Tc**, K		
Initial Zn substitution degree x_0	**0.2**	**0.6**	**0.8**
Sample before surface treatment	523	405	350
Sample after surface treatment	584	430	407

The dependence $\sigma(T)$ near certain temperature can be characterised by the thermomagnetic coefficient $k_T = -\Delta\sigma/\Delta T$, where ΔT is taken of 20-60 K. The magnetization σ is taken in **H**=5 kOe (if not specially mentioned) due to the fact that for the majority of samples k_T in this field achieves or is close to saturation.

The thermomagnetic coefficient k_T determined at 313 K (in the range of 303-323 K) for non-treated and treated samples with a varying Zn substitution degree **x** are plotted on Figure 4.1.-5. It is noticeable that a surface treatment leads to a significant growth of the thermomagnetic coefficient k_T for **x**>0.5. For example, in the case of weakly magnetic sample with **x**~0.8 the k_T grows in more than 2 times (at 313 K) (see Figure 4.1.-7.). For **x**~0.5 the surface treatment does not change significantly the thermomagnetic coefficient k_T. As a result, after a treatment maximum of k_T shifts to a higher **x** values (to **x** ~0.6). In the whole, the dependence k_T(**x**) after surface treatment becomes more smooth.

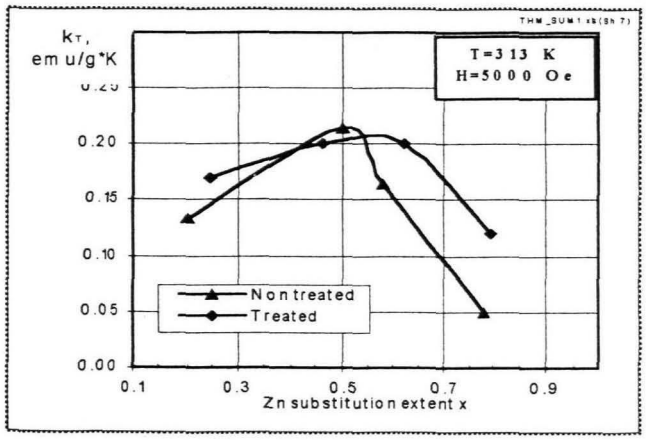

Figure 4.1.-7. The thermomagnetic coefficient k_T at 313 K for non treated and treated samples versus Zn substitution degree.

The thermomagnetic coefficient k_T depends on the magnetic field strength **H** (because of $\Delta\sigma$ depending of **H**). The shape of k_T(**H**) resembles the shape of a magnetisation curve. As non-treated

and surface treated particles have a different shape of the magnetisation curve, they have also a different shape of $k_T(H)$. Especially these differences are pronounced for $x>0.5$ (see Figure 4.1.-8.). For non-treated samples $k_T(H)$ is growing even in H_m= 20 kOe. After surface treatment the k_T reaches saturation in a certain magnetic field.

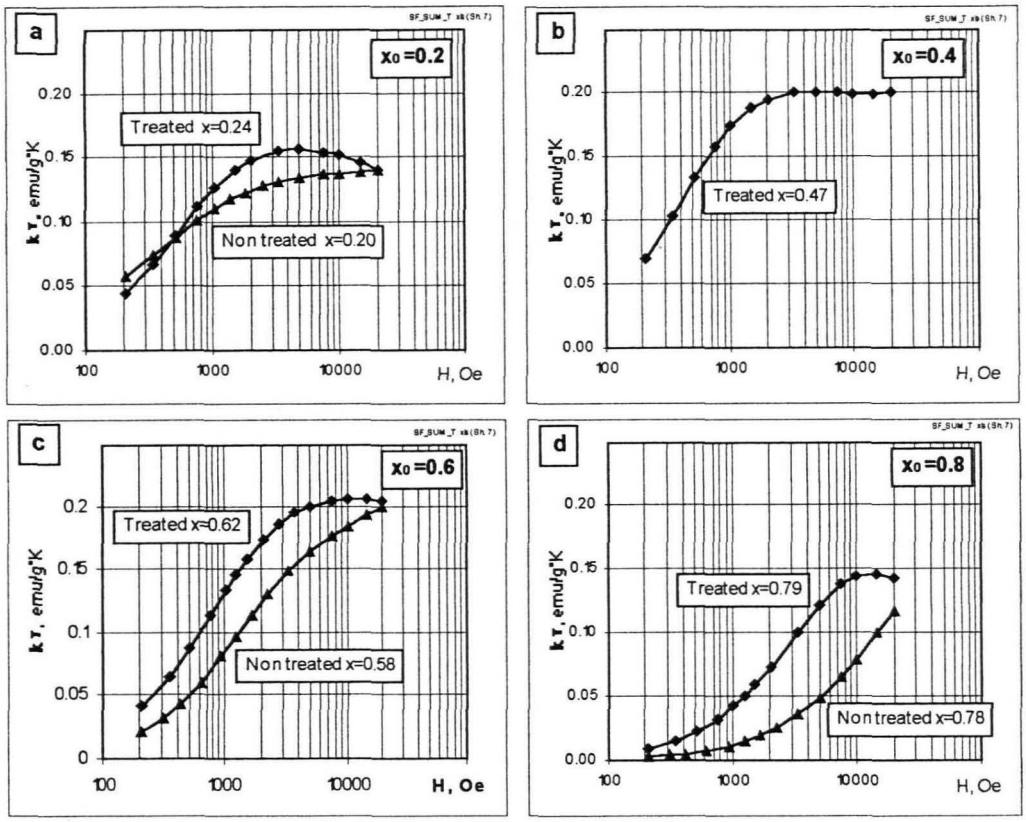

Figure 4.1.-8. Thermomagnetic coefficients versus magnetic field strength **H** (log scale) for non-treated and treated particles at a different initial Zn substitution degree x_0 : (a)-x_0=0.2; (b)- x_0=0.4; (c)- x_0=0.6; (d)- x_0=0.8.

The dependences $k_T(H)$ for treated samples with four different **x** values are collected together and shown on Figure 4.1.-9. It can be seen that growing of k_T takes place only to a certain field value and then a saturation is observed, but for sample with **x**=0.24 even a slight decrease of k_T in higher fields occurs. This saturation effect may be characterized by the field value H_1, where it is achieved. The maximal values of k_T and values of H_1 for four samples with a different **x** are given in Table 4.1-8. The minimal H_1~1.7 kOe is found for **x**=0.47 (x_0=0.4). In the **x** range of 0.4 - 0.8 H_1 strongly depends on **x**: the higher is the **x** the bigger is the H_1. For sample with **x**~0.8 k_T becomes saturated only in strong fields: H_1 ~ 8 kOe.

Table 4.1-8. The maximum values of thermomagnetic coefficients k_{Tmax} and values of magnetic field strength H_1 at **T**=313 K for surface treated particles with a different Zn substitution degree **x**.

Zn substitution degree **x**	0.24	0.47	0.62	0.79
$k_{T\ max}$, emu/g*K	0.156	0.205	0.206	0.147
H_1, Oe	2050	1680	3710	8005

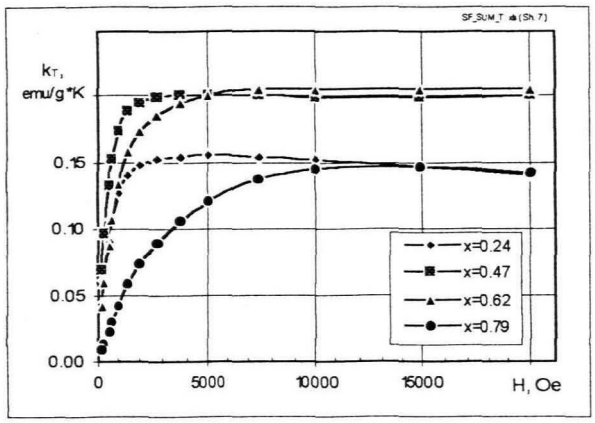

Figure 4.1.-9. Thermomagnetic coefficients k_T at 313 K for surface treated particles with different Zn substitution degree x versus magnetic field strength H.

The thermomagnetic coefficients k_T themselves depend on temperature. In Fig. 4.1.-9. (a), (b) and (c) the behaviour of $k_T(T)$ is shown for non-treated and treated samples with x_0=0.2, 0.6 and 0.8 respectively.

For nontreated samples the maximum k_T values for various x are reached at a different temperatures (see Table 3.2.-3.). After a surface treatment the positions of the maximum k_T shift in a temperature scale, however differently for samples with a various Zn substitution degree x : in the case of x_0 =0.2 the maximum of k_T shifts to a lower temperatures, for x_0 =0.8 - to a higher temperatures (for more than 100 K), whereas for x_0 =0.6 it does not change (at least its upper edge). For samples before and after surface treatment the maximal k_T values and temperature ranges, where they are achieved are summarised in Table 4.1-8.

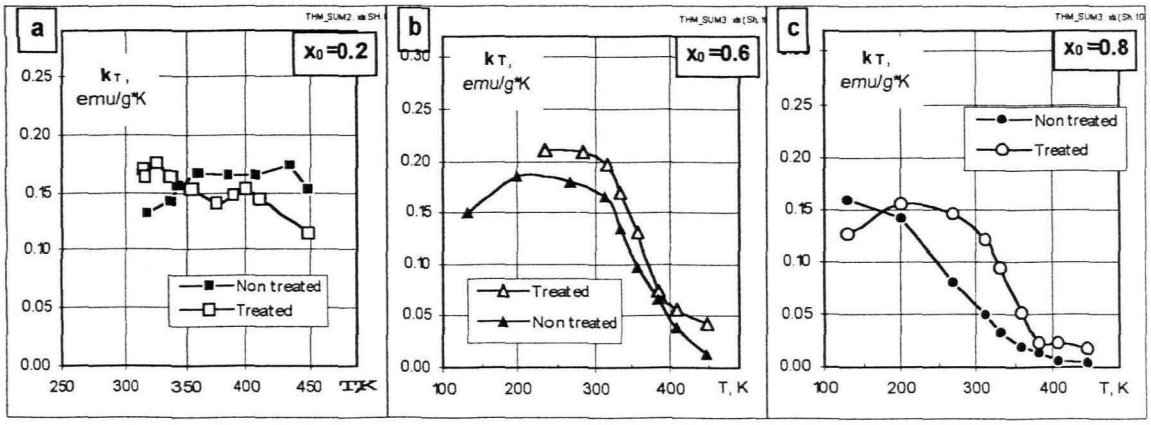

Figure 4.1.-9. Thermomagnetic coefficients k_T in the field H=5000 Oe versus temperature for samples before and after a surface treatment in the temperature range of 100-448 K: (a) x_0=0.2; (b) x_0=0.6; (c) x_0=0.8.

Table 4.1.-8. Maximal k_T values and temperature ranges, where they are achieved for non-treated and surface treated samples with a different initial Zn substitution degree x_0.

Initial Zn substitution degree x_0		0.2	0.4	0.5	0.6	0.8
Studied temperature range		303-448 K	303-413 K	303-413 K	120-448 K	120-448 K
Temperature range of maximal k_T	Samples before surface treatment	350-430 K	-	≤313 K	200-260 K	≤160 K
	Samples after surface treatment	303-333 K	≤333 K	≤313 K	240-280	200-260 K
Maximal k_T emu/g*K	Samples before surf. tr.	0.175	-	0.215	0.18	0.16
	Samples after surf. tr.	0.175	0.205	0.21	0.215	0.155

Conclusions (for 4.1.)

1. In the process of an acid treatment (by HNO_3) metals from particles dissolve in the following relative progressive sequence: Fe<Zn<Mn. As a result the molar ratio **X** decreases (content of Fe increases) and the Zn substitution degree **x** slightly increases.

2. Increasing of the Zn substitution degree **x** leads to a higher dissolution of particles material during acid treatment.

3. Zn ferrite particles heated in alkaline medium after coprecipitation for longer time demonstrate lower dissolution in HNO_3 and smaller changes in chemical composition after surface treatment.

4. $Fe(NO_3)_3$ treatment leads to the additional decrease of **X**, but does not change **x**.

As a result of the two treatments (by HNO_3 and subsequently by $Fe(NO_3)_3$) conventional Fe_2O_3 content in the particles grows from 51-52 up to 58-67 mol %.

5.The mean size of particles and associated water content after the surface treatment change negligibly.

6. Surface treatment procedures lead to the increase of the magnetisation σ and the parameter $i_m=\sigma_{2000}/\sigma_m$ in all studied temperature range. The shape of magnetisation curve becomes more steep and higher values of σ and k_T are reached in a lower fields. The thermomagnetic coefficients k_T are significantly increased for $x>0.5$. In the **x** range of 0.5-1.0 a relative changes in σ, parameter i_m and k_T arised by a surface treatment are more pronounced. After the surface treatment the maximal increase of σ, i_m and k_T is observed for samples with a higher Zn substitution degrees $x=0.8$-1.0.

7. The estimated Curie temperatures after surface treatment increase for 25-60 K.

8. For non-treated samples the especially strong decrease of magnetic parameters (σ, i_m and k_T) take place for $0.5<x<0.6$. Surface treatment leads to a diminishing of this dramatic decrease and to its shifting to a higher **x** values. After a surface treatment the magnetic parameters change more smoothly with varying of **x**.

9. For non-treated samples the thermomagnetic coefficients k_T does not reach saturation even in H_m=20 kOe. After the surface treatment the k_T becomes saturated in a certain magnetic field H_1 (1.7-8 kOe), whose value depends on **x**: the higher is the **x** the bigger is the H_1.

10. For non-treated samples the maximal k_T values for various **x** are reached at a different temperatures. After the surface treatment the maximums of k_T shift in a temperature scale differently for samples with a various initial Zn substitution degree x_0: for $x_0=0.2$ the maximum of k_T to lower temperatures, for $x_0=0.8$ - strongly to a higher temperatures (for more than 100 K), whereas for $x_0=0.6$ it does not change.

4.2. Formation and properties of surfacted ferrofluid in hydrocarbone medium

Introduction

In the chapter 3 and 4 the synthesis of an aqueous ferrofluids is described. It is shown how Mn-Zn ferrite particles of definite size can be synthesised and transferred into a water solution.

These particles can be as well dispersed in non-polar solution. To do this it is necessary "to surfact" them, in other words to cover their surface with amphiphil molecules, which cause a steric repultion between particles.

4.2.1. Preparation of surfacted ferrofluids

It is possible to peptise in non-polar medium particles initially got as ionic ones as well as particles obtained directly after a coprecipitation. Both two ways are used (see scheme on Fig. 4.2.-2) and properties of final ferrofluids are compared. A relatively low-evaporating hydrocarbon dodecane $C_{12}H_{26}$ is used as a non-polar carrier liquid.

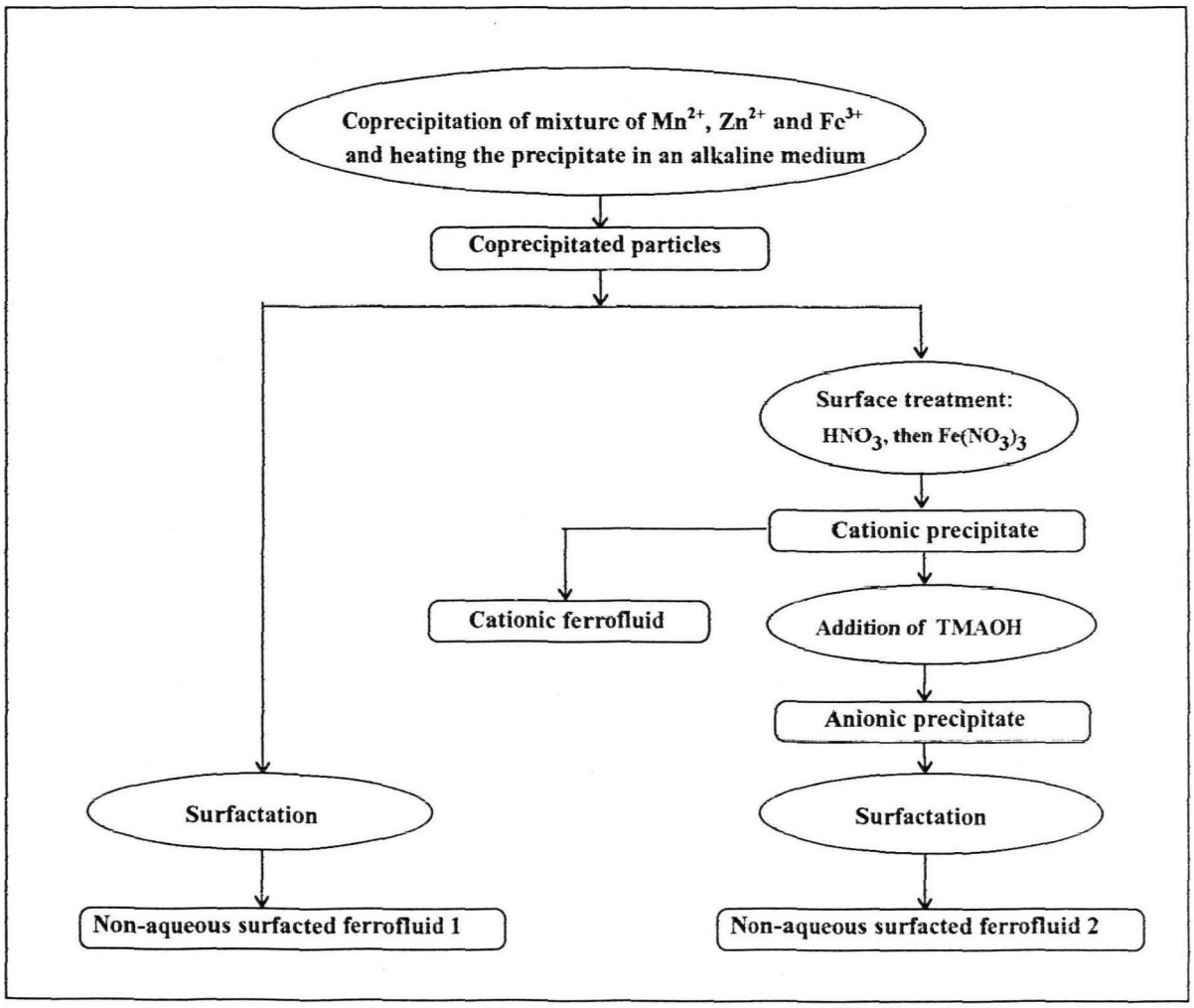

Figure 4.2.-2. A general scheme of synthesis for surfacted non-aqueous Mn-Zn ferrite ferrofluid. Two pathways are shown: starting directly from coprecipitated and heated particles or from cationic (surface treated) particles.

4.2.1.-A. Direct surfactation of coprecipitated particles (surfacted ferrofluid type 1)

The addition of oleic acid directly to the alkaline precipitate (after heating in a mature alkaline solution) at pH~12-13 does not success in obtaining a stable colloid in dodecane. Surfactation takes place at pH~11.

A surfacted ferrofluid of type 1 is prepared by the following procedure:

A precipitate is twice washed with a distilled water to lower pH to 10.5-11 and decanted on the magnetic plate. A surfactant (oleic acid) diluted in dodecane at a concentration of about 12 vol. % is added to the wet precipitate and the resulting mixture is stirred at 30 °C. The following proportion of surfactant to a total metal in particles is utilised: 1 mol oleic acid : 8 mol Me. Particles are surfacted and transferred into the organic phase. This phase is separated and then heated to ~120 °C under stirring in order to remove the remaining part of water. The excess of surfactant is eliminated by an extraction with methanol.

It is noted that the chemical composition of particles of surfacted ferrofluid type 1 is very close to the composition of coprecipitated and heated particles (see Table 4.2.-1.). The mean size of particles after surfactation does not change significantly.

4.2.1.-B. Preparation of surfacted ferrofluid from a cationic one (surf. ferrofluid type 2)

Surfacted ferrofluid can be also prepared using particles after a surface treatment (cationic precipitate) These particles are transferred into the anionic precipitate by the addition of tetramethyl-ammonium hydroxide (TMAOH). Subsequently, particles are surfacted with an oleic acid and transferred into a non-polar medium (see Figure 4.2.-2.).

TMAOH is added to the cationic precipitate in proportion 1 mol TMAOH : 10 mol Me under stirring. After that, the surfactant is added in a proportion 1 mol oleic acid : 5 mol Me. The mixture is stirred at 30° C. Then the excess of oleic acid in ferrofluid is extracted by methanol.

At the final stage the chemical composition of particles (surfacted ferrofluid 2) is very close to the composition of its precursor - cationic precipitate (see Table 4.2.-1.). The mean size of particles of surfacted ferrofluid 2 and cationic precipitate does not differ significantly. This also means that the stages of formation of anionic precipitate and surfactation do not lead to a changes of chemical composition and size.

Table 4.2.-1. Chemical composition of surfacted ferrofluids prepared by two different methods from the same initial molar composition (x_0=0.5).

Sample	Particles mean size	Chemical composition, mol%		
	D_{XR}, nm	MnO	ZnO	Fe_2O_3
Initial mixture of salts	-	25.0	25.0	50.0
Coprecipitated particles(precursor for SF1)	8.5	24.8	24.5	50.7
Surfacted ferrofluid 1	8.3	24.7	24.9	50.4
Cationic ferrofluid (precursor for SF2)	8.8	18.8	22.4	58.8
Surfacted ferrofluid 2	8.9	18.7	22.3	59.0

4.2.2. Magnetic properties of surfacted ferrofluids

After the surface treatment a certain changes in magnetic properties take place (see Section 4.1.3). Namely, a magnetisation grows and the magnetisation curve shape becomes more steep after a surface

treatment. For the surfacted ferrofluids prepared from the coprecipitated and heated particles (type 1) and from the surface treated particles (type 2) these differences in the magnetic properties remain.

The magnetisation curves for surfacted ferrofluids of type 1 and type 2 are measured and shown in Fig 4.2-3. Both surfacted ferrofluids are obtained from the same initial molar composition (x_0=0.5) and their chemical composition and the mean size of particles are summarised in Table 4.2-1. It can be seen that although the magnetisation in a maximum magnetic field (**H**=10.5 kOe) for both types of ferrofluids is close, the respective shapes of the magnetisation curves differs significantly. Ferrofluid obtained directly from the coprecipitated particles demonstrates a less steep magnetisation curve. These differences may be seen on Fig. 4.2-4, where the spectra of magnetic moments corresponding to these two magnetisation curves are shown. Non-treated sample demonstrate a much more pronounced paramagnetic part in a magnetic moment spectrum. This probably is connected with the paramagnetic component inherent in hydroxides of metals which are not completely transformed into ferrite. Hydroxides which are paramagnetic also are less resistant to the acid treatment than oxides (ferrites) [10]. Therefore, after a surface treatment the paramagnetic component may significantly decrease. In the magnetic fields lower than 3 kOe (usually used in practical applications) the ferrofluid of type 2 has significantly higher magnetisation (up to 25 %) than the ferrofluid of type 1.

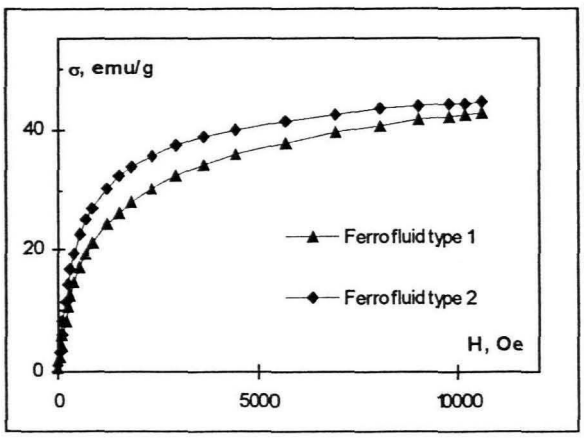

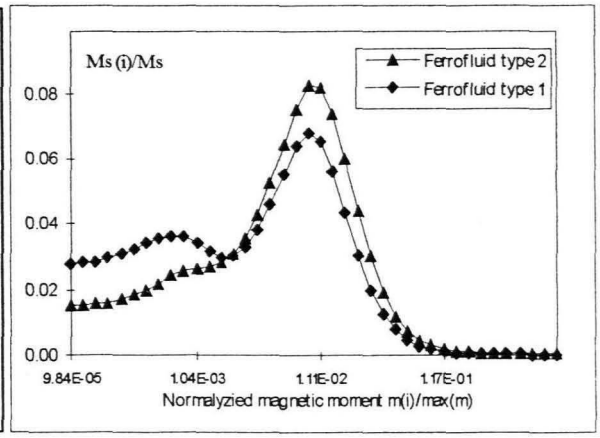

Figure 4.2.-3. Magnetisation curves for two types of the surfacted ferrofluid, obtained by two different methods: 1 - by directed surfactation of coprecipitated particles, 2 - by the surfactation of particles obtained through surface treatment.

Figure 4.2.-4. Spectra of magnetic moments for magnetisation curves for two types of the surfacted ferrofluid shown on Fig. 4.2.-3.

Conclusions (for 4.2.)

1. Surfacted ferrofluids are obtained with an oleic acid in dodecane by two different ways: directly from coprecipitated and heated particles or from surface treated particles.

2. Properties of particles (chemical composition and mean size) of the surfacted ferrofluids are very close to those of their respective precursors: coprecipitated and heated particles or the surface treated particles.

3. Differences in a magnetic properties for untreated and the surface treated particles remain also for two types of the surfacted ferrofluids: magnetisation of the surfacted ferrofluid of type 2 (prepared from surface treated particles) is higher than that of the type 1. This difference in magnetisation is more pronounced in less intensive magnetic fields (**H** < 5 kOe), whereas in **H**=10 kOe magnetisation is almost equal. The corresponding spectra of magnetic moments demonstrate difference as well: for SF1 there is a more pronounced paramagnetic part.

Chapter 5.

PROPERTIES OF PARTICLES OF DIFFERENT SIZE

Introduction

In the review of literature (see 1.1.2.) it is shown that physical properties of Mn-Zn ferrite ferrite ultrafine particles may depend on their size. Prepared nanoparticles demonstrate certain polydispersity in a size. It seemed interesting to compare properties of small and large particles fractionated from the same polydispersed sample. An attempt is made to fractionate Mn-Zn ferrite particles obtained after coprecipitation and heating by sedimentation in an aqueous solution. Particles of the cationic ferrofluids are fractionated by centrifugation.

5.1 Properties of particles after coprecipitation and heating fractionated by sedimentation

Particles with x~0.5 obtained after a coprecipitation and heating are fractionated by a natural sedimentation process in mature alkaline solution in the cillindrical volume ∅18×22 cm. Three fractions are collected according to the time of sedimentation: 5, 10 and 15 min. Fraction Ds3 sedimentated for 5 min is called "heavy" one and has weight of 48 % of the total sample. Other two fractions Ds2 and Ds1 are called "intermediate" and "light" and have weights of 41 and ~11 % of total respectively.

Properties of fractions: chemical composition, mean size from X-rays, associated water content (determined by the TG as relative weight loss at 750 °C) are summarised in Table 5.-1.

For a light fraction the content of Fe is a little lower and the Zn substitution degree is higher than for heavy fraction. Fraction Ds2 shows intermediate values. It must be mentioned that X-rays diffraction spectra reveal some additional peaks in the light fraction Ds1 that may be attributed to the hydroxide of Fe. For other two fractions (as well as for all fractions of the cationic ferrofluids) only peaks of spinel are observed. Particles of the light and the intermediate fractions may have different density, as the mean crystalline size is very close. This is confirmed by different content of the associated water, which is higher in the particles of light fraction (13.1 w%) than in two other fractions (11.8 w%).

Table 5.-1. Properties of particles after coprecipitation and heating in alkaline medium fractionated by sedimentation.

Name of fraction	Fraction's weight, w% of total sample	Chemical composition					Mean size of particles D_{XR}, nm	Assoc. water content w%, (TG)
		MnO, mol.%	ZnO, mol.%	Fe_2O_3 mol.%	The molar ratio X	Zn substitution degree x		
Ds1, light	10.7	23.4	25.9	50.5	0.328	0.525	8.8*	13.1
Ds2, intermediat.	41.1	23.8	24.7	51.4	0.321	0.509	8.7	11.8
Ds3, heavy	48.2	24.6	23.3	52.1	0.315	0.486	9.5	11.8

*X-rays diffraction spectrum of Ds1 has an additional peaks of hydroxide of FeOOH.

5.2. Properties of particles of the cationic ferrofluid fractionated by centrifugation

The surface treated particles in the form of cationic ferrofluid are fractionated by a centrifugation. Liquid the cationic ferrofluids at concentration of 2-3 mol/l Me are centrifuged at 12 000 rpm for 30 min and then separated into 2 or 3 fractions.

Cationic ferrofluid Df (x_0=0.5) is separated into 3 fractions taking ferrofluid from 3 parts of centrifugal tube (at a different height). The following fractions are obtained: Df1-light, Df2-intermediate and Df3-heavy. The cationic ferrofluid Bf (x_0=0.2) after centrifugation is devided into 2 fractions: the light one Bf1 remaining as liquid and the heavy one Bf2 concentrated on the bottom of the tube as viscous sediment, which is then separated and redispersed in distilled water.

Properties of particles from the different fractions of Dff and Bf are determined: chemical composition, mean size from X-rays, mean size from electronic microscopy and associated water content (determined by TG as relative weight loss at 750 °C). Data are summarised in Table 5.-2. For both Dff and Bf samples light fractions contain particles of smaller size. Therefore in further for Df and Bf the correspondence light fraction = smaller particles is used. The mean size values determined from the X-rays diffraction exceed those from the electronic microscopy. F.Tourinho reported a similar difference in size obtained by these two methods for particles of ferrite of Mn and Co [32]. This difference may be connected with a remained polydispersity in size even in obtained fractions.

Table 5.-2. Properties of fractions of the surface treated particles (cationic ferrofluids) separated by centrifugation for two samples Df (x_0=0.5) and Bf (x_0=0.2). Mean sizes, determined from X-rays (D_{XR}) and electronic microscopy (D_{EM}), chemical composition and associated water content (from TG). For fractions of Bf properties of precursor Bs (particles before surface treatment) are also given.

Name of fraction		Fraction's part of total sample	Particles mean size, nm		Chemical composition			Assoc. water content **Q**, w%
		mol% of Me	D_{XR}, nm	D_{EM}, nm	$MnO:ZnO:Fe_2O_3$	Molar ratio **X**	Zn subst. degree **x**	
Dff1	light	26.5	8.65	6.7	18.6:22.3:59.0	0.257	0.545	12.0
Dff2	intermed	33.8	9.5	n.d.	18.4:23:58.7	0.261	0.556	n.d.
Dff3	heavy	39.7	9.5	7.5	18.5:23.1:58.4	0.263	0.555	9.8
Bf1	light	13.5	9.5	4.9	29.2:9.7:61.1	0.241	0.249	n.d.
Bf2	heavy	86.5	11.7	10.5	35.8:11.0:53.2	0.305	0.235	n.d.
Bs	precursor	-	11.0	n.d.	39:10:51	0.325	0.20	n.d.

n.d.- not determined

For fractions of Df the difference in chemical composition is too small to make a definite conclusions, whereas for fractions of Bf a strong difference in metal content is found. In the light fraction Bf1 content of Fe as well as the Zn substitution degree **x** are higher than those in the heavy fraction Bf2 (see Table 5.-2.). Comparison of chemical composition of the coprecipitated precursor Bs with composition of fractions of cationic ferrofluid reveal that bigger particles are less chemically changed during the surface treatment than the small ones.

The light fraction Df1 has also a higher content of associated water than the heavy one Df3.

5.3 Magnetic properties of the fractionated particles and ferrofluids

5.3.1. Magnetic properties of the particles fractionated by sedimentation

The magnetisation curves for light and heavy fractions of particles after coprecipitation and heating Ds1 and Ds3 and corresponding spectra of magnetic moments are shown on Figures 5.-1. and 5.-2. respectively. The light fraction Ds1 has a less steep magnetisation curve and in a spectrum of magnetic moments there is much more pronounced weakly magnetic part. Difference in the magnetisation between two fractions is relatively higher in low fields.

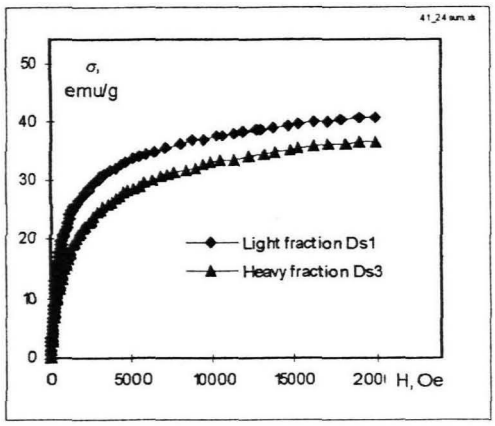

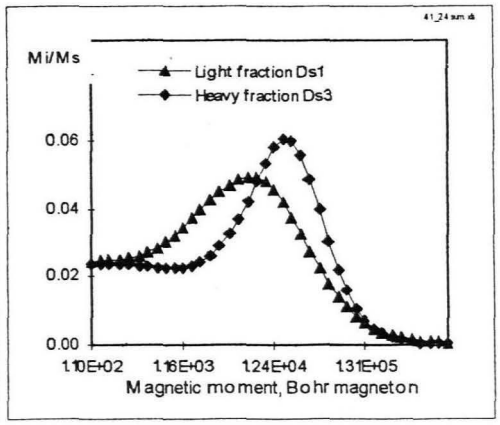

Figure 5.-1. Magnetisation curves for light and heavy fractions of sample Ds at **T**=294 K.
Figure 5.-2. Spectra of magnetic moments for light and heavy fractions of sample Ds at **T**=294 K.

5.3.2. Magnetic properties of the ferrofluids fractionated by centrifugation

For fractions of the cationic ferrofluids the magnetisation curves are measured at temperatures close to the room as well at the elevated temperature up to 373 K for fractions Df1and Df3 and up to 473 K for Bf1 and Bf2. The magnetisation curves for fractions Df1and Df3 at 294 K are shown on Figure 5.-3. The corresponding spectra of a magnetic moments are shown on Figure 5.-4. The difference in the maximum positions for these two fractions is clearly seen.

Magnetisation curves and the corresponding spectra of magnetic moments (at 303 K) for fractions Bf1 and Bf2 are shown on Figure 5.-5. and 5.-6. respectively. For both fractions of Df and Bf the smaller particles have a lower magnetisation than the bigger ones.

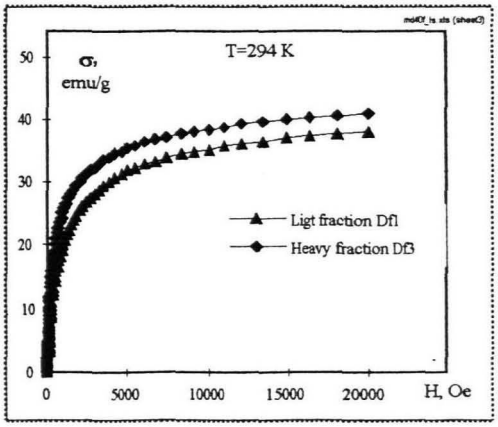

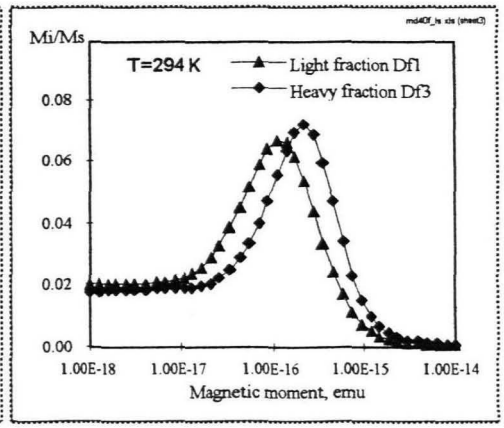

Figure 5.-3. Magnetisation curves for light and heavy fractions of sample Df at **T**=294 K.
Figure 5.-4. Spectra of magnetic moments for light and heavy fractions of sample Df at **T**=294 K.

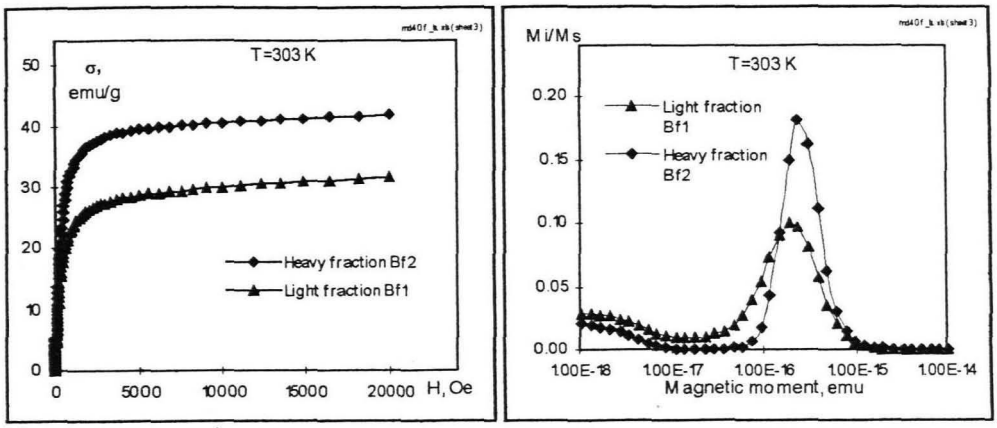

Figure 5.-5. Magnetisation curves for light and heavy fractions of sample Bf at **T**=294 K.
Figure 5.-6. Spectra of magnetic moments for light and heavy fractions of sample Bf at **T**=294 K.

The difference in magnetisation is relatively more pronounced in low fields. This is connected with the fact that for smaller particles higher fields are required to orientate their magnetic moments.

There is a difference for smaller and larger particles also in magnetisation on temperature dependence. The dependence of magnetisation on temperature for Df1 and Df3 in magnetic fields of three different intensities of 20, 5 and 1.025 kOe are shown on Figures 5.-7. (a), (b) and (c) respectively. In **H**=20 kOe the relative difference of magnetisation for two fractions $\Delta\sigma/\sigma_{Heavy}$ decreases with growing of temperature, whereas in **H**=1.025 kOe $\Delta\sigma/\sigma_{Heavy}$ it grows from 0.20 at 294 K to 0.27 at 373 K.

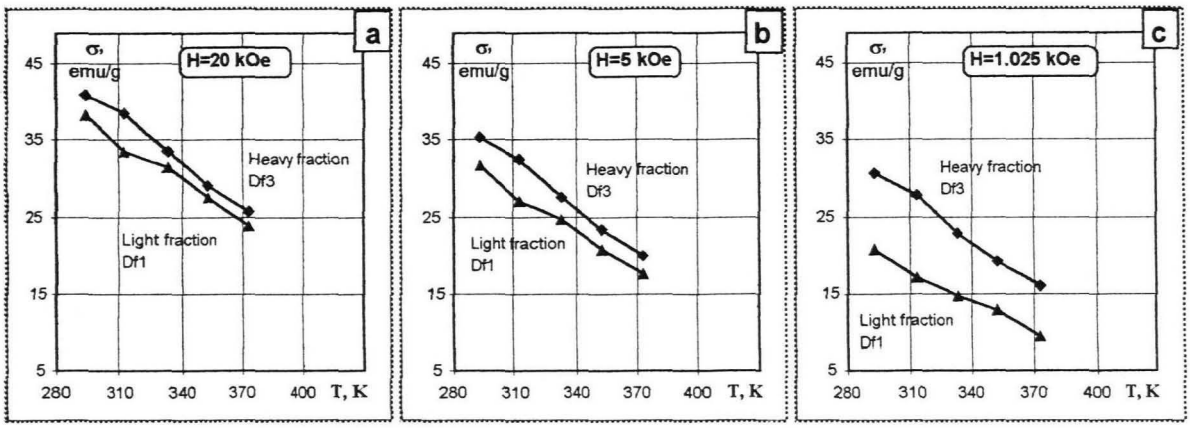

Figure 5.-7. Magnetisation versus temperature for light and heavy fractions of sample Df in magnetic fields of different strength: (a) - **H**=20 kOe, (b)-**H**=5 kOe and (c)-**H**=1.025 kOe.

Similar magnetisation on temperature dependence for Bf1 and Bf2 in the range of 303-473 K are presented in Figures 5.-8. (a), (b) and (c). The conclusion that the relative difference of magnetisation between heavy and light fractions $\Delta\sigma/\sigma_{Heavy}$ is higher in lower fields holds true for all taken temperature range. It can be seen that the slope of magnetisation - temperature curves is lower for light fractions for fractions of the both samples Df and Bf. This can be quantitatively expressed in a values of the thermomagnetic coefficient $\mathbf{k}_T$, determined by a linear approximation of experimental dependence in the temperature range of 294-373 K for the fractions of Df and in the range of 303-373 K for the fractions of Bf.

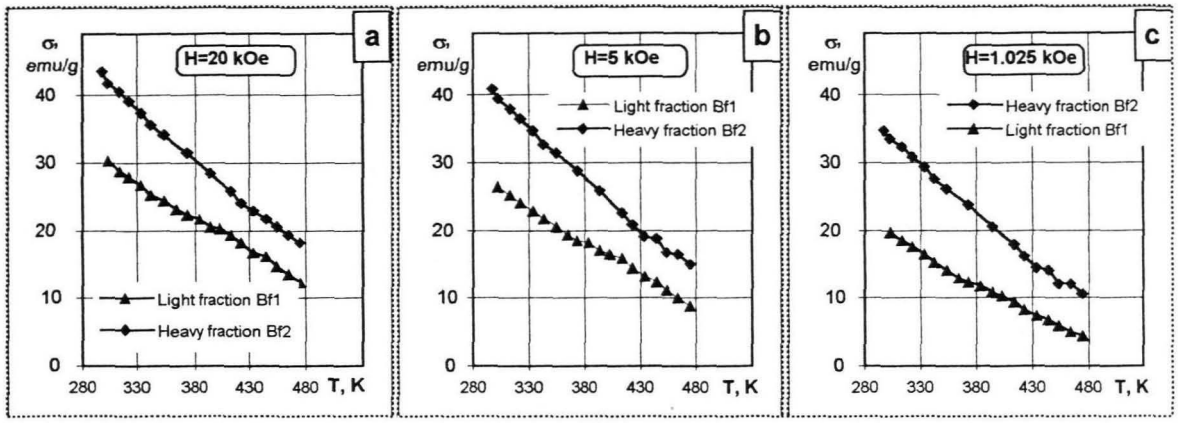

Figure 5.-8. Magnetisation versus temperature for light and heavy fractions of sample Bf in magnetic fields of different strength: (a) - **H**=20 kOe, (b)-**H**=5 kOe and (c)-**H**=1.025 kOe.

The thermomagnetic coefficients for Df1 and Df3 as well as for Bf1 and Bf2 in the magnetic field of different strength are presented on Figures 5.-9. (a) and (b) respectively. The character of the dependence $\mathbf{k_T(H)}$ for smaller and bigger particles is similar. It is remarkable that $\mathbf{k_T}$ increases with growing of H up to 5 kOe for Df1, Df3 and up to 3 kOe for Bf1, Bf2 and in stronger fields remains approximately constant. For Bf2 $\mathbf{k_T}$ reaches the maximal value in **H**~2 kOe and even slightly decreases in a stronger fields. The maximal value of $\mathbf{k_T}$ for Df3 exceeds that of Df1 for 1.15 times, whereas $\mathbf{k_T}$ for Bf2 exceeds that of Bf1 for 1.4 times.

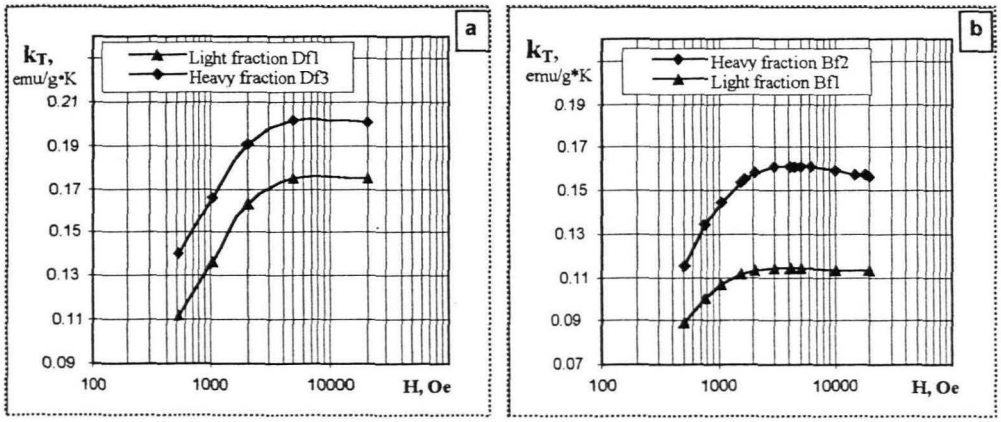

Figure 5.-9. Thermomagnetic coefficients $\mathbf{k_T} = -\Delta\sigma/\Delta T$ for light and heavy fractions of samples Df (a) and Bf (b) in the temperature range of 294-373 K versus magnetic field strength.

Conclusions

Particles after coprecipitation and heating separated by sedimentation

1. Particles of the light fraction have a lower Fe content, higher Zn substitution degree **x** and higher associated water content **Q** than particles of the heavy fraction.

2. The light fraction has a lower specific magnetisation than the heavy one. Especially this difference is pronounced in a low fields.

Cationic ferrofluids fractionated by centrifugation

3. In comparison with the coprecipitated particles separated by sedimentation, fractionation of the cationic ferrofluids by centrifugation leads to a better separation in size of particles.

4. Properties of particles (chemical composition, content of associated water, magnetic properties) are dependent on size of particles. Smaller particles are more chemically changed during a surface treatment than the bigger ones. They have higher content of Fe and a higher content of associated water.

5. Smaller particles possess a lower specific magnetisation and a lower thermomagnetic coefficients than the bigger ones in all the range of magnetic field of 0 - 20 kOe. In a low fields difference in the magnetisation for smaller and bigger ones is relatively more pronounced.

Chapter 6.

DISCUSSION

6.1. The role of Zn substitution degree x

Growing of **x** leads to particles with smaller sizes. Similar observations were reported by V. Chalyi for particles of 12-16 nm [29]. This may be partly caused by a different values of the ionic radii of Zn^{2+} (0.83 Å) and Mn^{2+} (0.91 Å) ions.

Growing of **x** leads also to higher content of associated water in particles. This may be connected with smaller size of particles with higher **x**: smaller particles have more developed surface, which may adsorb a higher quantity of water. This suggestment is also confirmed by a higher associated water content present in smaller particles fractionated from the polydispersed samples. Other reason for increased associated water content in particles with higher **x** may be a higher affinity of remained Zn hydroxide to water in comparison of Mn hydroxide [30].

6.2. Parameters of synthesis

6.2.1. The type of coprecipitating base

Three bases give particles with sizes decreasing in the following sequence: $D_{NaOH}>D_{CH3NH2}>D_{NH3}$. A similar regularities were found earlier for Mn and Co ferrites [25]. This may be connected with a different pH values, which are provided by these bases. Distinguishing feature of Mn-Zn ferrite is that for CH_3NH_3OH and NH_4OH the increasing of the initial Zn substitution degree $\mathbf{x_0}$ above the definite threshold values leads to formation of non-magnetic roenthgenoamorpthous product. It is remarkable also that for ferrite particles obtained by CH_3NH_2 below this threshold value a deficit in Zn content is found in respect to the initial reagent mixture. These phenomena may be explained by the soluble complex formation for Zn^{2+} and partly Mn^{2+} with CH_3NH_3OH or NH_4OH [49]. Fe^{3+} is not complexing with these bases and Fe (III) hydroxide may to some extent initiate the precipitating of Mn^{2+} and Zn^{2+} [50]. To widen **x** limits where ferrite is formed with CH_3NH_2 or NH_3, taking a nonstoichiometric initial compositions with the excess of Fe^{3+} may be proposed for further studies.

6.2.2. The duration of heating after coprecipitation

The process of ferrite formation requires a certain time. It is found that the most relevant changes occur during the first 20 min of heating in alkaline solution. It is remarkable that particles contain ~10 w% of associated water even after 90-180 min of heating. V. Chalyi also reported that the content of the associated water can be reduced only to a certain level (7-10 w%) after 24 hours of boiling and further boiling failed to reduce it. This long heating process, however, may lead to the growing of particles size and requires a special reaction vessel with reversed cooler to prevent evaporation of the base and decreasing the pH of the suspension. A different technique may be proposed as an improvement of the synthesis, namely, the hydrotermal treatment of coprecipitated particles in alkaline solution. This method known for ultrafine crystal growing [51] allows to subject an aqueous suspension to temperatures up to 250 °C under the pressures up to 70 atm. Hydrotermal treatment may accelerate the ferrite formation and lead to a more perfect crystalline structure of particles.

However, the hydrotermal treatment requires a hermetic stainless steel vessels, and stirring of suspension may be a serious technical problem.

6.3. Magnetisation and crystalline structure

Magnetisation (in magnetic field $\mathbf{H_m}$=20 kOe) of particles obtained by the coprecipitation method in the range of $\mathbf{x}$=0.2-0.7 is only 40-50 % from that of the bulk high temperature obtained ferrite [5].

In spite of the fact that in X-rays diffraction spectra no other crystalline structures are identified than the ferrite spinel one, there is, however, a pronounced noise signal. This may indicate to the roenthgenoamorthous component present in the particles. At least two reasons may be responsible for that: 1) non-complete transformation of hydroxides into ferrite, that is confirmed by the presence of 4-14 w% of associated water in particles (complete leaving of associated water from particles is achieved only by a high temperature heating up to 750 °C); 2) possible inhomogeneties in particles crystalline structure, which may be pronounced in our case of three metals ferrite.

Zn substitution degree $\mathbf{x}$ has a great influence on magnetic properties of particles. Synthesized samples with $\mathbf{x}$>0.3 do not reach the magnetic saturation in $\mathbf{H_m}$ =20 kOe. Nanoparticles with $\mathbf{x}\geq$0.5 (mean size of 6 - 10 nm) are found to be far from magnetic saturation even in a very strong magnetic field of 120 kOe due to significant paramagnetic contribution [14]. This hinder correctly determinate their saturation magnetisation. Authors of ref. [14] made an attempt to divide superparamagnetic and paramagnetic contributions of the whole magnetisation on the base of calculated spectrum of magnetic moments. Then a "spontaneous intrinsic magnetisation" is calculated as saturation of super-paramagnetic part of magnetisation. However, for our samples with $\mathbf{x}\geq$0.8 as well as for samples with lower Zn content at elevated temperatures spectra of magnetic moments become with "one maximum" and it is no more possible divide these two parts of magnetisation.

For particles obtained by NaOH a dramatic decrease of magnetisation σ, growing of paramagnetic part in magnetic moment spectra and a decrease of thermomagnetic coefficient $\mathbf{k_T}$ is observed for $\mathbf{x}$ growing from 0.5 to 0.6. The decrease of particles size is not so great for causing such strong effect. Progressive fall of σ and $\mathbf{k_T}$ continues up to $\mathbf{x}$=0.8. A similar regularities were reported by Chalyi for 14-20 nm particles [13] and by Corradi et al for bigger Mn-Zn ferrite particles (120 nm) [12]. For bulk ferrites at room temperature there is also a decrease of magnetic parameters for $\mathbf{x}$>0.3, but much more smooth [5]. Particles with $\mathbf{x}$>0.5 obtained by the coprecipitation may be considered as not true homogene ferrites, but rather as highly disordered systems constituted locally of paramagnetic regions with composition close to Zn ferrite and ferrimagnetic regions with mixed ferrite structure with $\mathbf{x}$ higher than average value [11, 52].

The magnetisation σ_m of Zn ferrite particles is 11 emu/g*K, whereas in the bulk ceramic Zn ferrites magnetisation is negligible. Pure bulk $ZnFe_2O_4$ is not ferrimagnetic. Transition from paramagnetic state to antiferromagnetic occurs at very low temperature (~15 K) [53]. The effect of increase of magnetisation for Zn ferrite particles of 6-11 nm in comparison with that for the bigger ones was reported by Japanese researchers [16, 19, 20]. Deviations in Zn^{2+} and Fe^{3+} cations distributions in sublattices from the completely direct spinel stricture are considered to be responsible for this anomalous magnetisation. Other reason of an anomalous magnetism of the obtained Zn ferrite particles may be the magnetisation caused by the amorphous Fe(III) hydroxide, which at room temperatures may reach values of σ~2–6 emu/g (in H=10 kOe) [50].

For practical applications samples with high thermomagnetic coefficient $\mathbf{k_T}$ are desired. It is remarkable that ferrite particles with a different $\mathbf{x}$ show their maximal thermomagnetic coefficients $\mathbf{k_T}$ at different temperatures. The sample with $\mathbf{x}$=0.2 has almost a constant $\mathbf{k_T}$ values (0.13-0.17 emu/g*K) in

wide temperature range of 313-448 K. High k_T (0.13-0.21 emu/g*K) in the temperature range of 303-413 K are reached by the samples with x=0.5. Samples with a higher x may be potentially used at lower temperatures, because at elevated temperatures (above the room one) their k_T is strongly decreasing.

Pronounced non-linear behaviour of $\sigma(T)$ at temperatures near the estimated Curie temperatures is observed for samples with x=0.58 and 0.78. The estimated Curie temperatures for these samples are inside the investigated temperature range (they are 405 and 370 K respectively) and a non-linear tail of σ above T_c up to 80-100 K long is observed. This phenomenon called 'paraprocess' was earlier reported for ceramic ferrites with nonmagnetic ions and for Mn-Zn ferrites it reached 70 K [54]. It was explained by the presence of chemical inhomogenities in 3-component ferrite. For particles obtained by the coprecipitation these inhomogenities may be even more pronounced and therefore the non-linear tail may be longer than for ceramic ferrite.

6.4. Surface treatment (formation of ionic ferrofluids)

Chemical stability of particles in solution and their maintenance in colloidal suspension requires the appropriate state of their surface. Agglomeration and sedimentation of particles is avoided by creating a sufficient repulsion forces between particles. Solubilisation is realised by HNO_3 treatment which apports superficial charges providing electrostatic repulsion between particles.

However, a partial dissolution of particles during HNO_3 treatment occurs. It is remarkable that three metals from particles dissolve differently, namely in the following relative sequence: Fe<Zn<Mn. Therefore the chemical composition of particles changes to the excess of Fe, as well as the Zn substitution degree x slightly grows. To explain this it can be pointed out that the formation of Zn ferrite occurs more readily than of the Mn ferrite [30]. Therefore Mn in a higher degree than Zn may remain in the form of hydroxide and then may be more readily dissolved in HNO_3.Other obstacle that may explain a different dissolution of three metals is that they have a different precipitation/ dissolution pH values: Fe(III) has the lowest pH~1.6, Zn – pH~5.8 and Mn(II) the highest – pH~8.6 [30].

A modification of particles surface to make it more resistant to acid action (to prevent a destruction in weakly acid medium) is realised by a ferric nitrate treatment. This treatment leads to the additional increase of Fe content in particles, however, not so strong as during an acid treatment. X-ray diffraction and IR-spectroscopy did not reveal any changes in positions and intensity of lines or absorbtion bands for particles before and after acid and ferric nitrate treatments. For some samples somewhat diminution of noise level in X-ray diffraction spectra is found after acid treatment.

F.Tourinho considered that the amorphous non-magnetic layer of Fe hydroxide is formed on the surface of Co ferrite particles, which leads to decrease of their magnetisation [25]. However, for Mn-Zn ferrite particles no any decrease in particles magnetisation is found after ferric nitrate treatment, moreover a slight increase in σ is observed.

As a result of two treatments, called together 'surface treatment', the shape of magnetisation curve becomes more steep. Higher σ and k_T are reached in lower fields. After 'surface treatment' paramagnetic component is strongly decreased (as it is seen on magnetic moment spectra) especially for samples with high Zn substitution degree x. Changes in magnetic properties after "surface treatment may be probably caused by following process: roentgenamorthous paramagnetic part of particles material is less resistant to acid treatment and therefore may be more readily dissolved than crystallised superparamagnetic part. At the same time there is another factor, which may be responsible for increasing of magnetisation and for higher Curie temperatures: increase of Fe content

in particles in favour of Mn and Zn. This may probably lead to formation of complex ferrite $Mn_{1-x}Zn_xFe_2O_4$ γ–Fe_2O_3. Maghemite γ–Fe_2O_3 has higher specific magnetisation σ_s=77 emu/g and much higher Curie temperature T_c=870 K [1, 2, 4, 10] (data are given for bulk material) than $Mn_{1-x}Zn_xFe_2O_4$ and even presence of small amount of Fe_2O_3 can lead to higher σ and T_c of the whole product.

6.5. Surfacted ferrofluids

The Mn-Zn ferrofluids based on non-polar liquids may keep their fluid properties in rather wide temperature range (if liquid carrier is low-evaporating) that is important for the practical applications [17]. Non-polar type of liquid carrier - liquid hydrocarbon medium requires a different approach to the solubilisation of particles than for the ionic ferrofluids. Surfactant is adsorbed on the surface of particles and only after that particles are transferred into the carrier liquid. Commonly particles directly obtained after coprecipitation are used for preparation of organic based ferrofluids. In this work two types of particles are applied: particles directly obtained after coprecipitation as well as cationic ones obtained after 'the surface treatment'. Chemical and magnetic properties of these two types of hydrocarbon based ferrofluids are determined by those of the correspondent precursor particles.

6.6. Influence of size on properties of Mn-Zn ferrite nanoparticles

Comparing the properties of smaller and bigger particles fractionated from polydispersed samples shows that the smaller particles a have higher content of the associated water as well as demonstrate lower magnetisation σ and thermomagnetic coefficients k_T. The decreasing of saturation magnetisation for smaller particles with size lower than 10 nm was reported by T. Sato et [9]. This may be connected with increasing of the relative part of less magnetic surface layer in smaller particles. The decrease in magnetisation in smaller particles is thought to be caused probably with the magnetically inactive surface layer or magnetic effects caused by the asymmetric environment of the atoms near the surface.

Conclusions

1. Mn-Zn ferrite nanoparticles (6-19 nm) are synthesised with the Zn substitution degree parameter **x** in the range $0 \leq x \leq 1$.

2. Influence of several synthesis parameters on the properties of obtained Mn-Zn ferrite particles is studied:

a) dependence of particle mean size upon the type of coprecipitating base is clarified. Three bases yield particles with the mean sizes decreasing in the following sequence: $D_{(NaOH)} > D_{(CH3NH3OH)} > D_{(NH4OH)}$. For CH_3NH_3OH and NH_4OH, however, the formation of ferrite occurs only if the initial Zn substitution degree x_0 does not exceed a definite threshold values: 0.6 and 0.3 respectively.

b) duration of heating in alkaline solution after coprecipitation significantly effects the properties of obtained particles: the most relevant changes in particles size and associated water content occur in the first 20 minutes of heating.

On the basis of obtained results an optimized operation protocol for preparation of Mn-Zn ferrite nanoparticles is ellaborated.

3. Varying of the Zn substitution degree parameter **x** causes changes in size, associated water content as well as in magnetic parameters:

a) increasing of the parameter **x** causes a significant decrease of particles mean size **D** and increase in associated water content **Q**: for **x** growing from 0 to 1 (coprecipitation by NaOH), **D** decreases from 19 down to 6 nm, and **Q** increases from 3-4 to 14 w.%.

b) near the room temperatures magnetic parameters - magnetisation σ and thermomagnetic coefficient k_T reach their maximum values at $x=0.4\text{-}0.5$: $\sigma_m=41$ emu/g and $k_T=0{,}215$ emu/g*K respectively in magnetic field of 20 un 5 kOe.. For **x** above 0.5 a dramatic decrease in σ and k_T as well as in i_m occurs. However, Zn ferrite particles ($x=1$) show relatively high magnetisation: σ_m value of about 11 emu/g, which is not found for bulk material.

c) particles with different **x** show their maximal values of thermomagnetic coefficients k_T at a different temperatures. Growth of **x** from 0.2 to 0.8 shifts the maximum of k_T to a lower temperatures: from 350-430 to 160 K respectively. These results allow to choose appropriate **x** values for preparing particles with maximal values of thermomagnetic coefficients for a different temperature ranges.

4. Cationic ferrofluids are synthesised using obtained Mn-Zn ferrite nanoparticles. A special "surface treatment" procedures (with HNO_3, then with $Fe(NO_3)_3$) are applied for formation of the appropriate particles surface state which provides colloidally and chemically stable cationic sol. A significant changes in chemical and magnetic properties of particles after surface treatment are found:

a) a significant increase in the relative content of Fe(III) in particles (conventional Fe_2O_3 content grows from 51-52 up to 58-67 mol %), Zn substitution degree **x** also increases, because of different dissolution of three metals at HNO_3 treatment. Metals relative dissolution increases in the following sequense: Fe→Zn→Mn;

b) changes in magnetic parameters of particles take place:

- the increase of magnetisation σ, parameter i_m and thermomagnetic coefficients k_T occurs, especially for samples with higher Zn content ($x>0.5$);
- higher values of σ and k_T are achieved in a lower magnetic fields and k_T shows saturation in a certain magnetic field H_1, which value grows with the increase of **x**.
- the estimated Curie temperatures increase for 25-60 K.

The above mentioned changes in magnetic properties may be caused by two probable reasons:
1) more pronounced dissolution of paramagnetic phase than of ferrite phase at HNO_3 treatment;
2) increase of Fe(III) content and respective Mn and Zn content decrease after HNO_3 and $Fe(NO_3)_3$ treatments, which may probably lead to formation of Mn-Zn ferrite and Fe(III) oxide compositions with higher Curie temperature.

5. Hydrocarbon-based ferrofluids are prepared by stabilisation of particles with surfactant (oleic acid). Two different types of particles are used:

1) particles directly obtained after the coprecipitation and heating in alkaline medium;

2) cationic particles, obtained by a surface treatment.

Particles surfactation and solubilisation in hydrocarbon medium does not effect their size and chemical composition. Differences in the magnetic properties for untreated and the surface treated particles remain also for two types of surfacted ferrofluids: the magnetisation of the surfacted ferrofluid of type 2 is higher than that of the type 1, especially in a low fields.

6. Properties of particles of different sizes obtained by fractionation of polydispersed samples are compared. Smaller particles show lower magnetic parameters σ, i_m and k_T than larger ones. Smaller particles have also higher content of associated water than larger particles. This may indicate to a higher presence of paramagnetic roentgen amorthous phase in a smaller particles.

References:

1. J.SMITH and H.P.J.WIJN, *Ferrites* John Wiley and Sons, N.Y., 1959.

2. S.TIKADZUMI, *Physics of ferrimagnetism* Tokyo, 1978 (Transl. to Russ. Moscow 1983).

3. A.H..MORRISH and P.E.CLARK, High-field Mossbauer study of Mn-Zn ferrites *Physical Review B* 11 (1975) 278-286.

4. LANDOLT-BORNSTEIN, *Numerical Data and Functional Relationships in Science and Technology* Vol. 4 (Magnetic materials) Part b Berlin, 1970.

5. Ch.GUILLAUD and H.CREVEAUX, Proprietes ferromagnetiques des ferrites mixtes de Co et de Zn et de Mn et Zn *C. R. Acad. Sci*. (Paris), 230 (1950) 1458.

6. Ch.GUILLAUD and ROUX, *C. R. Acad. Sci.* (Paris), 229 (1949) 1331.

7. K.OHTA, *J. Phys. Soc. Jap.* 18 (1963) 685.

8. J.K.GALT, W.A.YAGER, J.P.REMEIKA and F.R.MERRITT, *Phys. Rev.*, 81, (1951) 470.

9. T.SATO, T.IIJIMA, M.SEKI and N.INAGAKI, Magnetic properties of ultrafine ferrite particles *J.M.M.M.* 65 (1987) 252.

10. L.RABKIN, S.SOSKIN and B.EPSSTEIN, *Ferrites: structure, properties and technology* Leningrad 1968 (in Russ.) p.263.

11. M.PETRERA, A.GENNARO and N.BURRIESCI, Mossbauer study of Mn-Zn spinel ferrites prepared by a wet chemical method *J. Mater. Sci.* 17 (1982) 429.

12. A.R.CORRADI, L.BENZONI, N.BURRIESCI, C.A.NANNETTI, M.PETRERA and S.PIZZINI, Experimental evidence of the influence of the cation site occupancy and of its evaluation with temperature on magnetic properties of soft ferrites prepared by wet methods *Journal de Physique* Colloque C1 38 (1977), C1 291.

13. V.P.CHALYI and E.B.NOVOSADOVA, Phase transformation in the system of hydroxides of Mn (II), Zn (II) and Fe(III) *Neorganicheskie Materiali* 9 (1973) 2190 (in Russ.).

14. M. MAIOROV, E. BLUMS, M. HANSON and C. JOHANSON, High field magnetization of the colloidal Mn-Zn ferrite *J.M.M.M.* (1999) (in print).

15. Z.X.TANG, C.M.SORENSEN, K.J.KLABUNDE, Size-dependent Curie temperature in nano-scale $MnFe_2O_4$ particles *Phys. Rev. Lett.* 67 (1991) 3602.

16. J.L.KIRSCHVINK, D.S.JONES and B.J. MACFADDEN, *Magnetite biomineralisation and magneto-reception in organisms* ed. Plenum Press N.Y., 1985, vol. 1, p. 43.

17. T.FUJITA, M.MAMIYA and B.JEVADEVAN, Basic study of heat convention pipe using the developed temperature sensitive magnetic fluid *J.M.M.M* 85 (1990), 203.

18. E.BLUMS, M.M.MAIOROV and G.KRONKALNS, Thermomagnetic properties of ferrofluids containing chemically coprecipitated Mn-Zn ferrite particles *IEEE Trans. Magn.* 29 (1993) N6 3267.

19. T.KAMIYAMA, K.HANEDA, T.SATO, S.IKEDA and H.ASANO, Cation distributions in $ZnFe_2O_4$ fine particles studied by neutron powder diffraction *Solid State Communications* 81 (1992) 563-566.

20. T.SATO, K.HANEDA, M.SEKI and T.IIJIMA, Morphology and magnetic properties of ultrafine $ZnFe_2O_4$ particles *App. Phys.* A 50 (1990) 13.

21. B. JEYADEVAN, K. TOHJI and K.NAKATSUKA, Structure analysis of coprecipitated $ZnFe_2O_4$ by extended X-ray-absorption *J. Appl. Phys.* 76 (1994) 6325.

22. E. BLUMS, A. CEBERS and M. M. MAIOROV, *Magnetic Fluids* ed. W. de Gruyter, Berlin-New York, 1997, p. 298.

23. R.MASSART and V.CABUIL, Synthese en milieu alcaline de magnetite colloidale *J.Chim.Phys.* 84 (1987) N7-8 967 (in Fr.).

24. F.A.TOURINHO, R.FRANCK, R.MASSART, and R.PERZYNSKY, Synthesis and magnetic properties of Mn and Co ferrite ferrofluids *Progr. Colloid Polym Sci.* 79 (1989) 128.

25. F.A.TOURINHO, R.FRANCK and R.MASSART, Aqueous ferrofluids based on Mn and Co ferrites *J. Mater. Sci.* 25 (1990) 3249.

26. K.NAKATSUKA, Y.HAMA and J.TAKAHASHI, Heat transfer in temperature-sensitive magnetic fluids *J. Magn. Magn. Mater.* 85 (1990) 207.

27. O.I.IVANOVA and A.O.KUZUBOV, Temperature sensitive magnetic fluids *Magn. Gidrodin.* (1994) N1 47 (in Russ.).

28. T.ATARASHI, T.IMAI and J.SHIMOIIZAKA, On the preparation of the colored water-based magnetic fluids *Journ. Magn. Magn. Mater.* 85 (1990) 3.

29. V.P.CHALYI and E.B.NOVOSADOVA, Investigation of the conditions of the formation of Mn-Zn ferrites from hydroxides of metals *Neorg. Mater.* 6 (1970) N12 2170 (in Russ.).

30. V.P.CHALYI *Hydroxides of metals* Kiev, Naukova Dumka eds., 1972 (in Russ.).

31. N.M.GRIBANOV, E.E.BIBIK, O.V.BUZUNOV and V.N.NAUMOV, Physico-chemical regularities of obtaining highly dispersed magnetite by the method of chemical coprecipitation *J.M.M.M.* 85 (1990) 7.

32. E.MATIEVIC, *Acc. Chem. Res.* 14 (1981), 22.

33. F.TOURINHO, Ferrofluides a base de ferrite de Mn et de ferrite de Co. *Thesis*, Paris 1988 (in Fr.).

34. V.P.CHALYI and E.B.NOVOSADOVA, Kinetics and mehanism of the formation of Mn ferrite from hydroxides of metals *Neorg. Mater.* 6 (1970) N7 1301 (in Russ.).

35. V.P.CHALYI and E.N.LUKACHINA, Investigation of kinetics and mechanism of ferrite formation in the process of ageing of hydroxide metal systems *Neorg. Mater.* 1 (1965) N2 260 (in Russ.).

36. V.P.CHALYI, E.B.NOVOSADOVA and K.N.POTEMKIN, Investigation of the conditions of the formation of Mn ferrite from hydroxides of metals *Neorg. Mater.* 6 (1970) N7 1295 (in Russ.).

37. Z.X.TANG, C.M.SORENSEN, K.J.KLABUNDE, and G.C.HADJIPANAYIS, Preparation of Mn ferrite fine particles from aqueous solution *J.Coll. Interf. Sci.* 146, (1991) 38.

38. M.UEDA, SH.SHIMADA and M.INAGAKI, Synthesis of crystalline Zn ferrite near room temperature *J.Mater. Chem.*, 3 (1991) 1199.

39. V.P. CHALYI and E.N.LUKACHINA, Investigation of kinetics and mechanism of ferrite formation in systems ε-$Zn(OH)_2$–α-FeOOH in the process of ageing *Neorg. Mater.* 3 (1967) N8 1447 (in Russ.)

40. R.MASSART, Preparation of aqueous magnetic liquids in alcaline and acidic media *IEEE Trans. Magn.*, MAG-17, (1981), 1247.

41. J.P.JOLIVET, R. MASSART and J.-M. FRUCHART, Synthese et etude physicochimique de colloides magnetiques non surfactes en milieu aqueux *Nouv. Journ. Chim.* 7 N5 (1983) 325 (in Fr.).

42. C.ROCCHICCIOLO-DELTCHEFF, R.FRANCK, V.CABUIL and R.MASSART, Surfacted ferrofluids: interactions at the surfactant-magnetic iron oxide interface *J. Chem. Res. (S)* (1987) 126.

43. R.ROSENSWEIG, *Ferrohydrodynamics* Cambridge University Press, Cambridge 1985 p.61.

44. P.C.SCHOLTEN, Some material problems of in magnetic fluids *Chem. Eng. Commun.* 67 (1988) 331.

45. K.J.DAVIES, S.WELLS and S.W. CHARLES, The effect of temperature and oleate adsorption on the growth of maghemite particles *Journ. Magn. Magn. Mater.* 122 (1993) 24.

46. J.LECOMTE, Enciclopedia of physics, Springer Verlag, Berlin, 1958, Vol. 26, p.244.

47. V.C.FARMER, in *"The Infrared Spectra of Minerals"* ed. by V.C. Farmer Mineralogical Society, London, 1974 p.18.

48. A.GRANTS, A.IRBITIS, G.KRONKALNS and M.MAIOROV, Rheological properties of magnetite magnetic fluid *J.M.M.M.* 85 (1990) 129.

49. H.REMY, *Lehrbuch der Anorganischen Chemie, band II,* Leipzig, 1960 (in Germ.).

50. S.OKAMOTO, Iron hydroxides as magnetic scavenders *IEEE Trans. Magn.* MAG-10 (1974) 923.

51. T. PANNAPARAYIL, R.MARANDE and S.KOMARNENI, A novel low-temperature preparation of several ferrimagnetic spinels and their magnetic and Mossbauer characterisation *J. Appl. Phys* 64, (1988) 5641.

52. Y.ISHIKAWA, Superparamagnetism in magnetically diluted systems *J.Appl. Phys.* 35 (1964) 1054.

53. F.K.LOTGERING, *J. Phys.Chem. Solids* 27 (1966) 139.

54. K.P.BELOV, K.M.BOL'SHOVA and T.A.ELKINA, Investigation of magnetization of ferrites near Curie point *Izv. Acad. Nauk Ser. Fiz.* 21 (1957) 1047 (in Russ.).